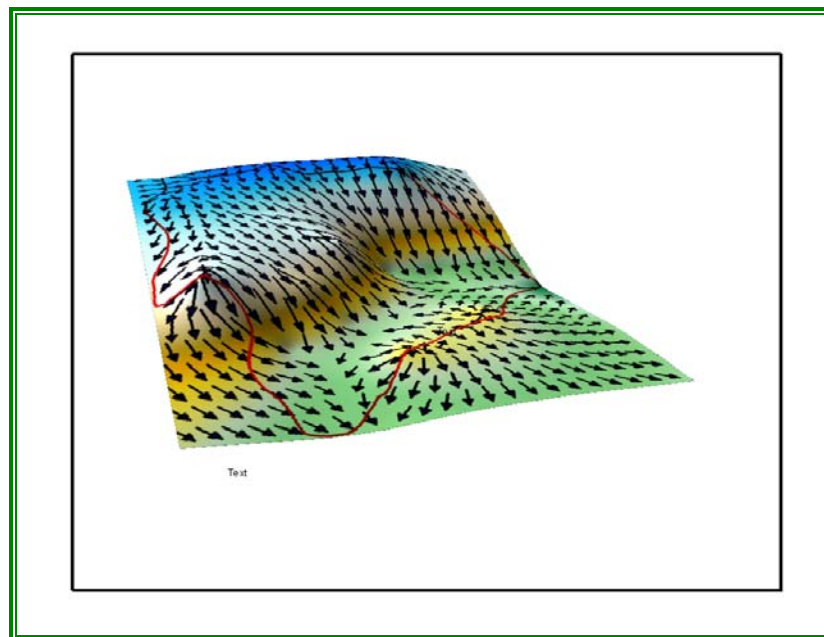


Addis Ababa  
University  
(Since 1950)



**ADDIS ABABA UNIVERSITY  
SCHOOL OF GRADUATES  
DEPARTMENT OF EARTH SCIENCES**

**GROUNDWATER POTENTIAL ASSESSMENT OF  
WELENCHITI AREA**



**A THESIS SUBMITTED TO THE SCHOOL OF GRADUATE STUDIES  
OF ADDIS ABABA UNIVERSITY IN PARTIAL FULFILMENT OF THE  
REQUIREMENTS FOR THE DEGREE OF MASTER IN HYDROGEOLOGY**

**BY  
GETACHEW ABRHA**

**JULY, 2007**

## **Acknowledgment**

I would like to forward my great thanks to my advisor Dr. Tamiru Alemayehu for his important and fruitful comments and willingness to assist me in any time of contact from the beginning. His guidance and valuable discussion had input to the successful completion of this thesis work.

I would like to thank Gambella building capacity bureau for their financial support during my stay in the university.

My sincere thanks go to Water Works Design and Supervision Enterprise for their encouragement and giving me valuable materials that were important reference to my study.

All organizations involved in this study deserve special appreciation. Geological survey of Ethiopia, National Meteorological Service Agency and Oromia Water Resource Bureau are greatly acknowledged for their data source.

My deepest heart felt thanks go to my family, who are my source of strength in every aspect of life and to my uncle Tequam Tesfamariam and his wife Shewaye Dirar for their endless support up to now.

In the last but not least, I offer my deepest gratitude to my friends, classmates and colleagues in and outside the University, organizations and individuals, who directly or indirectly involved in this study and their names are not listed are greatly acknowledged.

## **Abstract**

The welenchiti area is an extensive flat plain in the north Main Ethiopian Rift bounded by Western highland escarpment to the north and volcanic mountains to the south. It is situated between  $39^{\circ} 14' 57''$  to  $39^{\circ} 33' 16''$  East and  $8^{\circ} 27' 37''$  to  $8^{\circ} 48' 18.85''$  North covering a total area of  $780 \text{ km}^2$ . The average monthly temperature and the mean annual precipitation in the area are  $21.1 \text{ oc}$  and  $874 \text{ mm}$  respectively. Potential evapotranspiration for the area was calculated using Penman and Thornthwaite gives annual potential evapotranspiration value of  $1481 \text{ mm/year}$  and  $577 \text{ mm/year}$  respectively. Actual evapotranspiration for the area estimated, from Turc method gives value of  $697 \text{ mm}$ . While weighted actual evapotranspiration from soil water balance is  $842 \text{ mm}$  which is almost close to the annual precipitation. The annual surface water out flow, estimated using runoff coefficient methods, resulted  $129.5 \text{ Mm}^3$ . The overall water balance of the study area was computed with an aim of estimating the amount of annual recharge to the ground water. Accordingly; annual recharge to the ground water of the study area is approximated to be  $8.58 \text{ Mm}^3$ . The study area is characterized by deep groundwater systems encountered at an average depth of  $170 \text{ m}$ . Their hydraulic characteristics are spatially variable, which is the result of the complex nature of the lacustrine sediments and the degree of fracturing of the volcanic rocks. Fractured basalts, scoriaceous basalts and fractured ignimbrites are the main aquifer units in the area. These aquifers were found to be good groundwater potential zones. The general trend for groundwater flow observed from piezometric heads is from northern highland toward the plain in the direction of north west to south east of the study area. Groundwater type of the area evolves from  $\text{Ca-Na HCO}_3$  water type in areas close to northern escarpment into  $\text{Na-HCO}_3$  water type in the southern tip of the study area.

## **Acknowledgment**

I would like to forward my great thanks to my advisor Dr. Tamiru Alemayehu for his important and fruitful comments and willingness to assist me in any time of contact from the beginning. His guidance and valuable discussion had input to the successful completion of this thesis work.

I would like to thank Gambella capacity building bureau for their financial support during my stay in the university.

My sincere thanks go to Water Works Design and Supervision Enterprise for their encouragement and giving me valuable materials that were important reference to my study.

All organizations involved in this study deserve special appreciation. Geological survey of Ethiopia, National Meteorological Service Agency and Oromia Water Resource Bureau are greatly acknowledged for their data source.

My deepest heart felt thanks go to my family, who are my source of strength in every aspect of life and to my uncle Tequam Tesfamariam and his wife Shewaye Dirar for their endless support up to now.

In the last but not least, I offer my deepest gratitude to my friends, classmates and colleagues in and outside the University, organizations and individuals, who directly or indirectly involved in this study and their names are not listed are greatly acknowledged.

## Table of contents

<b>Acknowledgment</b> -----	<b>I</b>
<b>Lists of contents</b> -----	<b>II</b>
<b>Lists of Tables</b> -----	<b>V</b>
<b>Lists of Figures</b> -----	<b>VI</b>
<b>Lists of Annexes</b> -----	<b>VII</b>
<b>Abstract</b> -----	<b>VIII</b>

<b>CHAPTER ONE</b> .....	<b>1</b>
<b>Introduction</b> .....	<b>1</b>
1.1 Background.....	1
1.2 Objectives of the study.....	2
1.2.1 General objective .....	2
1.2.2 Specific objectives .....	2
1.3 Methodology.....	3
1.4 Previous Works .....	3
<b>CHAPTER TWO</b> .....	<b>5</b>
<b>General Over View of the Study Area</b> .....	<b>5</b>
2.1 Location.....	5
2.2 Climate .....	5
2.3 Physiography of the study area.....	7
2.4 Drainage.....	8
2.5 Land Use and land Cover .....	8
2.5.1 Cultivated Land .....	8
2.5.2 Vegetation Cover.....	8
<b>CHAPTER THREE</b> .....	<b>10</b>
<b>Geological setting</b> .....	<b>10</b>
3.1 Regional geology .....	10
3.1.1 Alaji Basalts .....	10
3.1.2 Anchar Basalts.....	11
3.1.3 Arba Gugu basalts.....	11
3.1.4 Chilalo and badda Trachytes .....	11
3.1.5 Post-Ashangi Group volcanic .....	11
3.1.5.1 Nazareth Group.....	12
3.1.5.2 Bofa Basalts .....	13
3.1.5.3 Wonji Group.....	13
3.1.5.4 Lacustrine sediments.....	14
3.1.5.5 Alluvial deposits.....	14
3.2 Geology of the study area.....	15
3.2.1 Ash flow tuffs, pantelleritic ignimbrites and unwelded tuffs.....	15
3.2.3 Bofa basalts.....	16
3.2.4 Pleistocene – Subrecent basalts .....	16

3.2.5 Alkali and peralkali Rhyolites, trachytes domes and flows.....	17
of Boseti.....	17
3.2.6 Lacustrine sediments.....	18
3.2.7 Recent to subrecent Rhyolite domes and flows.....	19
3.2.8 Recent aphyric basalts.....	20
3.3 Tectonics.....	22
<b>CHAPTER FOUR.....</b>	<b>23</b>
<b>Hydrometeorology.....</b>	<b>23</b>
4.1 Climate.....	23
4.1.1 Temperature.....	23
4.1.2 Wind speed.....	24
4.1.3 Sunshine hours.....	25
4.1.4 Relative humidity.....	26
4.2 Precipitation.....	27
4.3 Potential Evapotranspiration.....	32
4.4 Actual evapotranspiration.....	36
4.4.1 Empirical formula.....	36
4.4.2) Thornthwaite method (water balance method).....	38
4.5 Surface Runoff.....	44
4.6 Water balance.....	51
4.7 Cause of Flood in the study area.....	54
<b>CHAPTER FIVE.....</b>	<b>56</b>
<b>Hydrogeology.....</b>	<b>56</b>
5.1 Hydrostratigraphic units in the study area.....	56
5.1.1 The scoriaceous and fractured basalt aquifers with high.....	57
Productivity and permeability.....	57
5.1.2 Fractured and fissured Ignimbrites with Moderate permeability.....	59
and productivity.....	59
5.1.3 Lacustrine sediments with low permeability.....	60
5.1.4 Unwelded to poorly welded ignimbrites, ashflow tuffs with Low.....	61
Permeability and productivity.....	61
5.1.5 Massive rhyolite domes and flows with very low permeability.....	61
5.2 Aquifer characterization.....	63
5.3 Review of resistivity survey values in the study area.....	65
5.4 Groundwater Recharge mechanisms.....	69
5.4.1 Direct recharge from precipitation.....	70
5.4.2 Indirect recharge from highland mass through tectonic.....	71
discontinuities.....	71
5.5 Groundwater flow.....	71
<b>CHAPTER SIX.....</b>	<b>73</b>
<b>Hydrochemistry.....</b>	<b>73</b>
6.1 General.....	73
6.2 Evaluation of Hydrochemical parameters.....	73
6.2.1 Temperature and PH.....	73
6.2.2 Electrical conductance (EC).....	74
6.2.3 Total dissolved solids (TDS).....	75

6.2.4 Cations (Na + and Ca ++)	77
6.2.5 Anions	79
6.2.5.1 Fluoride	80
6.2.5.2 Chloride	84
6.2.5.3 Sulfates (SO <sub>4</sub> <sup>2-</sup> ) and Nitrates (NO <sub>3</sub> <sup>-</sup> )	84
6.2.6 Alkalinity	85
6.3 Geochemical Trend along flow paths	85
6.4 Evaluation of the hydrochemistry with respect to Drinking water quality standards in the study area	86
6.5 Water quality for irrigation purposes	87
6.5.1 Salinity and Sodium Adsorption Ratio	88
6.6 Water Types	90
<b>CHAPTER SEVEN</b>	<b>93</b>
<b>Synthesis</b>	<b>93</b>
<b>CHAPTER EIGHT</b>	<b>98</b>
<b>Conclusion and Recommendation</b>	<b>98</b>
8.1 Conclusion	98
8.2 Recommendation	99
<b>References:</b>	<b>100</b>

### List of Tables

<b>Table No</b>	<b>Type Description</b>	<b>Page No</b>
Table 4.1	Mean Monthly Air Temperature(0c) at Nazreth Station	23
Table 4.2	Mean Monthly Wind speed (m/s) at Nazreth Station	24
Table 4.3	Mean Monthly Sunshine hours at Nazreth station	25
Table 4.4	Mean Monthly Relative Humidity (%) at Nazreth Station	26
Table 4.5	Location and Mean Annual Rainfall of the Meteorological stations	28
Table 4.6	Annual weighted Rainfall depth using Thiessen Polygon	30
Table 4.7	Monthly mean Rainfall depth using Thiessen Polygon	30
Table 4.8	Mean Annual Rainfall using Isohytal method	32
Table 4.9	Mean Annual PET obtained from Thornthwaite method	34
Table 4.10	Mean Annual PET obtained from Penman method	37
Table 4.11	AET value for a soil with available water capacity of 250mm	41
Table 4.12	AET value for a soil with available water capacity of 200	42
Table 4.13	AET value for a soil with available water capacity of 150mm	42
Table 4.14	Weighted AET of The Study Area	43
Table 4.15	Runoff Coefficient for different Land covers	47
Table 4.16	CN value for different Land covers	49
Table 4.17	Peak discharges obtained from CN method	51
Table 4.18	Data sets for water budget calculation	54
Table 5.1	Summery of Resistivity value of Welenchiti Area	68
Table 6.1	Comparisons of water samples with water quality standards	87
Table 6.2	Suitability of natural water for Irrigation based on EC and SAR	89
Table 6.3	Suitability of Groundwater based on EC	90
Table 6.4	Suitability of Groundwater based on SAR	90

**List of Figures**

**Fig.2.1** Location map of The Study Area-----6

**Fig.2.2** Digital Elevation Model of The Study Area-----7

**Fig.2.3** Drainage map of The Study Area-----9

**Fig.3.1** Rhyolite domes in northeast of  
           Boseti Mt. -----18

**Fig.3.2** Pumice with intercalation of clay-----20

**Fig.3.3** Geological map of The study Area-----21

**Fig.3.4** Structural map of The Study Area-----22

**Fig.4.1** Mean Monthly Temperature in (°c)  
           at Nazreth Station-----24

**Fig.4.2** Mean monthly Windspeed(m/s)----- 25

**Fig.4.3** Mean Monthly Sunshine  
           Hours-----25

**Fig.4.4** Mean Monthly Relative  
           Humidity(%)-----26

**Fig.4.5** Thiessen polygon of The Area-----29

**Fig.4.6** Isohytal map of The Study Area-----31

**Fig.4.7** Results of the monthly water balance  
           For the weighted -----44

**Fig.4.8** Classified satellite image  
           Showing land cover -----46

**Fig.5.1** Vertical distribution of aquifers  
           From well log data-----58

**Fig.5.2** Fractured Ignimbrite Aquifer  
           In sekeklo Area-----60

**Fig.5.3** Hydrogeological Map of The Area-----62

**Fig.5.4** Hydrogeologic section on the welenchiti  
           Plain along NNE-SSW-----66

**Fig.5.5** Geoelectric section around welenchiti  
           Town-----67

**Fig.5.6** Groundwater Flow Direction Map-----72

**Fig.6.1** Temprature Map Of The Ground  
           Water samples-----75

**Fig.6.2** TDS-EC correlation for the Water sampled-----76

**Fig.6.3** TDS Map Of The Study Area-----77

**Fig.6.4** Correlation between Na and TDS-----78

**Fig.6.5** Correlation between Ca and TdS-----79

**Fig.6.6** Temprature-Fluoride Correlation-----81

**Fig.6.7** Ca-Fluoride correlation-----82

**Fig.6.8** Fluoride Map Of The Study Area-----82

**Fig.6.9** vertical distribution of fluoride-----83

**Fig.6.10** Piper plot for All water Samples-----92

**List of Annexes**

**Annex 1:** Location and pumping test data of the  
           Boreholes used in this work-----105

**Annex 2:** Hydrochemistry data used in this work-----106

**Annex 3:** Mean Monthly maximum T(°c)-----107

**Annex 4:** Mean Monthly minimum T(°c)-----108

**Annex 5:** Mean Monthly Rainfall (mm)-----109

**Annex 6:** Mean monthly Rainfall(mm)-----110

**Annex 7:** Mean Monthly Rainfall(mm)-----111

**Annex 8:** Mean Relative Humidity(%) -----112

**Annex 9:** Mean monthly Relative humidity hours-----112

**Annex 10:** Mean Monthly Sunshine hours-----113

## **Abstract**

The Welenchiti area is an extensive flat plain in the north Main Ethiopian Rift bounded by Western highland escarpment to the north and volcanic mountains to the south. It is situated between 39° 14' 57" to 39° 33' 16" East and 8° 27' 37" to 8° 48' 18.85" North covering a total area of 780 km<sup>2</sup>. The average monthly temperature and the mean annual precipitation in the area are 21.1 °c and 874 mm respectively. Potential evapotranspiration for the area was calculated using Penman and Thornthwaite gives annual potential evapotranspiration value of 1481 mm/year and 577mm/year respectively. Actual evapotranspiration for the area estimated, from Turc method gives value of 697mm. While weighted actual evapotranspiration from soil water balance is 842mm which is almost close to the annual precipitation. The annual surface water out flow, estimated using runoff coefficient methods, resulted 129.5 Mm<sup>3</sup>. The overall water balance of the study area was computed with an aim of estimating the amount of annual recharge to the groundwater. Accordingly; annual recharge to the groundwater of the study area is approximated to be 112Mm<sup>3</sup>. The study area is characterized by deep groundwater systems encountered at an average depth of 170m. Their hydraulic characteristics are spatially variable, which is the result of the complex nature of the lacustrine sediments and the degree of fracturing of the volcanic rocks. Fractured basalts, scoriaceous basalts and fractured ignimbrites are the main aquifer units in the area. These aquifers were found to be good groundwater potential zones. The general trend for groundwater flow observed from piezometric heads is from northern highland toward the plain in the direction of north west to south east of the study area. Groundwater type of the area evolves from Ca-Na HCO<sub>3</sub> water type in areas close to northern escarpment into Na-HCO<sub>3</sub> water type in the southern tip of the study area.

# **CHAPTER ONE**

## **Introduction**

### **1.1 Background**

Groundwater is the major and most feasible source of water supply particularly in areas of semi-arid zones like the Main Ethiopian Rift where there is high evaporation and limited amount of rainfall in a range of 800- 900 mm annually which is erratic in nature and with minimum associated perennial surface water resource distribution in the area. Therefore water resource studies on the availability, Sustainability and quality of the resource is very important for the effective and safe utilization of the resource in the area. Groundwater is becoming the major source of water for different purposes but one problem of this resource is the location of ground water resources that serves as a sustainable water source. So for this case groundwater recharge condition of an area must be fully understood.

The study area is situated in the northern Main Ethiopian Rift. All streams from highland escarpment and volcanic mountains are seasonal and intermittent which are not available as water supply source for most part of both rural and urban community. From the water supply point of view, Deep wells are the major source of water supply for domestic purpose as the streams are intermittent and dry up for most period of the year. Therefore groundwater development through deep wells is currently on going by regional water bureau and non-governmental organizations. These integrated activities will bring the potable water supply coverage in the area in the coming years. Groundwater development activities through shallow hand dug wells in the highland escarpment have also some challenges with regards to geology and topography. Fluoride concentration is among the most challenges and constraints with regard to water quality aspects in most deep groundwater sources. Therefore

these and other related problems need some further and detail hydrogeological investigations to indicate some possible ways and mechanisms for sustainable, potable and feasible water resource development programs in the area. On the basis of this concept this study is proposed to give some detail picture on groundwater characteristics.

The study in general focuses and incorporates water balance to estimate recharge condition, aquifer characterization, groundwater flow and evaluation of hydrochemistry.

## **1.2 Objectives of the study**

### **1.2.1 General objective**

The general objective of the study is to describe and give some detail picture on the hydrogeological feature with more focus on the flat areas or welenchiti plain. This makes an interest from the groundwater potential point of view to evaluate its water resource potential in relation to the deep groundwater resource of the study area on the basis of aquifer characterization, recharge mechanism, groundwater potential flow conditions and hydrochemical nature of the ground water.

### **1.2.2 Specific objectives**

The specific objectives of this study include:

- The description and characterization of the major aquifer systems and units in the area.
- Determining the amount of water recharging the groundwater system through water balance calculation.
- Defining the major structure and lithologic controls on the groundwater flow systems.
- Defining mechanism of recharge for the groundwater potential.

- Description of hydrochemistry of the groundwater from the analysis of the water chemistry data.

### **1.3 Methodology**

Various approaches and methodologies were applied in order to come up with the results. These are:

- ❖ Literature reviews of previous works and desk studies satellite image, topographic maps and other maps.
- ❖ Data collection and formation of data base under GIS environment such as hydro-meteorological, hydrochemical, well log data, etc and base map preparation.
- ❖ Field work accompanied by systematic field methods, measurement of relevant field variables such as EC, PH, Temperature, hydrogeological mapping, Georeferencing water points, observations of rock units and interpretations in terms of previous works and knowledge of the area.
- ❖ Data processing, analysis and interpretations of existing and field data, through use of existing maps such as geological, well log data, pumping test data, topographic maps, etc.
- ❖ The analysis and interpretation is supported by different Softwares and methods applicable in hydrogeology used for image interpretation, GIS application, hydrochemical analysis , etc (ERDAS 8.6, Arcgis 9.1, Global mapper, surfur 8, Aquachem).

### **1.4 Previous Works**

In relation to surface water and groundwater potential, studies were carried out on regional and local level at different times.

Hydrogeological investigation was carried out using the application of Geophysics by Ethiopian Institute of Geological Survey (1982) under the title of Geophysical survey for Hydrogeological Study in the Nazret area.

Groundwater exploration in Nazreth-Welenchiti Area was also studied by Taye Zewde (1987). The study revealed the lateral variation in thickness of the lacustrine sediments along North-South and East-West direction and identified the underlying water bearing formation using geophysical investigations.

The Hydrogeology of Nazreth was also studied by Getahun Kebede (1987). The study conducted to prepare 1:250,000 scaled hydrogeological map of the north main Ethiopian rift. The study concluded that the various rock units are classified as low, moderate and high permeability.

Adama Master Plan (2005) was also revised including small part of the study area.

A Surface water and groundwater potential for irrigation has also been studied for the partial part of the study area by Water Works Design and Supervision Enterprise (2007).

Some studies carried out, are almost general and are of regional scale and the local studies carried out using Geophysical investigation without well log data correlation depends highly on degree of interpretation. Therefore this study is proposed to give detail picture on Groundwater potential with respect to recharge estimation, aquifer characteristics, Groundwater flow and hydrochemistry of Welenchiti area.

## **CHAPTER TWO**

### **General Over View of the Study Area**

#### **2.1 Location**

The study area is located in the Northern part of the Main Ethiopian Rift, in east shoa zone of Oromia National State at 130 km from Addis Ababa. IT is situated between latitude of  $8^{\circ} 27' 37''$  and  $8^{\circ} 48' 18.85''$  and longitude of  $39^{\circ} 14' 27''$  and  $39^{\circ} 33' 16''$ .

The major focus of the study i.e Wolenchiti pain is located on the central of the area on the main Addis Ababa- Metahara road. The study area covers an area of 780 km<sup>2</sup>.

#### **2.2 Climate**

The Climate of the area in general comes under the influence of the Inter tropical Convergence Zone (ITCZ) which is a zone of low pressure that marks the convergence of tropical easterlies and moist equatorial westerly. The seasonal rainfall distribution is highly controlled by the annual migration of intertropical convergence zone across the area. The climate of the area in general falls under semi-arid and sub humid climatic zones. Based on the Ethiopian agro-climatic zoning, the plain with in the rift floor is grouped as kola climatic zones with altitude ranging from 1370 to 1750m while the northern highland covering small part of the study area is grouped as weinadega climatic zone with an altitude ranging from 2000-2400m.

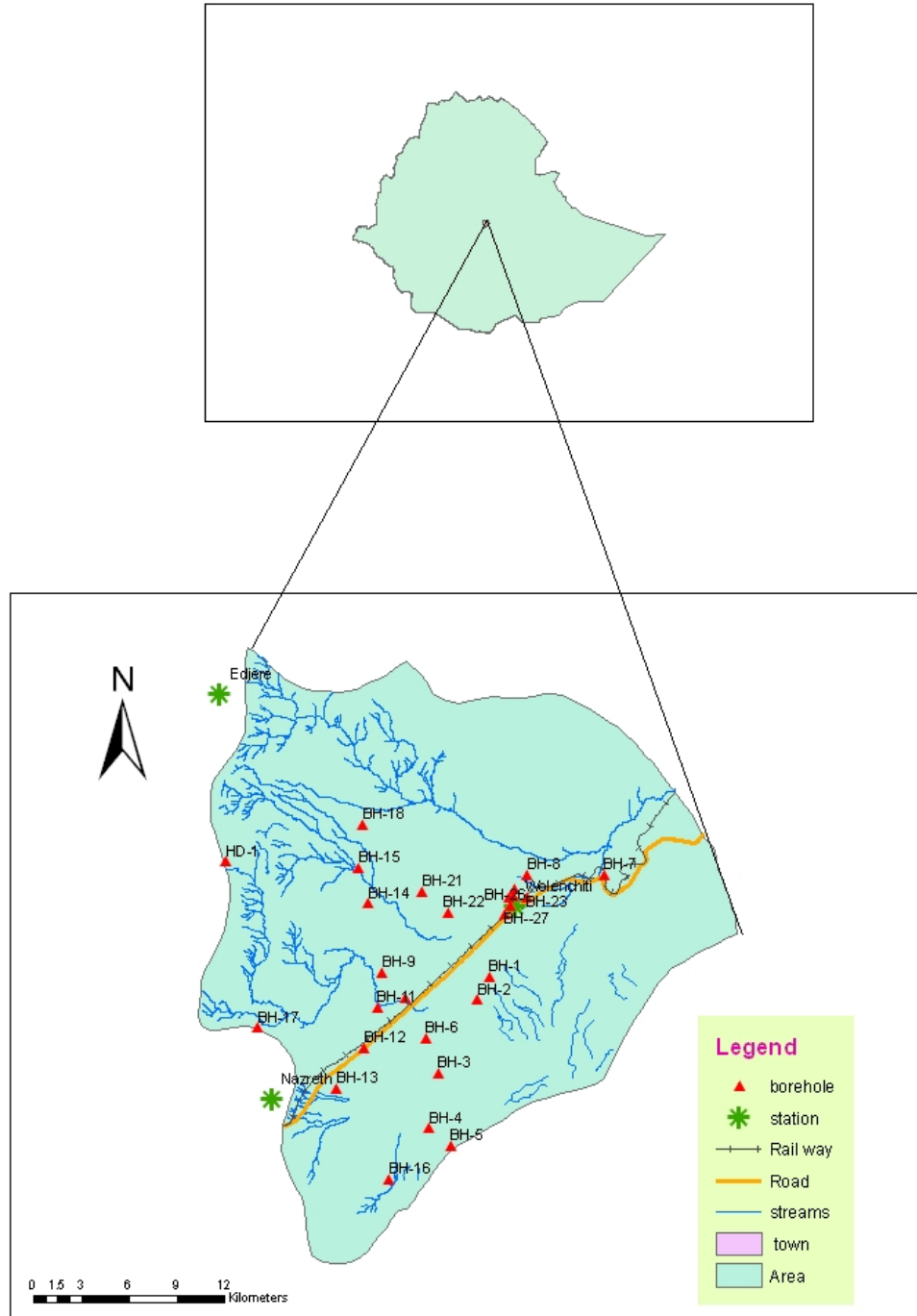


**Fig 2.1** Location map of the study area

### 2.3 Physiography of the study area

The major landform of the area consists of flat to undulating plain, hilly escarpment, volcanic cones and Mountains. Most part of the area is occupied by the flat and undulating topography with an altitude ranging from 1370-1760 m while the highland mass bounded the study area in the northern and north west part with an altitude ranging from 2000-2400m above mean sea level. Boseti Volcanic mountains such as Mt. Guda and Mt. Bariccia with peak altitudes of 2445m and 2135m respectively occurs in the southern and south west part of the area.

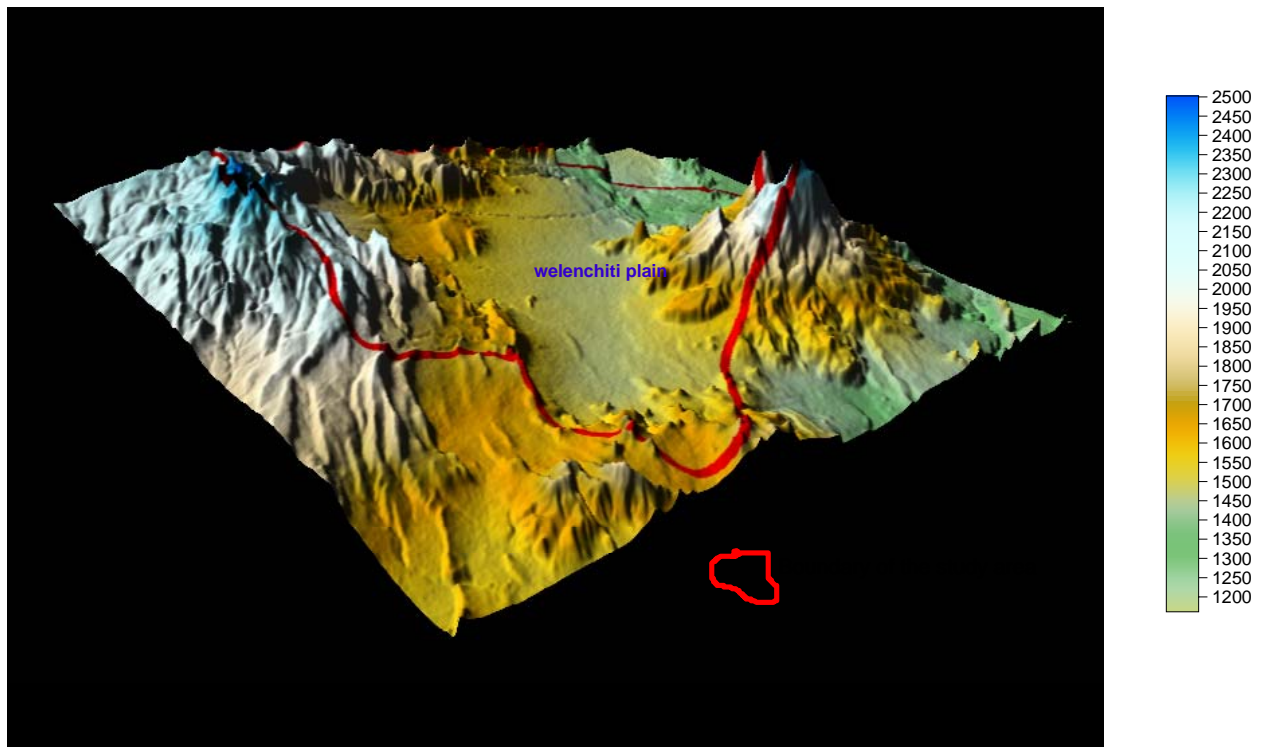


**Fig. 2.2** Digital Elevation Model showing Topography of the Area

## **2.4 Drainage**

The most dominant drainage pattern is the dendritic pattern. The major rivers flow in the north-south direction from the northern highland parallel to each other into the flat plain. The only surface water outlet from the study area is via the southeastern part of the study area.

The dendritic pattern of the streams shows the highland escarpment has the same resistance to erosion and uniform structure. It is influenced by the slope gradient. The streams have 2-3 order of hydrographic net.

Some of the major rivers in the study area are Tebo, Geldia and Marmarssa rivers shown in Fig.2.3.

## **2.5 Land Use and land Cover**

### **2.5.1 Cultivated Land**

Most part of the flat plain is cultivated for cereal crop production such as maize, teff and sorghum.

For the entire area, the Arable land is 38,041 hectare and 29,000 hectare is still cultivated.

### **2.5.2 Vegetation Cover**

The vegetation of the area is characterized by bushy wood lands, shrubs to a lesser extent of forests. The dominant vegetation cover of the area is the typical rift valley vegetation of flat-topped acacia trees that prevail in the flat cultivated area where as scattered and small thorny bushes cover the highland escarpment and hilly side of Boseti Mountains. In addition to these mixed type of vegetation small part of northeast and north west of the highland is covered with forests.

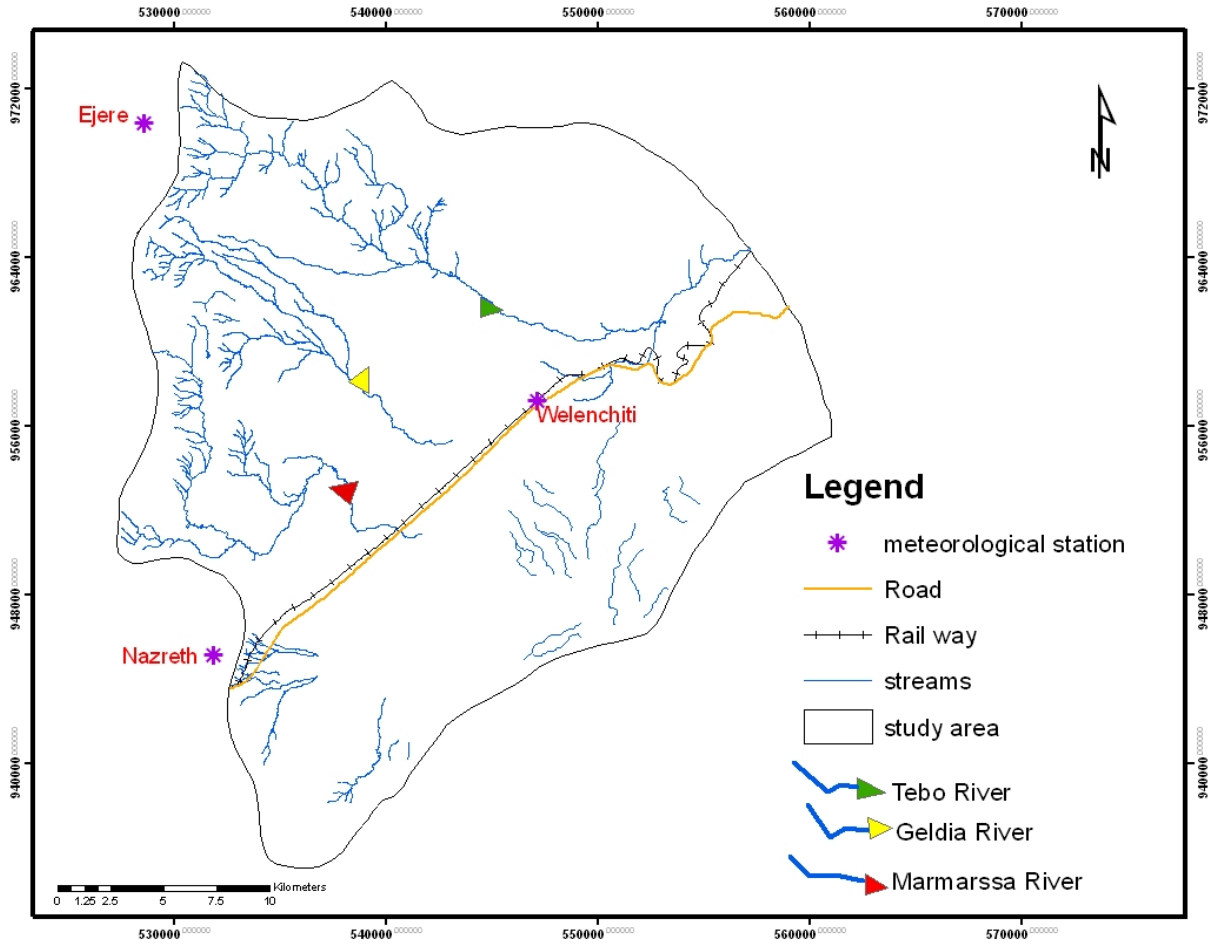


**Fig 2.3** Drainage map of the study area

## **CHAPTER THREE**

### **Geological setting**

#### **3.1 Regional geology**

In Ethiopia, the present morphology, physiographic, and geological setting are a result of two major post Paleozoic events which were followed by important phases of volcanic activity (Mohr, 1964). The first tectonic event which occurred in late Mesozoic and early Tertiary period produced the Afro Arabian and the associated fissure volcanic activities gave rise to the extrusion of the Trap series succession. The extrusion of the Trap series fissure basalts during Eocene-Oligocene time was the major and the largest volcanic episode on the south eastern and the western plateau of the country. Kazmin (1975). The second tectonic event resulted in rift development and related volcanic phenomenon during late Tertiary to quaternary period is the extensional tectonics which produced the Ethiopian Rift valley genetically related to the Rift valley of East Africa.

##### **3.1.1 Alaji Basalts**

A succession of up to 800m thick predominantly aphyric flood basalts rests unconformably on the eroded surface of the Mesozoic sediments. K-Ar age determinations place the basalts between 28 and 5 Ma (Kuntz et al. 1975; Morbidelli et al. 1975), suggesting correlation with the widespread Alaji Basalts of the Ethiopian plateau. Zanetti and Justin-Visentin (1973, 1974, 1975) and the Adole Basalts of Central eastern Afar (Barberi et al 1975).

### **3.1.2 Anchar Basalts**

Along the eastern margin of the Rift, Alaji basalts are conformably overlapped by a unit of flood basalts and siliceous rocks which is in turn partly covered with slightly unconformity by silicis of the Nazreth group. In the Anchar area the unit is represented by about 400m of basalts with general intercalation of ignimbrites, the one at the base being 12.4 Ma. To the south and north east, the basalts are laterally replaced by welded and unwelded ash flows.

### **3.1.3 Arba Gugu basalts**

This unit erupted from Arba Gugu Shield volcano and represented by successive lava flows up to 300m thick made up of mostly of porphyritic pyroxene or plagioclase basalts with an age of around 8.5 Ma.

### **3.1.4 Chilalo and badda Trachytes**

From the data obtained from Kuntz et al. (1975) two elliptical shield volcanoes on the eastern rift shoulder belong to numerous groups of trachyte volcanoes developed in the upper Pliocene on both sides of the rift. Chilalo volcano first erupted followed by trachytes while Badda evolved from basalts and trachy basalts to Trachytes. Lava flows of both volcanoes are contemporaneous with the young ignimbrites of Nazareth group and partly inter finger with them. The formation of these shield volcanoes coincide with the important stage of rifting around 4 to 4.5 Ma. This rifting is supposed to correspond to the peak of the silicic volcanism in the rift (Morbidegli et al 1975) and preceded of the fissure erupted Bofa Basalt.

### **3.1.5 Post-Ashangi Group volcanic**

This sequence includes Nazareth and wonji Group that is composed of a range of igneous rocks of different ages and occurrences.

### **3.1.5.1 Nazareth Group**

The group is composed of a thick succession of ignimbrite, unwelded tuffs, ash flows, rhyolites and Trachytes forming the larger part of the rift floor and also outcrop in the rift escarpments and on the adjacent plateau margins. In the rift, the group attains thickness up to 250m and possibly more, while on the rift shoulders only a few meters of ignimbrites are generally observed. According to Morbidelli and Piccirillo (1975); Brotzu et al (1974), the ignimbrites of the rift floor were fissure eruptions. However, the silicic centers such as Gara Gumbi (Gara Gumbi rhyolites) were active in the period between 7 and 5.5 Ma. (Christiansen et al. 1975) so that central type explosive eruptions played a significant part in the formation of the Nazareth volcanics. Silicic centers were especially abundant during the latest stages of the Nazareth volcanism, as is evident from the wide distribution of rhyolitic domes cutting through older ignimbrite sheets (Older Alkaline and Peralkaline Rhyolite domes).

The lowermost ignimbritic flows of the Nazareth Group intercalated with the Chorora sediments are 9.5 Ma. (Kuntz et al. 1975). An upper age limit of the group is older than 2.5 Ma. Possibly 3 to 3.5 Ma coincides with the age of the overlying Bofa basalts. Numerous K-Ar determinations on the Nazareth silicics (Morbidelli et al. 1975; Mohr 1974) fall between 7 to 6 and 1.5 Ma with maximum between 5.5 and 3.5 Ma. According to Kazmin (1978) its age is around 2 to 1.5 Ma long. The time of formation of the Nazareth group is between 9.5 and 3 to 4 Ma, which is close to the age established by Zanettin and Justinvisentin (1974) for the Balchi rhyolite.

Accumulation of the Nazareth Group was accompanied by formation of the shield volcanoes on the rift's eastern shoulder. The Arba Gugu shield volcano is synchronous with the early stages of the Nazareth volcanism. Chilalo and Badda volcanoes were formed during later stages.

### **3.1.5.2 Bofa Basalts**

In the rift the silicics of the Nazareth Group are overlapped by a unit of fissure flood basalts, which was named after its type locality in Bofa village. In the Awash Gorge near Kerayu Lodge, the lower part of the Bofa Basalts is dated as 2.5Ma and they are overlapped by ignimbrites 1.5 Ma. The Bofa Basalts include much older flows for example an age of 3.5Ma was established by Mohr (1971) for basalts in the Nazareth vicinity which possibly belong to the same unit. The Bofa Basalts are not restricted to the central part of the rift as younger units, but are rather evenly distributed over the rift floor. They represent an episode of fissure eruption, which immediately followed a major faulting episode.

### **3.1.5.3 Wonji Group**

As pointed out by many authors (Mohr 1967) and others; Meyer et al. 1975; Gibson 1970; Dankin and Gibson 1971) the latest volcanism in the Ethiopian Rift is related to its axial extensional zone, the Wonji Fault Belt. Although some volcanic manifestations such as eruptions of basalts and central volcanoes occur outside the belt this tectonic feature undoubtedly controls the bulk of the Pleistocene-Recent volcanism. According to Kazmin and Seifemichael Berhe (1978), the Wonji Group includes all rift volcanics formed after the last major episode of rift faulting which followed accumulation of the basalts. As observations in the Arba valley north of Abomsa village show the oldest volcanic of the Wonji Group, the Dino ignimbrites overlap strongly faulted Bofa Basalts, but are not themselves affected by this faulting.

The following major units comprise the wonji Group:

- Dino ignimbrites
- Pantelleritic Volcano Centers
- Sub-Recent and Recent fissure basalts

#### **3.1.5.4 Lacustrine sediments**

The lacustrine deposits are purely lake or swamp deposits or those of volcano-lacustrine type of the rift valley. The lacustrine sediments consisting of clay, silt, tuffs, travertine, and diatomites with intercalation of pumices are widely distributed. They are Pleistocene to Holocene in age and they are deposited from extensive lakes during the Pleistocene pluvial. In Nazareth, Welenchiti, Wonji and koka the thickness of the lacustrine sediments varies from 30 to 40 meters.

#### **3.1.5.5 Alluvial deposits**

The alluvial deposits are of two types: those spread out in alluvial plains and those strips along rivers and streams. Alluvial plains are filled up gravens and large stretches of flat land in the rift valley and long the whole length of the western border of the country. These are troughs in the lowland where during the pluvial period streams deposited large amounts of sediments carried down from the highlands. The thin strips of alluvium along streams occur in most places both in the highlands and the lowlands. The alluvial sediments occur in Metehara and Abadir area in the rift proper. Their grain size ranges from silt to gravel.

## **3.2 Geology of the study area**

### **3.2.1 Ash flow tuffs, pantelleritic ignimbrites and unwelded tuffs**

This unit covers wide area of the escarpment and adjacent plateau surrounding the lacustrine sediments in the northern and western sides. Central type explosive eruptions played a significant part in the formation of the Nazareth volcanic.

The west part of the study area near to Nazareth, the unit consists of strongly welded coarse-grained, green ignimbrite characterized by vitrophyric fiamme and lithic fragments interleaved with aphyric flood basalts and paleosols (Alula Damte, 1982).

While in the south of Nazareth town the unwelded ignimbrite units interbedded with paleosols, are characterized by fine-grained, brown-pink matrix containing small pumice clasts and few lithic fragments. This unit is principally made up of thick rhyolite lava flow at a base and top thick pumice fall deposits. The pumice fall deposit is constituted by fine depleted, coarse, angular pumice clasts, and lithic bearing ignimbrite set in a glassy matrix (Alula, Damte 1980)

On the upper part of the escarpment in Wake Tiyo area, a massive, finely crystalline having thin horizontal layer probably travertine is found along the exposed lithology. On the valleys of the escarpment units are, relatively medium grained of poorly welded per alkaline pantelleritic pyroclastic flows with sparse intercalated ashflows tuffs and basaltic lava flows. Texturally the ignimbrite layer shows variation from bottom to top. The bottom top portions is less welded with relatively lithic fragments. While middle portion on the other hand is densely welded and characterized by lenses of fiamme and lithic fragments composed of alkali feldspar, quartz, hornblende and pyroxene.

This unit is found on the north western on the Boru Teru Mt and north eastern of the study area. This unit is made up of pantelliritic lava flows and domes with layers of some times pumice fall, plagioclase–Porphyry pantelleritic lava domes with associated obsidian layers, phyolitic and trachytic lava domes associated with lava flows. However, in the field it was difficult to distinguish clear Stratigraphic relation with respect to the surrounding rock units.

### **3.2.3 Bofa basalts**

This unit is found on the southern tip and on the eastern across the main road of the study area. Bofa basalts represent an episode of fissure eruption that immediately followed a major faulting episode (kazmin and Siefemichael Berhe). The assemblages of the unit are mainly olivine, clino pyroxen, apatite and rare plagioclase–rich basaltic andesites (Gezahagn yirgu, 1980). Plagioclase basalts with subordinate fine-grained and scoraceous varaites represent the predominant types of lava flows. Bofa basalts in the southern part of the study area is Plagioclase phorphyry basalts rich in phenocrysts of plagioclase set in an interstitial ground mass containing plagioclase clinopyroxene (augite), olivine and opaque minerals (Alula Damite, 1982). The Bofa basalts, which are south west of wolenchiti, are low viscous flood basalts minor covered by pumice.

### **3.2.4 Pleistocene – Subrecent basalts**

This unit is found in the southern and south eastern of the study area. Basalts in the eastern part occur as black to grey some times brownish, dense to porous rock formed from low viscosity basalts while most basalts towards the southern part are highly viscous. And the scoraceous basalts occur in the area are high vesicular basaltic fall out bounded on basaltic sinters and scoria cones. It is reddish-brown to reddish-grey and fragments often show an internal flow structure.

The scoria cones with associated basaltic flows erupted by number of emission centers are probably related to tensional tectonism of recent wonji fault episode.

The scoria cones formed from fall out deposits, with dominant phenocrysts of olivine are scattered in the unit. Well-stratified scoria units and pyroclastic bombs are common rock types found near the vents. They are coarse in texture and reddish in colour.

### **3.2.5 Alkali and peralkali Rhyolites, trachytes domes and flows**

#### **of Boseti**

This unit covers Guda Mt. (2447m) and Bariccia Mt. (2132m) mountains extending upto the lacustrine sediments on the plain.

Three important volcanic events, which created Guda and Bariccia volcanoes, may be distinguished as:

- Highly explosive activity responsible for the formation of the two Volcanoes structurally linked by an open fissure.
- Formation of a caldera,
- A cycle of post- calderic activity, mainly of an effusive nature (BROTZU et al)

The huge eruption was followed by lava domes and flows particularly trachytes evolved from alkali basalts which are found towards the south east of Guda. Alkali and Peralkaline rhyolites: pantelleritic on the bottom of Guda and comenditic on the bottom of Bariccia are found.

The peralkaline rhyolite domes found in the south east of welenchiti town (Fig.3.1) can easily be identified by its flanks formed from high viscosity of lava. The most commonly occurring minerals are alkali feldspars, quartz, clino pyroxene and biotite.

Acidic volcanic glass (obsidian) marks one of the youngest volcanic products of Boseti and occurs mainly as flows and domes on the top and on the face of Guda. IT is massive and dense or finely vesicular having a porphyric texture.



**Fig 3.1** Rhyolite domes in northeast of Boseti Mt.

### **3.2.6 Lacustrine sediments**

This unit covers the central part of the study area. The lacustrine sediments are composed of clay, sand, gravel and underlain by weathered basalts and ignimbrites of the Nazareth group. The major components of the sediments are of volcanic origin, such as pumice, volcanic ashflow, rhyolite and basaltic rock fragments. The lacustrine beds are interbedded with Pliocene – Pleistocene ignimbrites on the rift shoulders (Mohr, 1966). The sub aqueous pyroclastic deposits can be distinguished by reverse graded bedding of the pumice layers. Rounded rock fragments reflecting abrasion during transportation by the rivers and waves of the lakes. Poor consolidation, fine lamination of the recent lake sediments, presence of evaporite deposits and micro-organic deposits (diatomites) can distinguish sub aqueous pyroclastic materials from reworked deposits. The diatomite bearing lacustrine sediments are exposed along the

gorge of Tebo River. Between Nazreth and welenchiti the unit is yellow to grey, fine sandy to silty sediments. Towards the SW of welenchiti town close to Mt. Guda, pumice deposits from pyroclastic fall out most possibly from the main vent of Boseti volcano, is clearly visible (Fig-3.2) along the dissection of small seasonal rivers.

Depending on the level of alteration, the pumice deposit is grey to yellow and highly vesicular from minor millimeters to more than 2cm, may be deposited and transported during the formation of Boseti then retransported and redeposited later.

### **3.2.7 Recent to subrecent Rhyolite domes and flows**

Large part of this unit is found bounded within two adjacent parallel faults and sparsely outcropped intercalating with lacustrine sediment and wonji group sub recent basalts. This unit is compact porphyritic phylitic lava flow described as the remnant wall of the volcano tectonic sub circular collapse of the pleistocene volcanics. Berehane et al, 1978.



**Fig 3.2** pumice intercalated with clay

### **3.2.8 Recent aphyric basalts**

This is one of the youngest rock units of wonji group found in the south of the study area and in between Guda Mt and Bariccia Mt. This unit resulted from fissure eruption and is highly vesicular with coarse texture. This unit consists mainly of alkali to olivine basaltic lava flows vary from strongly porphyritic to aphyric, with dominant phenocrysts of olivine. Between the tops of Guda and Bariccia, different small cones and domes exist along the trend of the main fault consists of very recent basalts.

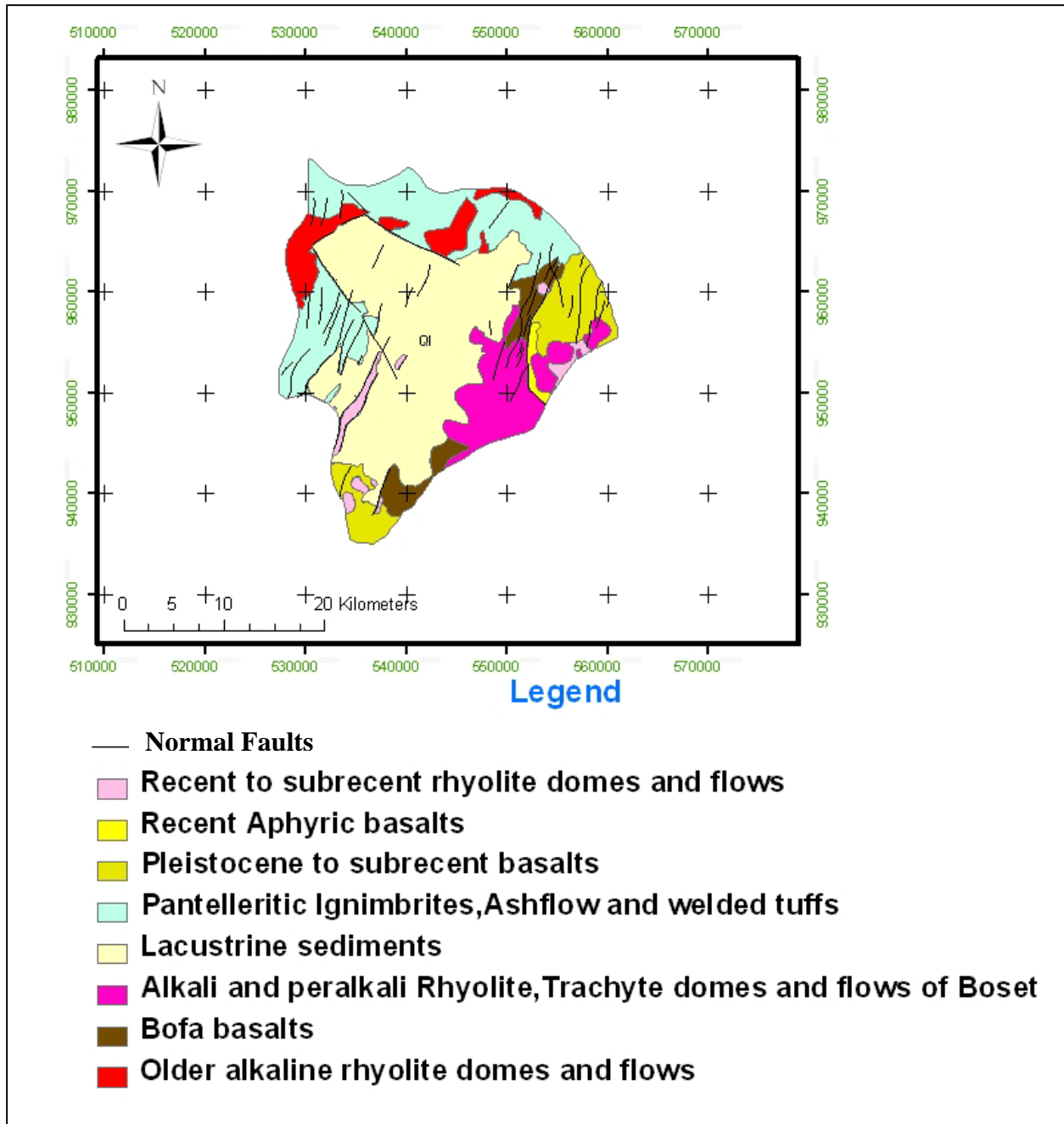


**Fig 3.3** Geological map of the study Area (modified from Geological map of Nazreth EIGS, 1978)

### 3.3 Tectonics

The study area is affected with tectonic structures. Normal faults, fracture zones, volcanic domes and flows are dominantly found.

In the study area there are three major faults. One strike NNE-SSW to the west and east of the area and sub-parallel faults west of welenchiti confines the lacustrine sediment in both sides striking NNW-SSE direction. The lacustrine sediments are also bounded to the north by minor faults striking NE-SW direction across the major NNW-SSE faults. The graven covered with lacustrine sediments is dissected by several NNE-SSW striking faults in to blocks between 100 and 700m in width. The throws of the faults range up to about 50m.

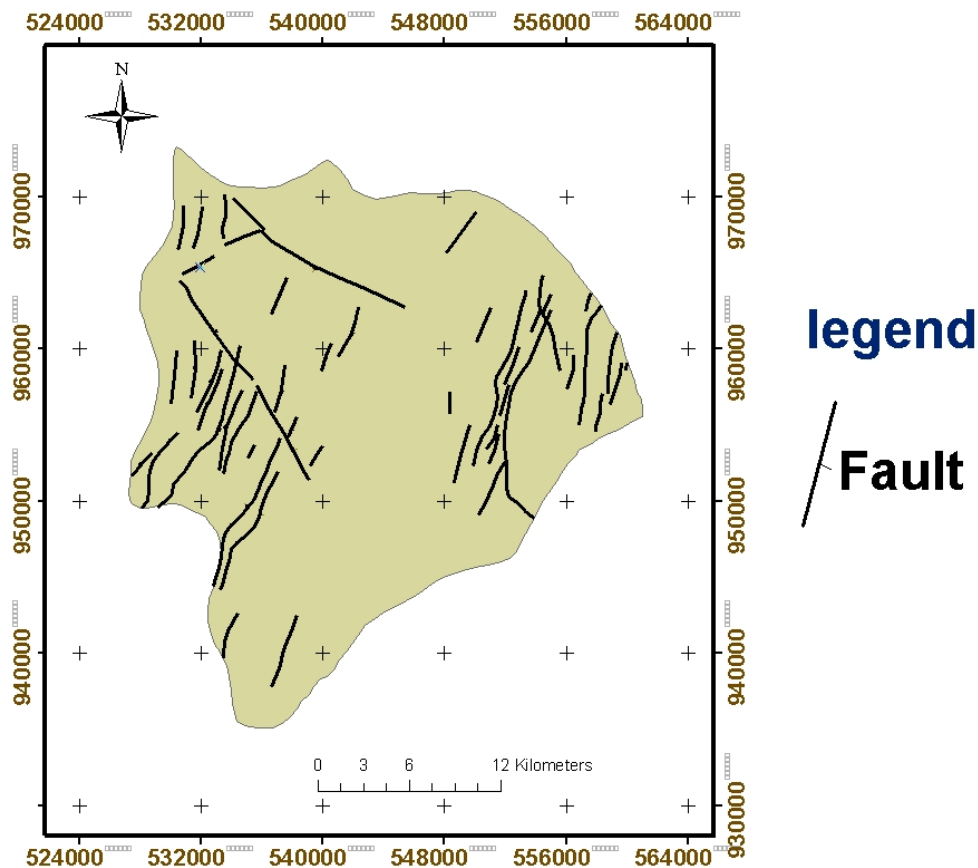


**Fig.3.4** Structural map of the Study Area

## CHAPTER FOUR

### Hydrometeorology

#### 4.1 Climate

Using the data obtained from National Meteorological Services Agency (NMSA), various climatological parameters of the study area have been summarized below.

##### 4.1.1 Temperature

Mean monthly temperature was computed as the arithmetic average of 20 years (1985-2004) from Nazreth station. The study area has an average temperature of 21.1<sup>0</sup>c with mean monthly minimum temperatures of 14.3<sup>0</sup>c and mean monthly maximum temperature 27.8<sup>0</sup>c. Maximum temperature values were recorded in the months of May and June while minimum temperature record was obtained in the month of December.

**Table 4.1** Mean monthly minimum, maximum and average air temperature at Nazreth station.

	Jan	Feb.	Mar.	Apr.	May	June	July	Aug	Sept.	Oct.	Nov	Dec
Max. T(o <sub>c</sub> )	27.2	29	29.6	29.8	31	29.9	26.1	25.8	27.2	27.6	26	27
Min. T(o <sub>c</sub> )	12.4	14.4	14	15	15.8	16.8	15.3	15.5	14.8	12.5	12	12
Mea n(o <sub>c</sub> )	19.8	21.7	21.8	22.4	23.4	23.4	20.7	20.6	21	20	19	19

Max. T (o<sub>c</sub>) = mean monthly maximum Temperature of the study area

Min. T (o<sub>c</sub>) = mean monthly minimum temperature

Mean. T (o<sub>c</sub>) = mean monthly temperature of the study area

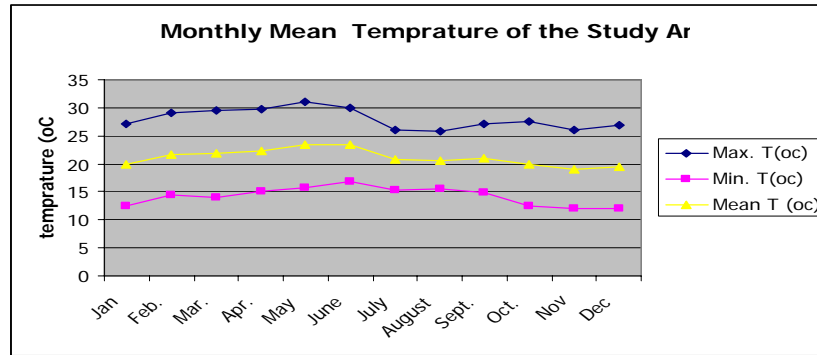


**Fig 4.1** Mean monthly temperature in (°C) at Nazreth station.

#### 4.1.2 Wind speed

Presence of atmospheric turbulence can greatly increase the rate of evaporation by removing vapor from evaporating surface and giving space for fresh air capable of holding additional vapor in the atmosphere.

A station located in Nazreth town has records of wind speed at 2m above the ground surface.

The mean monthly wind speed of the area varies from 1.7m/s to 3.3 m/s with average value of 2.8 m/s and maximum values observed in the months of December and January and minimum values were observed in the months of September.

**Table 4.2** Mean Monthly Wind speed (m/s) at Nazreth station.

Jan	Feb	Mar	Apr	May	Jun	July	Aug	Sep	Oct	Nov	Dec
2.8	2.6	2.4	2.5	2.4	2.6	2.7	2.6	1.7	2.6	2.7	3

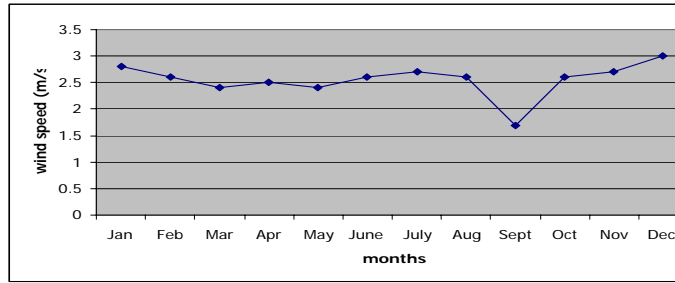


**Fig 4.2** Mean Monthly wind speed (m/s)

**4.1.3 Sunshine hours**

Since the evaporation requires continuous supply of energy, which is derived mainly from solar radiation, the radiation will be a factor of considerable importance.

The area consists of one sunshine hour recording station at Nazreth. The area has mean monthly sunshine hour value of 8.4.

**Table 4.3** Mean monthly sunshine hours

Station	Recording period	Jan	Feb	Mar	Apr	May	Jun	Jul	Aug	Se	Oct	Nov	Dec
Nazret	1992-2005	9.1	8.8	8.3	8.3	9	8.6	6.6	7.3	7.5	8.8	9.8	8.7

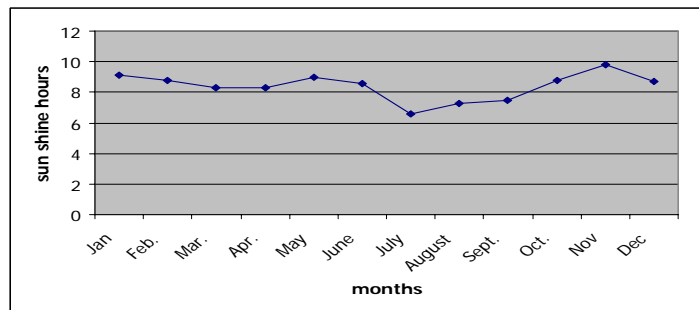


**Fig 4.3** Mean monthly sunshine hour

#### 4.1.4 Relative humidity

Relative humidity is the relative measure the amount of moisture in the air to the amount needed to saturate the air at the same temperature. The relative humidity of the air is largely dependent on temperature and rainfall. For the data ranging from 1990-2004, Mean monthly relative humidity is calculated to be 47.8 where maximum value was observed in the months of July and August and minimum value during May.

**Table 4.4** Mean monthly Relative humidity (%) at Nazreth station.

Months	Jan	Feb	Mar	Apr	May	June	Jul	Aug	Sept	Oct	Nov	Dec
MeanRelative Humidity (%)	44	41	46	44	40	46	61	63	58	48	42	41

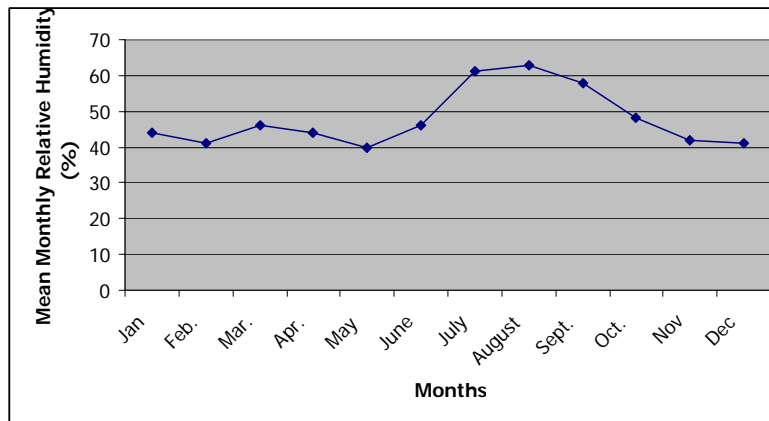


**Fig.4.4** Mean monthly relative humidity (%)

## 4.2 Precipitation

The seasonal distribution of rainfall over the country is governed by the position of Inter Tropical Convergence zone. During its movement to the north and south of the equator, the ITCZ passes over Ethiopia twice a year and this migration causes the onset and withdrawal of winds from north and south. The ITCZ represents a low-pressure area of convergence between dry tropical Easterlies and moist Equatorial westerly along which equatorial wave disturbance takes place. When the ITCZ is located north of Ethiopia, the northeasterly winds from southwest reach to most parts of Ethiopia. During this time the trade winds from the north retreat. When the ITCZ is located in the south, the trade winds from north drifts the equatorial winds. This periodical anomaly of winds causes seasonal rainfall variability.

The summer rains or keremt rains occur when the ITCZ is found north of the country. During this period the whole country is under the influence of equatorial westerlies from South Atlantic Ocean and southerly wind from the India Ocean. When the ITCZ moves to the south, the country will be under the influence of continental air currents from north and northeast. These winds originate from north Africa and north easterly trade winds traversing Arabia, dominate the region (march, April, may) and the ITCZ lies in the southern part and a strong cyclonic cell (low pressure aerial develops over Sudan. Winds from the Gulf of Aden and Indian oceanic (anticyclone) blow across central and southern Ethiopia and form the relatively belg rains.

The study area is located in the eastern part of the country experience bi modal rainfall distribution. These are belg rains (march to may) and kiremt rains (June to September). Mean annual rainfall gradually decreases to wards the north east and east (Tenalem Ayenew and Tamiru Alemayehu, 2001). According to the data obtained from National meteorology service agency (NMSA), the area obtains the highest rainfall in the months of July and August. This can easily be shown on the mean monthly rainfall in millimeters for the area over a time of 20 years.

Arial depth of rainfall of the area was calculated using three approaches:

**A)** Arithmetic mean average method **B)** Thiessen polygon method **C)** Isohytal method

**a) Arithmetic mean**

It was computed as the arithmetic mean of the amounts measured by the three gauges with in and outside the area.

Arithmetic mean computed using these three gauges gives a value of **877 mm** of rainfall.

Since the study area includes escarpment from highland to the floor of rift valley and widely spaced gauges, the value obtained by this method is unreliable.

**Table 4.5** Location and mean annual RF of the meteorology stations

Staions	UTME	UTMN	Elevation (m)	Mean Annual Rainfall (mm)
Wellenchiti	547118.16	957213.37	1551	875
Nazreth	531846.41	945223.16	1650	850
Ejere	528627.99	970465.71	2100	905

**b) Thiessen polygon method**

This method considers random nature of topography and distribution of stations. As a result good rainfall depth values are expected when the rain gauges not evenly distributed over the area in both flat and hilly terrains. The method assumes that the recorded rainfall in a gauge is representative for the area half way to the adjacent gauges. The method involves the connection of the stations on the map by lines and drawing the perpendicular bisector of the lines

joining the adjacent stations. And the observed precipitation ( $P_i$ ) is weighted according to the area ( $a_i$ ) of the polygon associated with it. Three stations, one with in and two out of the study area are used.

Using this calculation, areal rainfall depth of the study area is equal to **874mm**. The table used to compute the average rainfall depth using Thiessen polygon is given in Table 4.6.

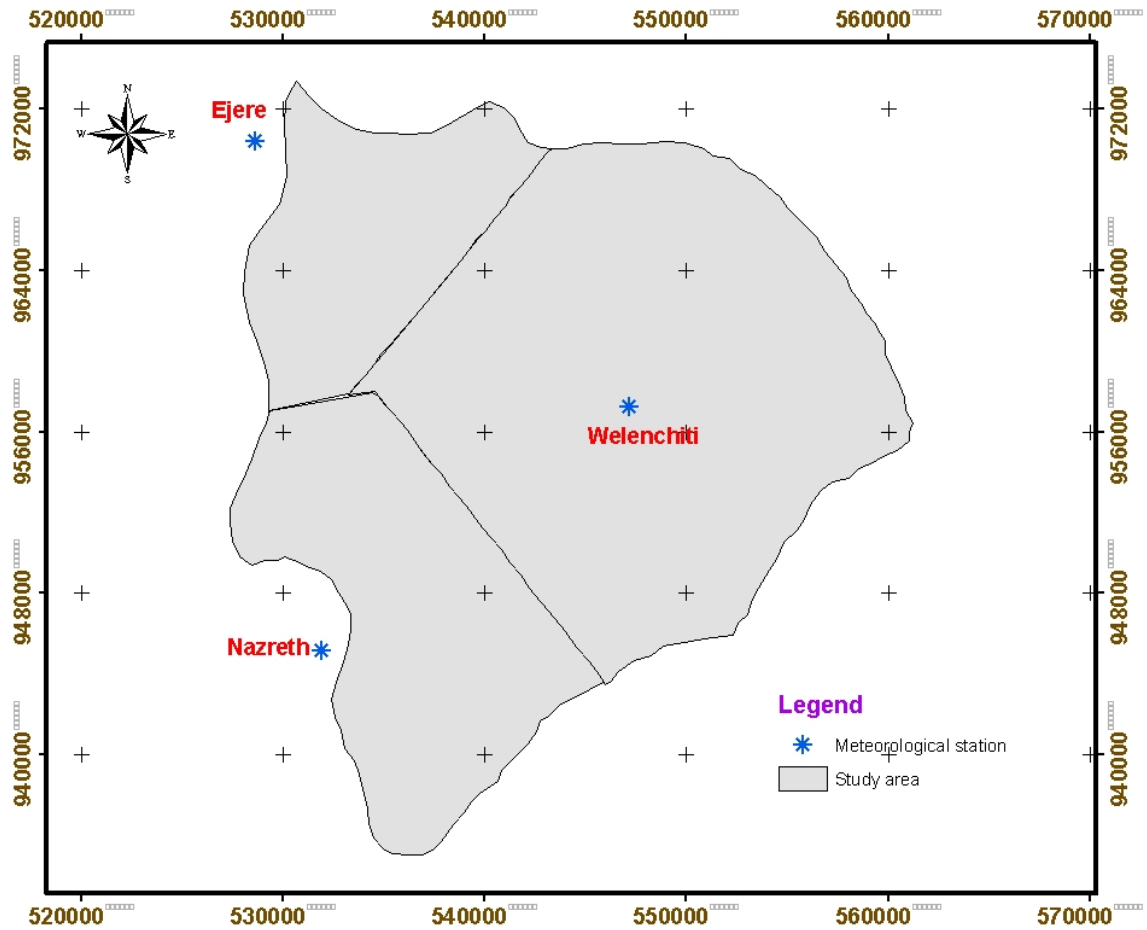


**Fig4.5 Thiessen polygon of the study area**

**Table 4.6** Annual weighted rainfall depth using Thiessen polygon

Meteorological station	Area of influence (Km <sup>2</sup> )	Mean RF (mm)	Weighted area %	Weighted RF (mm)
Ejere	135km <sup>2</sup>	905	17.31	156.67
Nazreth	217km <sup>2</sup>	850	27.82	237.33
Welenchiti	428km <sup>2</sup>	875	54.87	480.00
Total	780		100%	<b>874</b>

**Table 4.7** Monthly mean rainfall depth using Thiessen polygon

Station	Area	Jan	Feb	Mar	Apr	May	Jun	Jul	Aug	Sep	Oct	Nov	Dec
Nazreth	217	11.5	30.7	51.9	60	48	56	230	210	101	34.8	8.1	8
Wele nchiti	428	17.2	54.2	85.6	80	32.6	58.7	195	210	86	40.3	7.2	9.2
Ejere	135	17.5	35.3	44.5	46.5	56.3	78.7	230	253	99.6	29.2	7.4	7.7
Total	780	15.66	44.39	69.1	68.6	40.9	61.4	210.3	217.4	92.5	36	2	25

### c) Isohytal method

Contours of equal precipitation (isohytes) are drawn for the area. The area between successive isohytes is calculated and multiplied by the average rainfall on that area. The average rainfall is the average value of the two adjacent isohytes. The advantage of this method for determining averages is that it allows the influence of physiographic parameters to be taken into account. These factors include elevation, slope and exposure to rain bearing winds (shaw, 1988)

$$Pa = \frac{p_{12}a_{12} + p_{23}a_{23} + \dots + P_{n-1,n}a_{n-1,n}}{A_T}$$

Where  $P_{12}$  - Rainfall depth between 1 and 2  
 $a_{12}$  - Area enclosed by successive 1 and 2  
 $A_T$  - total Area

Based on this calculation, mean annual precipitation of the study area has been obtained **874.5 mm**

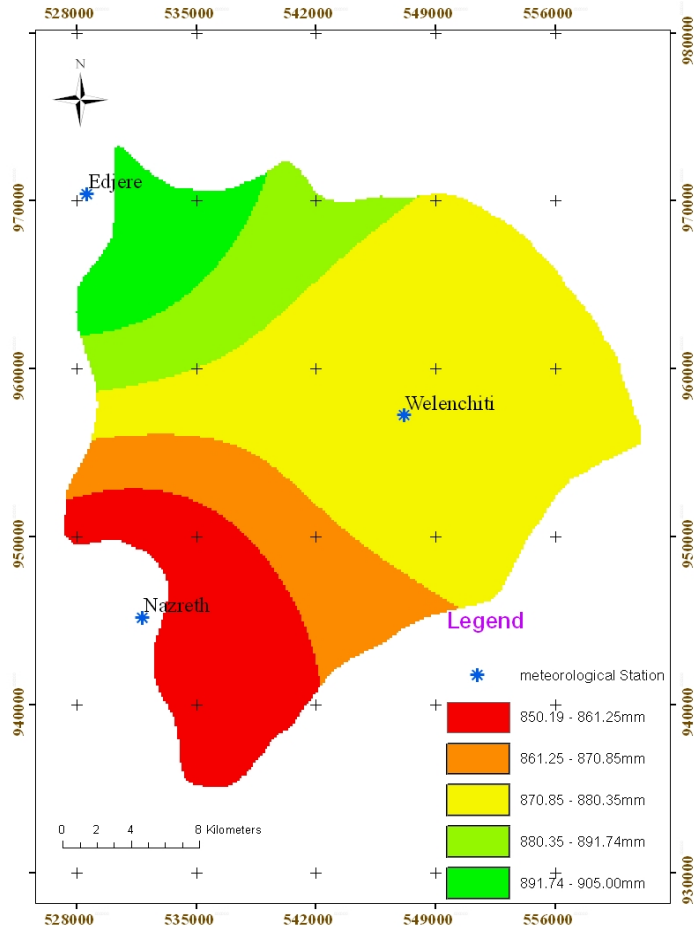


**Fig. 4.6** Isohytal Map of the study area

**Table 4.8** Mean annual rainfall using Isohytal method

Isohyte (mm)	Average	Net Area (km <sup>2</sup> )	Percent of the area (%)	Weighted precipitation(mm)
850.2-861.25	863.25	86	11.02	94.96
862.25-870.86	866.56	106	13.6	117.85
870.86-880.35	875.60	450	57.7	504.87
880.35-891.74	886.04	86	11.02	97.46
891.74-905	898.37	52	6.6	59.29
Total		780	100	<b>874.5</b>

### 4.3 Potential Evapotranspiration

Potential evapotranspiration is the water loss if at no time there is a deficit of water in the soil for the use of vegetation (Thornthwaite, 1944). Several methods have been developed to estimate potential evapotranspiration such as using pan evapotranspiration upto empirical formulas. Due to lack of pan evaporation data, empirical formulas that use different meteorological data are used to calculate potential evapotranspiration.

#### a) Thornthwaite method

Thornthwaite method is based upon the assumption that Potential evapotranspiration is dependent only on meteorological conditions and ignores the effect of vegetation density and maturity. The only necessary factors to calculate potential evapotranspiration using these methods are mean monthly air temperature (T), Latitude and month (Thornthwaite and mather 1955, 1957). The last two factors yield average monthly sunlight.

PET<sub>m</sub>, calculated on a monthly basis is given by:

$$\mathbf{PET_m = 16N_m (10t/I)^a}$$

Where:

M: months

N<sub>m</sub>: is monthly adjustment factor depending on latitude and season

t: mean monthly temperature

I: annual heat index obtained by adding monthly heat index (i<sub>m</sub>)  
of 12 months.

$$i_m = (t/5)^{1.514}$$

$$a = 6.75 \times 10^{-7} I^3 - 7.71 \times 10^{-5} I^2 + 1.8 \times 10^{-2} I + 0.49$$

$$I = 106$$

$$a = 2.32$$

Potential evapotranspiration of the study area using this method is **655.4mm/year.**

**Table 4.9** Mean annual PET obtained from Thornthwaite method

Par.	Jan	Feb.	Mar.	Apr.	May	June	July	Aug	Sept.	Oct.	Nov	Dec
$T_m(^{\circ}C)$	19.8	21.7	21.8	22.4	23.4	23.4	20.7	20.6	21	20	19	19.5
n	9.1	8.8	8.3	8.3	9	8.6	6.6	7.3	7.5	8.8	9.8	8.7
N	11.6	11.8	12	12.3	12.6	13	12.6	12.4	12.1	12	12	11.5
$N_m$	0.78	0.75	0.69	0.67	0.72	0.66	0.52	0.6	0.62	0.73	0.8	0.76
$i_m$	8	9.2	9.3	9.7	10.3	10.3	8.6	8.5	8.7	8.2	7.5	7.8
$PET_m$	53.2	63.3	58.8	58.1	72.4	66.3	39.3	44.9	48.5	51	49.6	50

## b) Penman method or combination method

The most general and widely used equation for calculating PET is the penman equation. The penman monteith variation is recommended by the Food and Agriculture Organization. This equation uses climatic data such as vapor pressure, sunshine hours, net radiation, wind speed and mean temperature. The basic equation of penman to calculate potential evapotranspiration,  $PET_m$  is

$$PET_m = \frac{(\Delta/\gamma)H_T + E_{at}}{\Delta/\gamma + 1}$$

The procedures followed during calculation for the data presented in (table 4.9) are given below

$H_T$  is the available heat and is calculated from the formula given by;

$$H_T = R_I (1-r) - R_0,$$

Where  $r$  is the average albedo of the area based on land cover type. In our case  $r=0.24$  and  $R_I$  and  $R_0$  are incoming and out going radiation respectively and their empirical formulas take the form:

$$R_I (1-r) = 0.76 R_a f_a (n/N)$$

$R_I$  is a function of  $R_a$ , the solar radiation (fixed by latitude and season) modulated by a function of the ratio,  $n/N$ , of measured to maximum possible sunshine duration. And “ $n$ ” is bright sunshine hours over the same period.

Since the study area is located south of  $(54 \frac{1}{2})^0N$  ( $10^0N$ ),

$f_a (n/N)$  is calculated as:

$$f_a(n/N) = (0.16+0.62 n/N).$$

The empirical formula of the out going radiation takes the formula,

$$R_0 = ET^4 (0.47-0.75ed \frac{1}{2}) (0.17+0.83n/N)$$

Where:  $T^4$  is the theoretical black body radiation at  $T_a$ , which is then modified by functions of the humidity of the air ( $ed$ ) and the cloudness ( $n/N$ ).

Temperature in  $^{\circ}k$  is converted result of temperature in  $^{\circ}c$ .

The parameters  $e_a$  saturated vapor pressure at air temperature.

$T_a$  is obtained from standard table of air temperature and saturation as:

$$e_a(T_a) = 6.11 \exp (17.3 T_a / T_a + 273.3)$$

Relative humidity (RH) in % used to calculate the value of actual Vapor pressure(  $e_d$ ) as :

$$e_d = e_a \text{ RH}\%$$

Wind speed ( $u_2$ ) in m/s was converted to mile/ day

The energy for evaporation  $E_{at}$  is given by

$$E_{at} = 0.35 (0.5 + u_2 / 100) (e_a - e_d)$$

The value  $\Delta/\gamma$  is found from weighing factor  $\Delta/\gamma$  versus temperature from (FAO, 1967) given in (E.M Shaw, 1996) where  $\Delta$  is the slope of saturated vapor pressure versus temperature and  $\gamma$  is the hydrometric constant with a value of 0.4859 mm Hg °C RAMI, 1996

PET was calculated using this formula and accordingly a potential evapotranspiration of **1481mm/year** found over the area.

#### 4.4 Actual evapotranspiration

Actual evapotranspiration is the amount of evapotranspiration that occurs under field conditions (Fetter, 1988). This actual evapotranspiration is one of the components that are vital in calculating the water balance of the area. Since large part of the study area is located in the warm rift system, high actual evapotranspiration is expected. The methods by which AET is calculated are:

##### 4.4.1 Empirical formula

###### a) Formula developed by Turc (1954, 1955)

Where:  $p$  = mean annual precipitation (mm)

$$I = 300 + 25T + 0.05T^3$$

$T$  = mean temperature (°C)

Actual evapotranspiration of the study area using this method is equal to **697** mm/year.

**Table 4.10** Mean annual PET obtained from Penman method

Parameters	Jan	Feb.	Mar.	Apr.	May	June	July	Aug	Sept.	Oct.	Nov	Dec
Temprature	19.7	21.7	21.8	22.4	23.4	23.4	20.7	20.6	21	20	19	19.5
Sunshine hours (n)	9.1	8.8	8.3	8.3	9	8.6	6.6	7.3	7.5	8.8	9.8	8.7
Wind speed (miles/day)	150	140	129	135	129	140	145	140	91	140	145	162
N	11.6	11.8	12	12.3	12.6	13	12.6	12.4	12.1	12	12	11.5
n/N	0.78	0.75	0.69	0.64	0.42	0.66	0.52	0.6	0.62	0.73	0.8	0.76
Ra	12.8	13.9	14.8	15.2	15	14.8	14.9	15	14.8	14.2	13. 1	12.5
e <sub>a</sub> (mm Mg)	17.01	19.1	19.2	21	22.1	22.1	18.2	18.16	18.68	17.53	16. 47	16.97
e <sub>d</sub>	7.5	7.8	8.8	9.2	8.8	10.2	11.1	11.47	11.83	8.41	6.9 2	6.93
e <sub>a</sub> -e <sub>d</sub>	9.5	11.3	10.4	11.8	13.3	11.9	7.1	6.72	6.9	9.12	9.5 5	10.03
ET <sup>a</sup> <sub>a</sub> (mm/d)	14.75	15.17	15.18	15.28	15.5	15.5	15.13	15.12	15	14.8	14. 6	14.7
R <sub>1</sub> (1-r) (mm/day)	6.26	6.6	6.61	6.43	6.9	6.4	5.5	6.04	6.12	6.6	6.5 3	6
R <sub>0</sub> (mm/day)	3.2	3.13	2.8	2.59	2.94	2.56	1.99	2.18	2.44	2.9	3.1	3.2
H = R(1-r)-R <sub>0</sub>	3.01	3.47	3.8	3.84	3.96	3.84	3.5	3.86	3.68	3.7	3.4 3	2.8
$\Delta / \gamma$	2.2	2.39	2.39	2.5	2.62	2.62	2.33	2.32	2.36	2.23	2.1 1	2.17
E <sub>at</sub>	7.2	8.38	7	7.4	8.3	8.8	5.25	4.5	3.4	5.39	6.9	7.44
PET (mm/day)	4	4.4	4.2	4.4	4.5	4.5	3.8	3.7	3.2	3.8	4.1	4.2
PET (mm/month)	124	123.2	130.3	132	140	135	117.7	114.7	96	117.8	123	130.5

**4.4.2) Thornthwaite method (water balance method)**

This method calculates actual evapotranspiration using precipitation and soil moisture deficit values. Always actual evapotranspiration is less or equal to potential evapotranspiration. When the soil is saturated, it will hold no more water. In this condition, actual evapotranspiration is equal to potential evapotranspiration (shaw, 1988). Given the fact that the values of soil moisture deficit and actual evapotranspiration vary with soil type and vegetation, during times when there is no rain to replenish the water supply, the soil moisture gradually becomes, depleted by the demand of vegetation to produce a soil moisture deficit. As a result the actual evapotranspiration becomes less than the potential evapotranspiration. To evaluate actual evapotranspiration over an area, the proportions of different types of vegetation covering the area must be known. The main components that basically influence the water balance is presented in the following way;

Since the value of annual rainfall depth calculated using Thiessen polygon and Isohyte methods is almost similar, the monthly precipitation (p) values obtained from Thiessen polygon method presented in raw 1 of each table.

The mean evapotranspiration calculated using penman is listed in raw 2. Changes in the balance of the precipitation and meteorological demand of each month is computed and presented in raw 3, following the computation, the accumulated potential water loss, which is obtained by adding meteorological demands(the negative values (P-PET)of consecutive months are listed in raw4.

The available water capacity of soil for three different land uses is obtained from a table developed by Thornwaite and Mather, 1957.

The tables give for moderately deep-rooted crops grown on a clay loam soil having a rooting depth of 0.8m with available water capacity of 200mm, for deep-rooted shrubs having a rooting depth of 1m with available water

capacity of 150mm and for a matured forest having a rooting depth of 2.5m with available water capacity of 250mm.

Using the graph, water retained in the soil against an accumulated potential water loss, and the available water capacity for the soil, the amount of water that will be retained by the soil (soil moisture, SM) for each month is calculated and listed in row 5.

If  $P_m > PET_m$  the value of soil moisture at the end of that month  $S_m$  is given as:

$$S_m = S_{m-1} \exp\left[-\frac{PET_m - P_m}{S_{max}}\right]$$

If for a given month  $P_m < PET_m$ : a soil moisture deficit develops or increases, the soil moisture for this case is given as:

$$S_m = \min\left[\left((P_m - PET_m) + S_{m-1}\right), S_{max}\right]$$

The change in the soil moisture during the month is obtained by deducting the soil moisture of the month under consideration from the soil moisture of the preceding month. These values are entered in row 6.

The actual evapotranspiration equals the potential rate during the months when the precipitation exceeds potential evapotranspiration this is because the rain water is considered to be easily available to the plant even if the soil moisture of the whole root zone is not raised to the available water capacity. At times when the potential evapotranspiration exceeds the precipitation amount, the actual evapotranspiration will be equal to the sum of precipitation and the amount of soil moisture withdrawn from storage.

The monthly actual evapotranspiration ( $AET_m$ ) is found as:

$$AET_m = PET \text{ if } P_m > PET_m$$

$$AET_m = P_m + S_{m-1} - S_m$$

The soil moisture deficit is calculated easily by subtracting the actual evapotranspiration from the potential. The moisture surplus (amount of water

that can not be stored), which is attained after the soil moisture reaches its field capacity, is obtained by subtracting the change in soil moisture from values of (P-PET).

**Table 4.11** AET values from soil water balance for a soil with available water capacity of 250mm. The soil is fine sand and the vegetation is mature forest with a rooting depth of 2.5m

parameter	Jan	Feb	Mar	Apr	May	Jun	Jul	Aug	Sept	Oct	Nov	Dec	Total
P	15.7	44.9	69.1	68.6	40.9	61.5	210.5	217.5	92.5	36.85	7.49	8.64	874
PET	124	123.2	130.3	132	140	135	117.7	114.7	96	117.8	123	130.5	1481
P-PET	-108.3	-78.3	-61.2	-63.4	-99.1	-73.5	92.7	102.7	-3.5	-80.19	-115.5	-121.8	-607
Acc.p ot. WL	-430	-508. 3	-569.5	632	-732	-805.5			-3.5	-84.45	-199.95	-321.75	
S <sub>m</sub>	45.95	39.28	25.53	20.6	13.98	10.47	103.17	205.85	246.6	179.2	168.6	70.5	
ΔS <sub>m</sub>	-24.55	-6.67	-13.75	4.87	-6.68	-3.51	92.7	102.68	40.75	-67.4	-10.6	-98.1	
AET	40.25	51.57	82.85	73.7 7	47.58	65.01	117.7	114.7	51.75	104.25	18.09	106.74	874
D	83.75	71.63	47.48	59.3	92.42	70	0	0	44.25	13.55	104.9	23.75	
S	0	0	0	0	0	0	0	0	0	0	0	0	0

Where:

**P** = monthly precipitation

**PET** = monthly potential Evapotranspiration

**ACC.Pot. WL** = Accumulated potential water loss

**SM** = Soil moisture

**ΔS<sub>m</sub>** = Change in soil moisture

**AET** = monthly actual evapotranspiration

**D** = moisture Deficit

**S** = Moisture surplus

**Table 4.12 AET** values from soil water balance for a soil with available water capacity of 200mm. The soil is mainly clay loam and the vegetation is moderately deep-rooted crops (cereals) with an average root depth of 0.8mm.

	Jan	Feb	Mar	Apr	May	Jun	July	Aug	Sep	Oct	Nov	Dec	Total
P	15.7	44.9	69.1	68.6	40.9	61.5	210.5	217.5	92.5	36.85	7.49	8.64	874
PET	124	123.2	130.3	132	140	135	117.7	114.7	96	117.8	123	130.5	1481
P-PET	-108.3	-78.3	-61.2	-63.4	-99.1	-73.5	92.7	102.7	-3.5	-80.19	-115.5	-121.8	-607
Acc.pot. WL	-430	-508.3	-569	632.9	-732	-805.5			-3.5	-84.45	-199.95	-321.7	
S <sub>m</sub>	23	16	9	5	3	95.7	198.4	196	131	74	40	70.5	
DS <sub>m</sub>	-17	-7	-4	-3	-4	-2	92.7	102.7	-2.4	-65	-57	-34	
AET	32.7	51.9	73.1	71.8	44.9	63.5	117.7	114.7	94.9	101.8	64.5	42.6	874
D	91.3	71.3	57.2	60.2	95.1	71.5	0	0	1.1	16	58.5	87.9	
S	0	0	0	0	0	0	0	0	0	0	0	0	0

**Table 4.13 AET** values from soil water balance Model for a soil with available water capacity of 150mm. The soil is fine sandy loam and the vegetation is made up of deep-rooted shrubs with a rooting depth of 1m.

	Jan	Feb	Mar	Apr	May	Jun	July	Aug	Sept	Oct	Nov	Dec	total
P	15.7	44.9	69.1	68.6	40.9	61.5	210.5	217.5	92.5	36.85	7.49	8.64	874
PET	124	123.2	130.3	132	140	135	117.7	114.7	96	117.8	123	130.5	1481
P-PET	-108.3	-78.3	-61.2	-63.4	-99.1	-73.5	92.7	102.7	-3.5	80.19	-115.5	-121.8	-607
Acc.pot. t.WL	-430	-508.3	-569.5	632.9	-732	-805.5			-3.5	84.45	199.95	321.75	
S <sub>m</sub>	9	5.3	3.5	2.3	1.2	0.7	93.4	150	146	85	40	18	
DS <sub>m</sub>	-9	-3.7	-1.8	-1.2	-1.1	-0.5	92.7	56.6	-4	-61	-45	-22	
AET	24.7	48.6	70.9	69.8	42	62	117.7	114.7	96.5	97.8	50.5	30.5	825.8
D	99.3	74.6	59.4	62.2	98	73	0	0	-0.5	20	72.5	100	
S	0	0	0	0	0	0	0	46.1	0	0	0	0	46.1

**Table 4.14** Weighted AET of the study area

Land cover	Available water capacity (mm)	Area (km <sup>2</sup> )	AET (mm/year)
Cultivated land	200	261	874
Deep rooted shrubs	150	502	825.8
Forest	250	17	874
Weighted		780	842

$$\text{Weighted AET} = \frac{\text{AET}_1 + \text{AET}_2 + \dots + \text{AET}_n}{A_1 + A_2 + \dots + A_n}$$

Where:  $\text{AET}_1, \text{AET}_2 \dots \text{AET}_n$  are actual evapotranspiration lost on each area covered by each Landuse.

$A_1, A_2 \dots A_n$  are areas covered by each land uses

Based on this calculation, weighted actual evapotranspiration of the study area is equal to **842mm/year**.

From this computation it can be observed that except for the Months (July and August) where  $P > PET$  value the rest shows lower precipitation below potential evapotranspiration.

Since the balance shows annual AET is similar to annual precipitation value, most of the rainfall received annually goes out as evapotranspiration, and small surplus (46mm) for the whole months of the year is observed.

According to David.N, (1990) soil moisture budgeting is developed for humid climate and has less validity in arid and semi-arid zones and this works best for seasonal patterns of recharge, well developed soil which donot dry completely and when AET is similar with PET with relatively uniform precipitation.

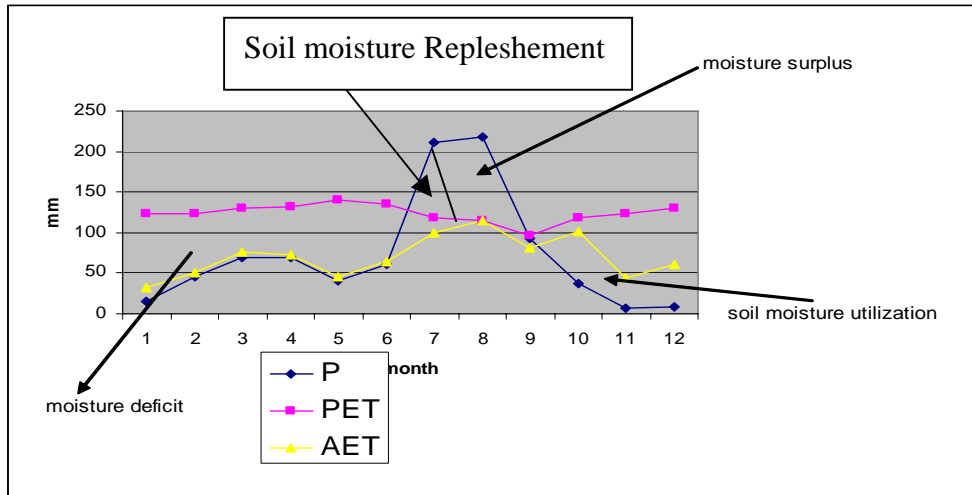


**Fig 4.7** Results of the monthly water balance for the weighted AET

#### 4.5 Surface Runoff

Runoff is a component of stream water which is generated from precipitation as flowing water in a basin. Runoff occurs when the rate of precipitation exceeds the rate of infiltration into a soil.

Runoff from a given area due to rainfall depends on climatological and physiographical.

The climatological factors that affect the runoff are:

- Type and form of rainfall
- Evaporation characteristics of the area
- Transpiration

The main physiographical factors on which the runoff characteristics depend are;

- Area and shape of the area
- Average slope of the area
- The permeability of soil and geological characteristics like the soil, type, land use, position of rock layer and aquifer characteristics.
- The presence of depression and natural reservoirs in the area.

All streams in the study all are seasonal and intermittent hence they are not gauged and have not measured flow data. Therefore the runoff component for water balance of the area was determined using empirical formulas and other runoff coefficient methods.

#### **a) Runoff Coefficient method chow (1980)**

The runoff coefficient is the fraction of rainfall converted in to runoff. This method estimates the runoff by multiplying the runoff coefficient to the rainfall depth of the area.

It is given by:  $R = K.P$

Where,  $R$  = runoff in mm

$P$  = rainfall depth in mm

$K$  = runoff coefficient

The values of runoff coefficient for different landuses/Land cover given by Barlow were used to estimate the runoff coefficient for the study area. Mathematically it is written as;

$$R = KP$$

$$K = \frac{k_1A_1 + k_2A_2 + \dots + k_nA_n}{A_1 + A_2 + \dots + A_n}$$

Where:  $k$  is weighted runoff coefficient

$K_1, k_2 \dots K_n$  : runoff coefficient for different land uses

$A_1, A_2 \dots A_n$  : area covered by each land use/Land cover

Therefore using this empirical formula, value of runoff coefficient for the study area is equal to **0.19**

This value is checked with adjacent area or catchments for more reliability. Therefore runoff coefficient for Mojo basin having similar geology, structure and rainfall distribution with the study, area is 0.138. (Tamiru Alemayehu). The reason for the little difference value of runoff coefficient for the study, area is due to relatively, steeper escarpment in the study area.

Based on this calculation surface runoff for the study area is **166 mm** or **129.5 Mm<sup>3</sup>**.

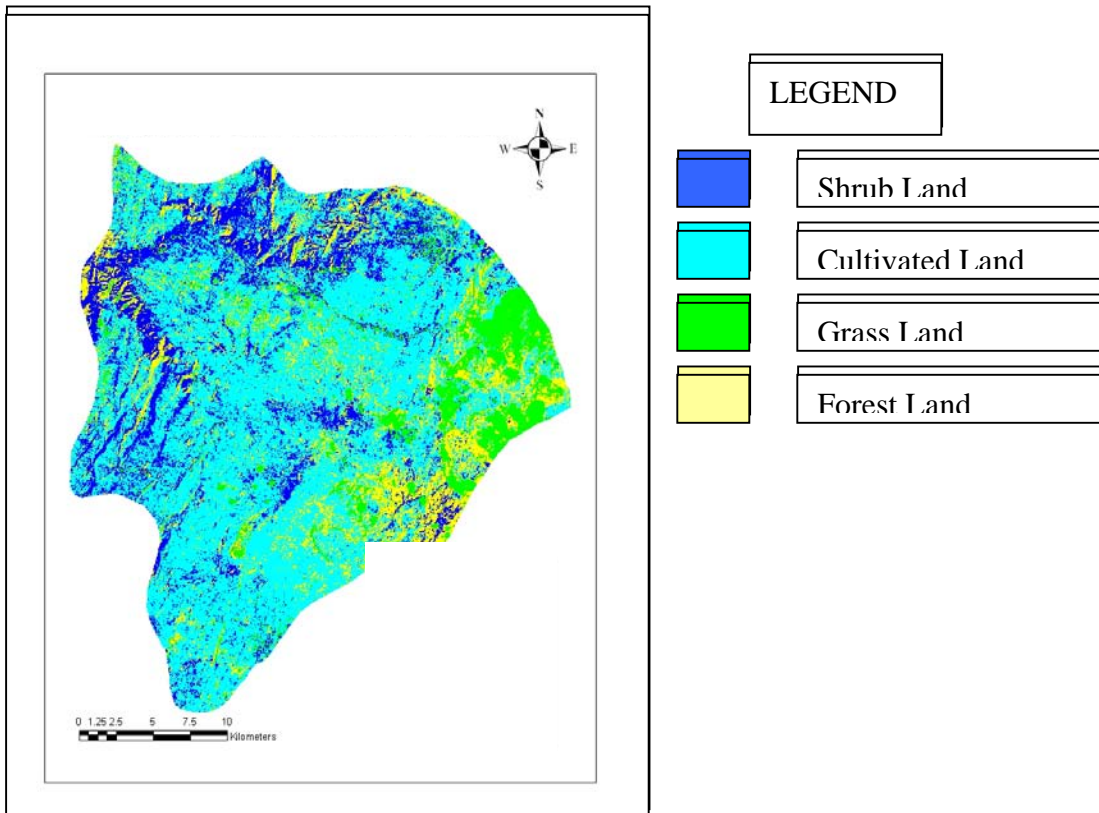


**Fig. 4.8** Classified Satellite Image showing Land cover of the study Area

**Table 4.15** Runoff coefficients for different landcovers

	Land use/Landcover type	Area (Km <sup>2</sup> )	value of run off coefficient
1	Flat, cultivated, various soil. Suitable for the soil dominated with different intercalation of clay, silt, sand and tuff covering large part of the plain.	377	0.15
2	Flat, cultivated, absorbent Soil. - Suitable for the soil dominated with coarse grained pumice deposit covering the plain, adjacent to Boset and bericca mountains.	170	0.1
3	Hills with little vegetation. - Suitable for hill side of Escarpment and Boset Mt.	216	0.35
4	Forest -Suitable for the forest covered small part of the highland.	17	0.1

**b) Curve Number Method (SCS Rainfall-Runoff Relation)**

The runoff curve number method for the estimation of direct runoff from storm rainfall is well established. Its popularity is rooted in its convenience, its

simplicity, and its responsiveness to four readily grasped catchments properties: soil type, landuse, and surface condition. The method was developed in 1954 by the USDA Soil Conservation Service (SCS, 1985).

In developing the SCS rainfall-runoff relation ship, the total rainfall was separated into three components: direct runoff (Q), actual retention (F), and the initial abstraction ( $I_a$ ). Conceptually, the following relationship between P, Q,  $I_a$  and F was assumed.

$$\text{i.e. } \frac{Q}{P - I_a} = \frac{p - Q - I_a}{S}$$

Where:

$I_a$  : initial abstraction, such as interception, infiltration and

Depression storage made in the water shed during rain fall

Q: direct runoff

P: rainfall depth

S: retention capacity of the soil

The value of  $I_a$  is usually takes  $0.2S$

$$\text{There fore: } Q = \frac{(P - 0.2S)^2}{P + 0.8S}$$

The retention capacity of soil (S) is determined by using the curve number (CN), developed by U.S. Soil conservation service (1972), given as

$$CN = \frac{2540}{25.4 + S}$$

In which, CN is the curve number which depends on land use pattern, treatments, hydrologic condition and hydrologic soil group of water shed.

The curve number (CN) for the study area is taken as following;

**Table 4.16** CN value for different landcovers

land use/Land cover	Hydrologic Soil group	Curve number value (CN)
Farm Cultivated	B	66
Shrub land	C	81
Wood or forest land	C	73

Based on the hydrologic characteristics, the soils are classified into two groups:

**Soil group (B):** Soils having moderate infiltration rate.

Soils are composed of moderately fine to moderately coarse particles.

**Soil group (C):** soils contain low infiltration rate:

The soil is composed of hard layer which impedes the down ward movement of water. Soils are generally constituted with moderately fine to fine particles.

Then weighted CN for the study area is calculated as 74. The wetness status of the area or Antecedent Moisture content (A.M.C is classified as A.M.C – II in which the conversion factor for the calculated CN is 0.73.

Based on this Runoff depth for the streams along with their sub catchments during flooding periods is calculated and is equal to 211.6 mm.

Peak runoff rate or discharge by all streams into the study area is calculated using the formula.

$$Q_p = \frac{0.0208 \cdot A \cdot Q}{T_p}$$

Where:  $Q_p$  = peak run off rate or discharge ( $M^3/S$ )  
 $A$  = area of the sub catchments ( $Km^2$ )  
 $Q$  = Runoff depth  
 $T_p$  = Time to peak discharge

In which  $T_p = 0.6 T_c + \sqrt{T_c}$  and  $T_c$  is the time required to reach the surface runoff from remotest point of the watershed to its out let. In this case from the highland escarpment and mountain peak up to the point it joins the swampy area or temporal ponds near Welenchiti town.

$T_c$  is calculated using SCS formula as:

$$T_c = \frac{(0.87 L^3)}{H}^{0.385}$$

Where:  $T_c$  = Time concentration (hr)  
 $L$  = Stream length (km)  
 $H$  = fall or elevation difference (m)

**Table 4.17** Peak discharges obtained from Curve Number (CN) method

Rivers with their Sub catchments	Subcatchment Area (km <sup>2</sup> )	Elevation difference or Fall H(m)	Stream length L(km)	Time of concentration Tc(hr)	Curve number (CN)	Run off depth (mm)	Peak run off (m <sup>3</sup> /s)
Tebo	100	760	30.5	3.3	97	73	70.6
Geldia	50	850	22.4	2.4	74	36.8	48
Mermersa	90	940	29.6	3.1	74	63	64
Nazareth creeks	40	280	6	1.4	74	21.7	34
Boset creeks	35	460	4	1.1	74	17.1	28

All streams, flows from south west of (near to Nazareth town ) of the study area and Boseti Mt. into the plain are grouped as Nazareth creek and Boseti creeks respectively.

Based on this calculation direct runoff depth for the study area is obtained as 211.6 mm/year or 185 Mm<sup>3</sup>/year.

Curve Number method computes the direct runoff storm wise or the runoff depth for peak discharges during flooding periods. Therefore this value is expected to be higher than the usual annual surface runoff.

#### 4.6 Water balance

Water balance represents the hydrological gains and losses of a given system (reservoir, column of soil, aquifer, river basin, etc) over a specific period of time. Quantification of the rate of natural groundwater recharge is a basic prerequisite for efficient groundwater resource management. However, the rate of aquifer recharge is one of the most difficult factors to measure in the evaluation of groundwater resources. It is a complex function of meteorological conditions, soil, vegetation, physiographic characteristics and properties of the geologic material with in the paths of flow.

Water balance models were developed by Thornthwaite (1948) and revised by Thornthwaite and Mather (1955). The method is essential procedure, which estimates the balance between the inflow and outflow of water.

Generally water balance has the following form:

$$\text{Inflow} = \text{out flow} + \text{change in storage}$$

The general form of the water balance of a given basin or catchment can be given by:

$$P+I+A_i+Q_i = R+Et+D+Q_o+W+S$$

Where:

P = precipitation

I = infiltration from surface water

A<sub>i</sub> = Artificial recharge

Q<sub>i</sub> = groundwater inflow

R = surface runoff

Et = evapotranspiration

D = drainage (including up ward seepage)

Q<sub>o</sub> = groundwater outflow

W = withdrawal

±s = change in storage

The main purpose of this computation is to make a quantitative evaluation of the amount of water that percolates in to the ground to recharge the groundwater circulation occurring in the investigated area. Therefore assumptions made to derive the water balance equation for the study area, are summarized as follows:

- a)** Since the computation is made annually, net change of the soil moisture and groundwater storage are assumed to be zero.
- b)** The area is part of the regional groundwater flow system and

groundwater is not in closed system. Therefore groundwater inflow from adjacent basin or area is equal to groundwater outflow in to the adjacent basin or area.

Since rain fed agricultural activities for cereal crop production takes place in the study area and no mechanized state farms and irrigation schemes, artificial recharge is taken to be zero.

The estimation of water reaching the ground water table can be calculated as;

$$R = P - AET - Q - W$$

Where: R is estimated recharge to the ground water

P: precipitation

Q: surface runoff

AET: actual evatranspotranspiration

W: withdrawal

Apart from Tebo river, all rivers in the area usually haven't outlet from the study area. Therefore the surface runoff from Tebo river as well as it's subcatchment covering 156 km<sup>2</sup> has been included in the water balance calculation. Surface runoff in the Tebo river sub catchment is estimated to be 33Mm<sup>3</sup>.

Because all streams in the area are seasonal, the only water supply for domestic purposes is from deep boreholes water withdrawn from bore holes anually approximately equal to **0.6Mm<sup>3</sup>**

Based on this calculation groundwater recharge is estimated to be **144mm/year**.

The flat area or welenchiti plain is exposed to flooding from the northern highland and covered with stagnant water for weeks during intensive rainfall usually in July and August, the amount of water to percolate deep into groundwater table is small due to the low permeability of the lacustrine sediments consists of clay, silt, sand, ash flow, tuff and pumice intercalated with each other. However surface water percolates deep into groundwater through hidden tectonic discontinuity and fracture zones particularly in the

downstream of Geldia stream Where the water body is lost quickly from the area. And water percolates down into pumice dominated soil towards the bottom of Mt. Boseti. The southern and eastern part of the study area is covered with scoraceous basalts having pore spaces interconnected each other and highly affected by deep faults and joints are expected to be high recharge zones.

**Table 4.18** Data sets for water budget calculation

Parameter	Amount
Total area (km <sup>2</sup> )	780
AET depth (mm)	697
AET (Mm <sup>3</sup> )	543.66
Precipitation depth (mm)	874
Precipitation (Mm <sup>3</sup> )	681.73
Ground out flow –Groundinflow	0
Artificial recharge	0
Runoff depth (mm)	166
Runoff (Mm <sup>3</sup> )	129.5
With drawal depth (mm)	0.0008
With drawal (Mm <sup>3</sup> )	0.6
Groundwater recharge depth(mm)	144
Groundwater recharge (Mm <sup>3</sup> )	112

#### 4.7 Cause of Flood in the study area

Surface runoff is the source of flood. When volume of incoming runoff becomes greater than the outflowing volume from the river or stream, then excess runoff tends to accumulate in the river course and increase the water level. If rises of water level is continued for longer time period, then excess water starts spreading in the adjoining areas and thus resulting into occurrence of flood. Floods are affected by the characteristics of precipitation and watershed, in

which precipitation, intensity of rainfall, the soil type, soil texture, structures and shape of the area.

The main cause of flood occurrence in the study area is occurrence of high intensity rainfall over small catchment surrounded by hilly terrain. The severness of flood in the study area due to intense storm mainly depends on;

**a) Intensity and duration of rainfall**

The rainfall intensity and its duration during summer season particularly in July and August, directly affect the size of flood. An intense storm occurring over the northern highland, results in high flooding over the plain. Because whatever rainfall takes place in the highland escarpment, is quickly drained to the outlet, which meets to the major rivers such as Tebo, Geldia and Marmarssa.

**b) Land slope**

The runoff rate and its volume is highly controlled by the land slope of the area. The study area extends elevated mass with an altitude of 2400m in the highland up to welenchiti plain with an altitude of 1500m with in average distance of 20km. Therefore, the steep side of the escarpment results in low time of concentration.

**c) Landuse**

The nature of land surface affects greatly by affecting the runoff producing characteristics of the area. Similarly, the deforested hilly side of the escarpment generates high rate of runoff very quickly to the outlet in the down stream of the rivers close to welenchiti town.

## **CHAPTER FIVE**

### **Hydrogeology**

There is limited data availability on the hydraulic characteristics of the rock units in the study area, however existing data, fieldwork, indirect and direct approach was used in order to characterize the different aquifer units in the area. The characterization involves the use of existing pumping test data, lithology obtained from well logs, water table depth, structures, topography and geophysical investigation so as to see the lateral distribution and the nature of the aquifers.

The hydraulic parameters (K,T) are determined from existing data of pumping tests that were conducted in the past years.

#### **5.1 Hydrostratigraphic units in the study area**

Geological descriptions of Stratigraphic units have been presented in chapter two. These lithologies have been grouped into four aquifer units based on hydraulic parameters, field observations of primary and secondary porosity, pumping tests and properties of well log data.

Pumping test analyzes using Jacob's method was the primary approach to assign the permeability group.

High permeability if  $K > 5\text{m/day}$

Moderate permeability if  $k = 0.5\text{-}5\text{m/day}$

Low permeability if  $K = 0.1\text{-}0.5\text{m/day}$

Very low permeability if  $K < 0.1\text{m/day}$

Where: k is permeability of the aquifer

### **5.1.1 The scoraceous and fractured basalt aquifers with high**

#### **Productivity and permeability.**

These aquifer units belong to sub recent basalts, recent aphyric basalts and Bofa basalts spatially distributed on the southern tip and eastern part of the study area. The most distinctive feature of the Bofa basalt is its prominent well-developed columnar joints, which favor for transmitting groundwater. Groundwater is deep and the deep nature of the vertical joints favors infiltration of precipitation with out meeting on impermeable bed in between. Recent aphyric basalts are products of fissural eruption and highly vesicular with interconnected pore spaces (Getahun Kebede, 1987). Wells drilled deep into fractured basalts in Gorowagilo (Fig5.1a) are good aquifers in relation to water productivity yielding 6.5L/s with transmissivity value of 310 m<sup>2</sup>/day, and permeability of 8m/day. While wells drilled deep into scoraceous basalts (Fig 5.1b) in Golbomitimiti area yields 4.6L/s with transmissivity value of 170 m<sup>2</sup>/day. Well drilled in Feto area (BH-7) has also high transmissivity and permeability of 180m<sup>2</sup>/day and 5.7m/day respectively.

The younger volcanic centers are highly fractured and in several places they are scoraceous and fragments often show an internal flow structure which favors groundwater transmitting in the area.

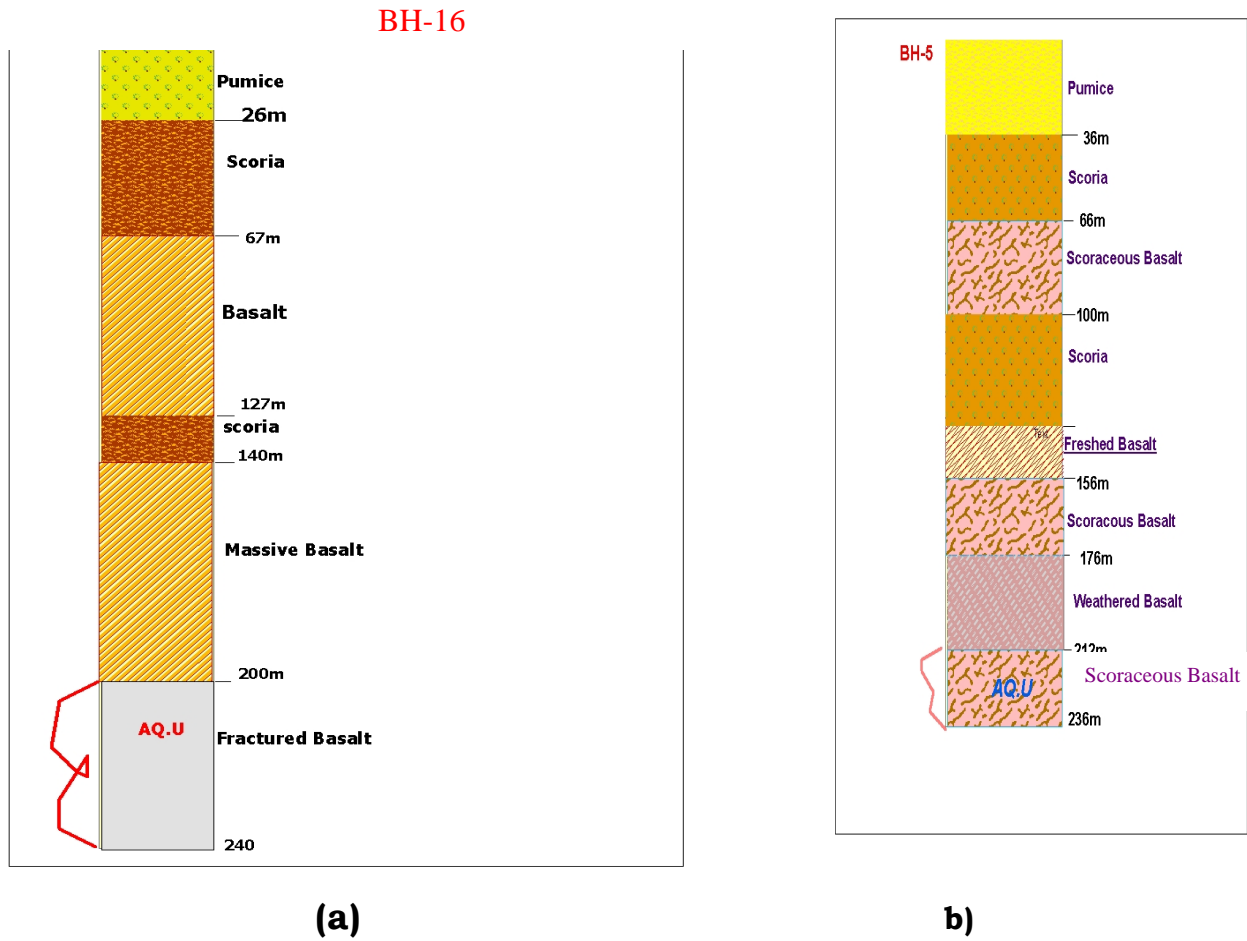


**Fig 5.1** vertical distributions of aquifers from well log and pumping test data **(a)** fractured basalt aquifer in Gorowagilo area **(b)** Scoraceous basalt aquifer in Golbomitimiti, **AQ.U** and **AQ.U** are potential Aquifer units.

### **5.1.2 Fractured and fissured Ignimbrites with Moderate permeability and productivity**

Ignimbrites exposed in the western part of the study area and in the form of intercalations are strongly welded pyroclastic flows unlike the northern part of the study area. The welded ignimbrites are intercalated with basaltic lava flows forming flow structures and also affected with Wonji type faults and associated fractures striking NNE-SSW direction, which favors groundwater transmitting. This type of ignimbrites extends beneath the lacustrine sediments throughout the plain, making the main aquifers.

Ignimbrites encountered in warka area in the form of intercalation have an aquifer unit of fractured ignimbrite at a depth of 145m with permeability and transmissivity of 0.62/day and 16.9 m<sup>2</sup>/day respectively. Well drilled towards the west highland in sekeklo (BH-17) area has permeability and yield of 0.53m/day and 4.43L/s respectively. The existence of deep groundwater in the western part of the area is due to tectonic structures particularly, faults striking NNE-SSW direction. The well was drilled with in a graven bounded by two parallel faults.

In general Welded ignimbrites in the form of intercalation with lacustrine sediments in the plain and out cropped in the west escarpment have moderate permeability.

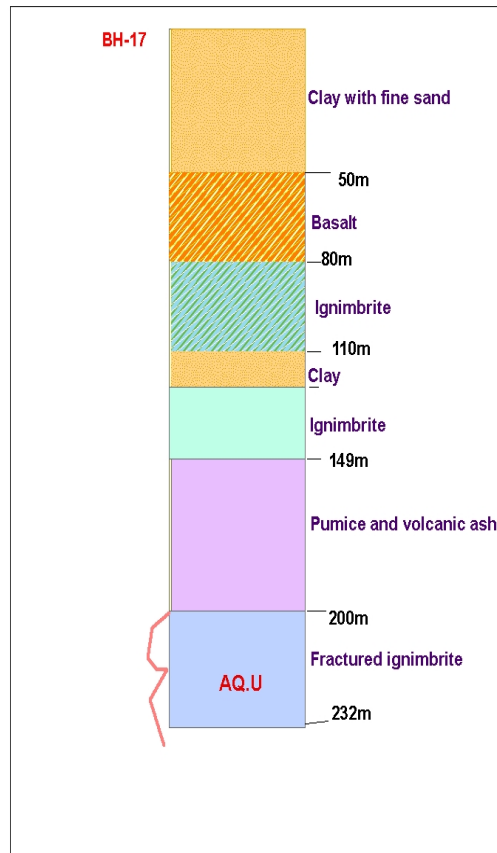


**Fig 5.2** Fractured Ignimbrite Aquifer in Sekeklo Area, **AQ.U**-  
Aquifer unit.

### 5.1.3 Lacustrine sediments with low permeability

The lacustrine sediments, which are composed of clay sand and gravel, occupy large proportion of the area. The average thickness of the lacustrine sediments according to the log data is generally 50m-60m. These sediments consist of sands, silts, clays, tuffs, pumice and diatomite. The permeability of sands and pumice fall deposits is reduced due to intercalation of clay and tuff layers which is visible along the layers dissected by small seasonal rivers. From NE to SW, the thickness of lacustrine sediment varies from 5 to 110m having an average thickness of 45m. However in places where there are thick sediment deposits, the sand and pumice deposits are underlain by clay and silt layers, which

highly reduce permeability. While from NW to SE, the thickness of lacustrine sediment varies from 6 to 29 having an average thickness of 15m subdivided by several intercalations of Bentonitic clay, silt, volcanic ash and diatomite clearly visible along the gorge of Tebo River. Therefore shallow aquifers with in the lacustrine sediments are limited in the study area.

#### **5.1.4 Unwelded to poorly welded ignimbrites, ashflow tuffs with Low**

##### **Permeability and productivity**

Nazreth group of ignimbrite mainly consists of pyroclastic materials such as pumice, poorly welded ignimbrite. Tuff, commenditic rhyolites and trachaytes bound the study area to the north and north east sides. Though this unit has unfortunately no wells drilled in order to characterize the vertical extent of the aquifer, From field observations and previous works, pyroclastic deposits consist of unwelded to poorly welded, volcanic ash flow and tuffs. Which are predominantly distributed in the area and less affected by tectonic discontinuity and fractures makes the unit low productive. In addition: steep topography of the escarpment is favorable for surface runoff rather than infiltration and site for groundwater exploitation.

#### **5.1.5 Massive rhyolite domes and flows with very low permeability.**

These units are distributed in a scattered way as massive rhyolite domes and flows. The prominent Boseti Mountain is characterized by obsidian flows with layered pumice in addition to rhyolite domes and flows. Due to the mineralogical composition of these rocks and the fact that most of them are not affected by different structures, makes them highly impermeable. The steep topographic feature of Boseti Mountain and northern highland escarpment favors quick runoff rather than infiltration. Productive deep wells are not penetrated in this formation. However there is hand dug well in mukeyero area in the weathered part of older alkaline and peralkaline rhyolite domes. In general due to massive

nature and steep topography these units are classified as very low productivity and permeability.

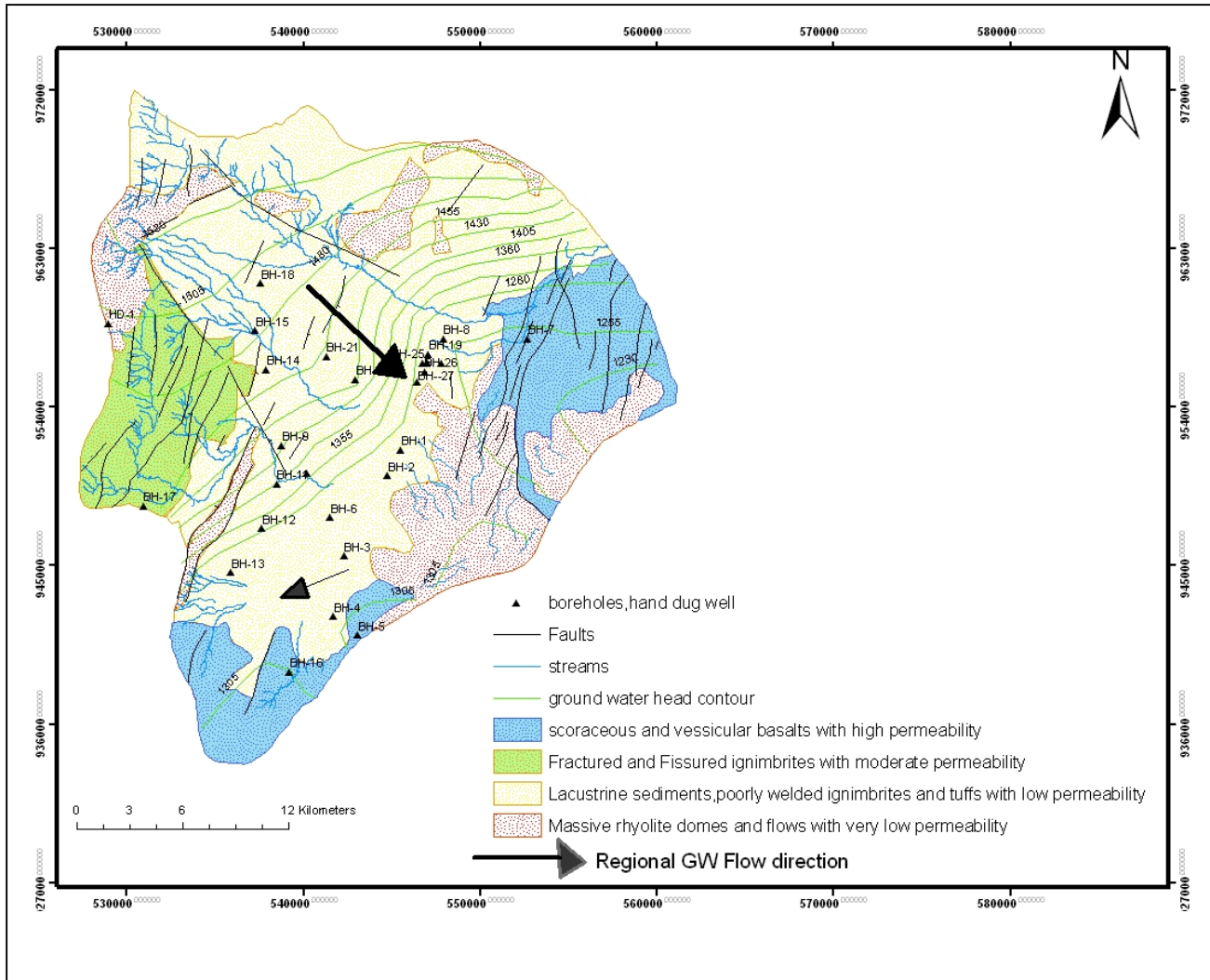


**FIG 5.3** Hydrogeological Map of the study Area

## 5.2 Aquifer characterization

Major Aquifer system classifications have been made from the hydro geologic patterns of the area for the depth of groundwater level in wells and aquifer units in relation to the prevailing hydrochemistry of the groundwater. This is based on the observation and analysis of all the compiled well log data and pumping test data for the existing wells in the study area.

There exists in general deep groundwater or aquifer system in the study area. The only hand dug well of shallow aquifer system exists in the weathered part of rhyolite domes in mukiyero area.

The deep aquifer system in general extends through out the lacustrine sediment plain as well as sub recent and recent aphyric basalts and Bofa basalts.

According to well log and pumping test data, the fractured and weathered Nathreth group of ignimbrites and basalts that under lay the lacustrine sediments are the main aquifer zone of welenchiti plain.

These aquifer units in welenchiti area are situated deep occurring at a depth ranging from relatively shallow depth of 126m in Dibibisa area up to 260m in chemerijawis area with a possible aquifer thickness of from 30-50m. The aquifer unit in Dibibisa area (BH-13) is fractured basalt with water depth of 126m. The aquifer unit has thickness of 40m and overlain by massive basalt, making the aquifer unit locally confined. This aquifer unit has permeability and transmissivity value of 4.5 m/day and 124 m<sup>2</sup>/day respectively. The relatively higher well yield and lower drawdown value of 8.4L/S and 4m respectively show that the fractured basalt aquifers, which are close to the foothill of the western escarpment, are potential aquifers.

The aquifer units in areas close to northern highland of the study area are fractured ignimbrite. Well drilled in Wersecha area (BH-15) with water depth of 199m, has permeability and transmissivity value of 5.3 m/day and 127m<sup>2</sup>/day respectively and yielding 4.6 l/s. The aquifer unit has a thickness of 30m

overlain by ashflow and tuffs. Wells drilled in the central part of the study area have relatively lower permeability and productivity. Well drilled in Buta Dengore have low permeability and transmissivity value of 1m/day and 35m<sup>2</sup>/day. This is most probably due to intercalation of volcanic rocks and remoteness from the escarpment which acts as potential recharge zone.

Aquifer units in the southern tip and southeast of the study area are scoriaceous and fractured basalts with water depth ranging from 205-236m. The potential aquifer unit of scoriaceous basalt in Golbomitimiti has a thickness of 30m overlain by weathered basalt. High permeability and transmissivity value of 6.4 m/day and 170m<sup>2</sup>/day respectively is due to the highly vesicular nature of the scoriaceous basalts. And the fractured basalt aquifers in the same area also have high permeability and transmissivity with moderate drawdown. Well drilled in Goro Wagilo area has water table depth of 205m and static water level of 176m with aquifer thickness of 40m. The deep nature of columnar joints and fractures make the aquifer unit good potential aquifers with permeability and transmissivity value of 8m/day and 310m<sup>2</sup>/day respectively.

The lateral lithology and thickness variation of the aquifer units is difficult to characterize due to scarcity in enough boreholes with well compiled log data and pumping test data. However from the existing log data and geophysical data, the lateral variation in aquifer characteristics shows that the fractured water bearing ignimbrite decrease in thickness or pinch out from the plain close to the highland escarpment into southern and south east of the study area. While the thickness of the fractured basalts which are potential aquifers increase from southwest highland upto the southern tip of the study area where potential aquifers are of scoriaceous basalts. According to Skuthan Bohmir et al (1982), the thickness of the volcanic rocks (tuff, ashflow, fractured ignimbrite) shows an average depth of 270m in the north part of the plain.

### **5.3 Review of resistivity survey values in the study area**

From resistivity survey conducted previously to a maximum spread of 1000m (AB) on the central part of the plain. 5 to 6 layers were identified almost consistent with the borehole log data on the area. Apparent resistivity values for the identified layers in general range from  $8\Omega.m$  to some high values around  $846.5\Omega.m$ . Except for ves# 4 and VES#6 the bottom 5<sup>th</sup> layer with resistivity values in the range of  $7.8\Omega.m$  to  $54\Omega.m$  signifies the major aquifer zones of fractured and weathered ignimbrites and basalts. The thickness of this aquifer unit varies from 44m in VES#3 to 63m in VES#4. The massive basalt layer exhibit values ranging from 500-800 $\Omega.m$  in VES#6 and VES#7 having thickness of about 50m makes the bottom water bearing formation semi-confined. The top soil has an apparent resistivity value of 5-25 $\Omega.m$  with thickness of 1-1.6m.

The bottom layer at an average depth of 170m with apparent resistivity value of 5-25 $\Omega.m$  is due to nature of fracturing of water bearing ignimbrite rocks rather than salinity and EC value of the groundwater.

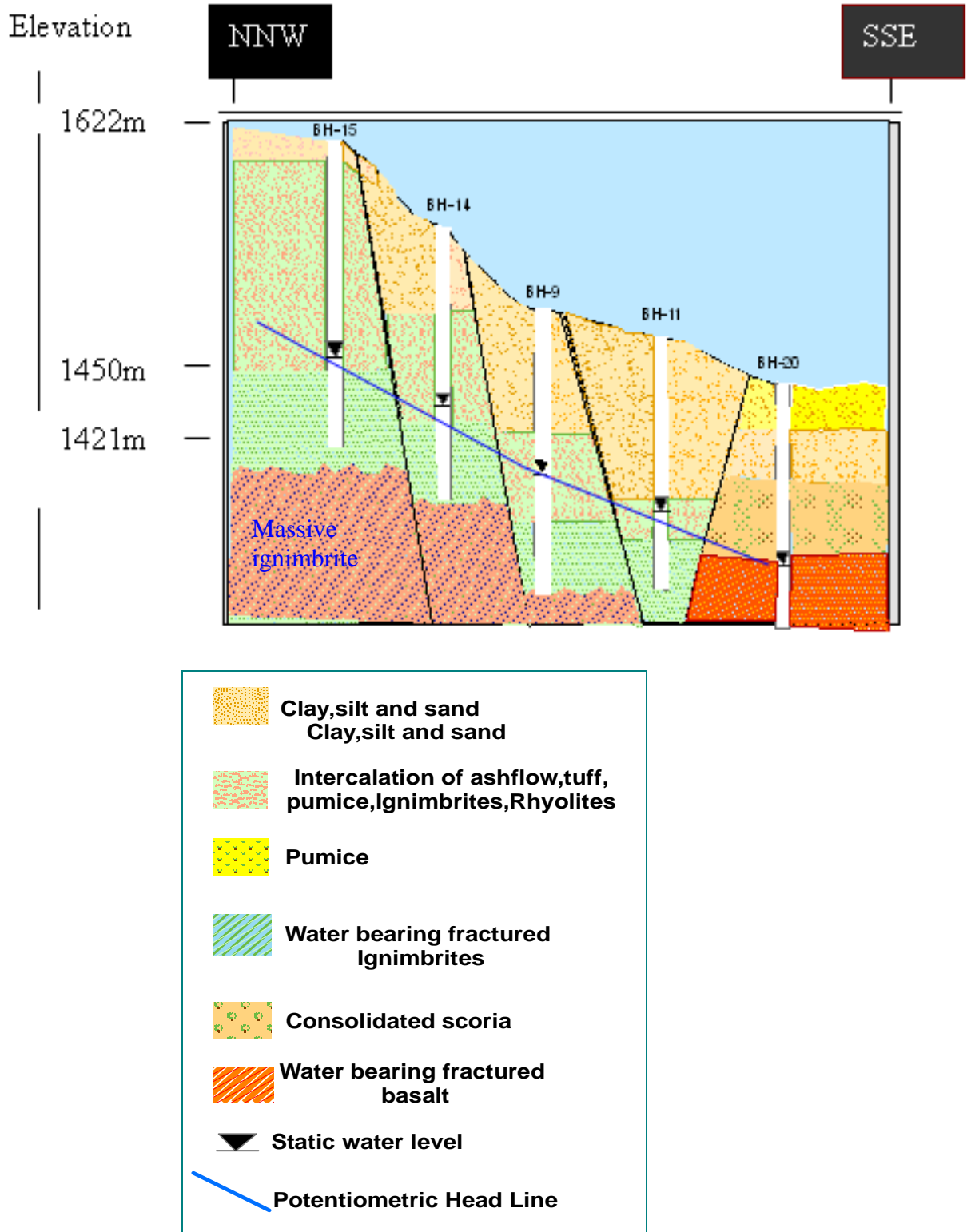


**Fig 5.4** Hydrogeological section on the Welenchiti Plain along NNW-SSE direction (not scale)

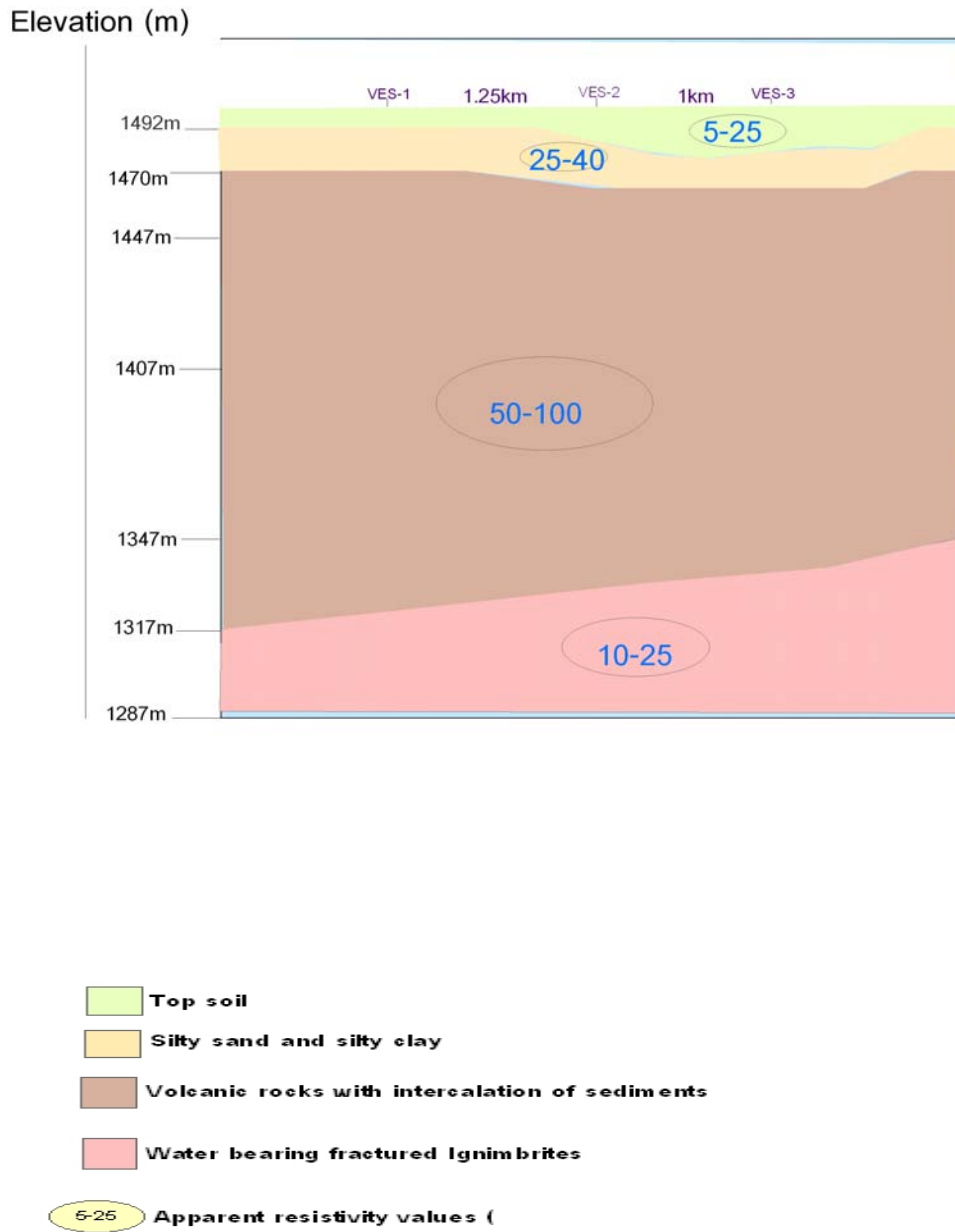


**Fig 5.5** Geoelectric section around welenchiti town

**Table 5.1** summery of Resistivity values of welenchiti area

VES# No and Location of shot or VES point (UTM) and Elevation(m)	Resistivity (ohm) and depth (m )	Layers					
		Layer 1	Layer 2	Layer 3	Layer 4	Layer 5	Layer 6
#1 0541235E 0957691N 1497m	Resistivity	25.5	36.9	9.1	93.9	19.6	
	Depth (m)	1.2	4.5	13.4	189.9		
#2 0542159E 0957135N 1497m	Resistivity	11.3	37.3	9.1	41.1	19.7	
	Depth (m)	1.3	3.4	8.5	154	-	
#3 0542976E 0956657N 1492m	Resistivity	39.2	26.5	5.4	42.3	12.3	
	Depth (m)	1.6	3.3	5.9	98.9	143	
#4 0537696E 0957023N 1477m	Resistivity	14.6	123.3	17.9	180.2	54.6	
	Depth (m)	1	3.2	24.5	72.1	-	
#5 0539536E 0596106N 1528m	Resistivity	3.8	51.5	8.2	71.8	7.8	846.5
	Depth (m)	0.9	2.1	8.3	13	73.7	-
#6 0541498E 0954592N 1485m	Resistivity	23.7	61.6	20.3	535	21.5	
	Depth (m)	1.5	5.8	41.6	81.9	-	

## **5.4 Groundwater Recharge mechanisms**

Recharge can be broadly defined as water that reaches an aquifer joining the water table from any direction, which contributes an addition to the groundwater reservoir. There are three principal mechanisms of recharge defined by Lerner et al. (1990) as:

- Direct recharge (Diffuse): water added to the groundwater reservoir in excess of soil moisture deficits and evaporation by direct vertical percolation from precipitation or irrigation.
- Indirect recharge: recharge to the water table through the beds of surface water courses.
- Localized recharge: an intermediate form of groundwater recharge resulting from the horizontal, near surface concentration of water in the absence of well defined channels such as small depressions, joints and faults.

The above mechanisms usually do not occur individually rather in combination which makes the assessment complex. On the other hand, the recharge and discharge conditions of an area is controlled by several factors such as; climate, topography, drainage, geologic framework, soil condition, landuse/landcover and vegetation etc.

Classification of the area into different recharging zones was not a simple task because no perennial stream is found in the area to measure base flow for the streams and categorize the region into different recharge zone. Therefore recharge mechanism in the study area has been explained based on lithology, stratigraphy, topography and structures of the area.

Recharge to the deep groundwater system of the plain most probably occurs in the following ways;

#### **5.4.1 Direct recharge from precipitation**

Due to the relatively higher annual potential evapotranspiration over the total annual precipitation in the flat plain, direct and local recharge from precipitation for this lower valley part i.e. Welenchiti plain is rare. During intensive rainfall in the north highland escarpment, Geldia and marmersa rivers cause flooding covering large part of the plain close to welenchiti town for weeks. However the relatively thick layer of lacustrine sediments consists of clay, silt, sand, ash flow and pumice intercalated each other reduces direct recharge or infiltration into ground water table. This can be justified by the absence of shallow aquifers with in the lacustrine sediments having a thickness of around 70m and no static water level rise is observed in most deep wells in different seasons. However the contribution of hidden tectonic structures, particularly normal faults that are the extensions of the NE-SW striking faults in the southwest of the study area, may have significant role in downward movement of water from the water body, accumulated during flooding period particularly at the down stream of Geldia river where the surface runoff is lost quickly than other areas. In general most of the surface water as swampy area around welenchiti town during summer season is lost by evapotranspiration and to some extent infiltrated in to pumice dominated soil as getting close to the foot Hill of Boseti Mountain. However the scoraceous and vertical basalt aquifers, belongs to recent aphyric basalts and Bofa basalts spatially distributed in the south and eastern part of the study area, have well developed columnar joints which favor for transmitting ground water. The deep nature of the vertical joints favors infiltration of precipitation with out meeting an impermeable bed in between.

### **5.4.2 Indirect recharge from highland mass through tectonic**

#### **discontinuities.**

Fault zones can act either as barrier to groundwater flow or as groundwater conduits depending up on the nature of filling material in the fault zone and orientation of the faults lines, particularly faults in poorly consolidated rocks with low displacement exhibited good permeability (fitter, 1996). In the study area, there exist a number of faults, which can act both as barriers or conduits to groundwater flow. Joints and deep fault lines striking NNW-SSE from highland escarpment and dipping towards the lacustrine sediment plain are expected to act as conduits for groundwater flow from highland escarpment most probably the recharge zone potential. Tectonic discontinuity and the associated fractures of the escarpment are a potential recharge zones for deep aquifer system of the plain. The groundwater table declining from NNW to SSE direction can manifest this. While the southwest part of escarpment is highly affected by number of wonji type of faults striking NNE-SSW favors groundwater flow direction similar to the direction of the strikes. This is manifested in wells drilled in sekeklo (BH-17) close to the lower end of such faults having relatively high productivity than wells on the central part of the plain close to Welenchiti town.

### **5.5 Groundwater flow**

On the basis of the potentiometer head distribution from various deep wells drilled in the aquifer system, Potentiometer contour map has been constructed to show the groundwater flow direction. Topography, geology and structures are the primary controlling factors on the flow system of the groundwater. Tectonics and many major and minor structures have affected the study area. Thus groundwater occurrence of the area is of much complex. But the general trend of ground water flow is towards SSE from the surrounding highland escarpment along which there exists a general potentiometric head decline as observed from groundwater contour map. However wells drilled in south west of Boseti Mountain particularly in Golbomitimiti area has higher potentiometric head or

static water levels may be due to elevated topography. Static water levels from wells in the study area exhibit replica of topography. Orientation and dip direction of faults and fracture system also influenced groundwater flow and direction. Most of fault controlled groundwater of the area move parallel to the direction of fault strike.

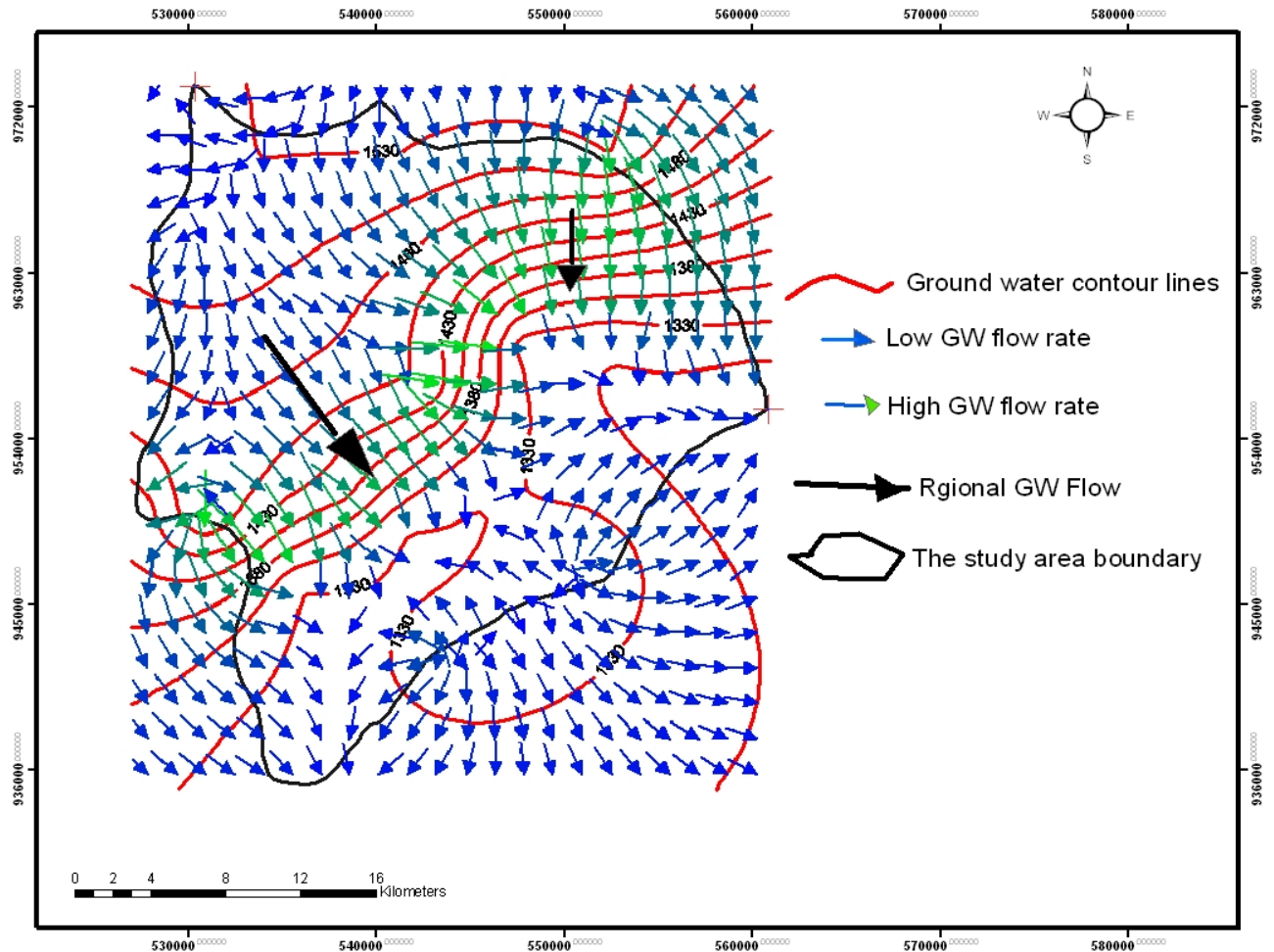


**Fig 5.6** Groundwater flow direction map

## **CHAPTER SIX**

### **Hydrochemistry**

#### **6.1 General**

Natural water consists of dissolved minerals, dissolved oxygen, suspended particulate materials and etc. The chemical composition of natural water is derived from different sources of solutes including gases from the atmosphere, weathering and erosion of rocks and soil, solution or precipitation, reactions occurring below the land surface and effects resulting from human activities (Hem, 1989). Water quality is defined by physical, chemical and biological characteristics. The significant physical characteristics include temperature, hardness, hydrogen ion activity (PH), electrical conductance (EC) and redox potential (Eh) etc of the water. Water chemistry studies require the identification and determination of different constituents, such as major ions, bicarbonates, carbonates, sulfates, chlorides, calcium, magnesium sodium, minor and trace elements. For the purpose of the hydrochemical characterization of the groundwater and explanation of the major geologic controls on the hydrochemical variations and concentrations, water quality analysis has been done on water samples. This water quality analysis in general includes water samples taken from 26 deep bore holes and 1 hand dug well .In situ or field measurements for some water quality parameters like PH and EC has been performed to observe the behavior of the physical and hydro chemical behavior of some parameters at the time of sampling.

#### **6.2 Evaluation of Hydrochemical parameters**

##### **6.2.1 Temperature and PH**

Temperature for groundwater from deep wells is observed to be in the range of 19-52<sup>o</sup>c. The highest value is observed for Dibibisa deep well (BH-13) around 52<sup>o</sup>C. The second highest value is observed for chele kiltu (BH-4) deep well around 48<sup>o</sup>c. Deep wells on the northern part of the study area close to escarpment have lower temperature. Some lowest value is observed for

worsecha (BH-15) deep well around 19<sup>o</sup>c and for sekeklo (BH-17) deep well is around 21<sup>o</sup>c. For chemeri jawis (BH-18) is around 23<sup>o</sup>c. Deep wells close to Boseti Mountain and southern tip of the study area have higher temperature values. Heat from deep thermal source in this area is the major factor for the high temperature values of water samples.

The southern tip of the area is highly affected by wonji type faults and recent faults favouring circulation of deep thermal waters.

Most of the deep wells display PH values close to 8 of alkaline condition and some deep wells such as Goro Wagilo (BH-16) and chele kiltu (BH-4) deep wells have PH value of 8.71 and 8.37 respectively. The only hand dug well in the study area has PH value of 8.75.

### **6.2.2 Electrical conductance (EC)**

Electrical conductance or conductivity is the ability of a substance to conduct an electric current. Conductance is expressed as mhos or micro siemens (it is the reciprocal of resistance). The presence of charged ionic species in water makes it conductive. In other words, EC is a measure of the total concentration of ion.

High electrical conductivity occurs in area at south and south west of Boseti Mountain. The maximum EC value is observed in Golbomitimiti (BH-5) with 1800  $\mu\text{S}/\text{cm}$  where as lowest value is observed in northern area named sekeklo (BH-35) having value of 435 $\mu\text{s}/\text{cm}$ . generally EC increases to wards south and south west of the study area. This is because of higher values of total dissolved solids in the southern tip of the study area. The water quality result shows that electrical conductivity (EC) and total dissolved solid (TDS) have a good correlation of  $\text{TDS} = 0.56\text{EC} + 91.3$ .

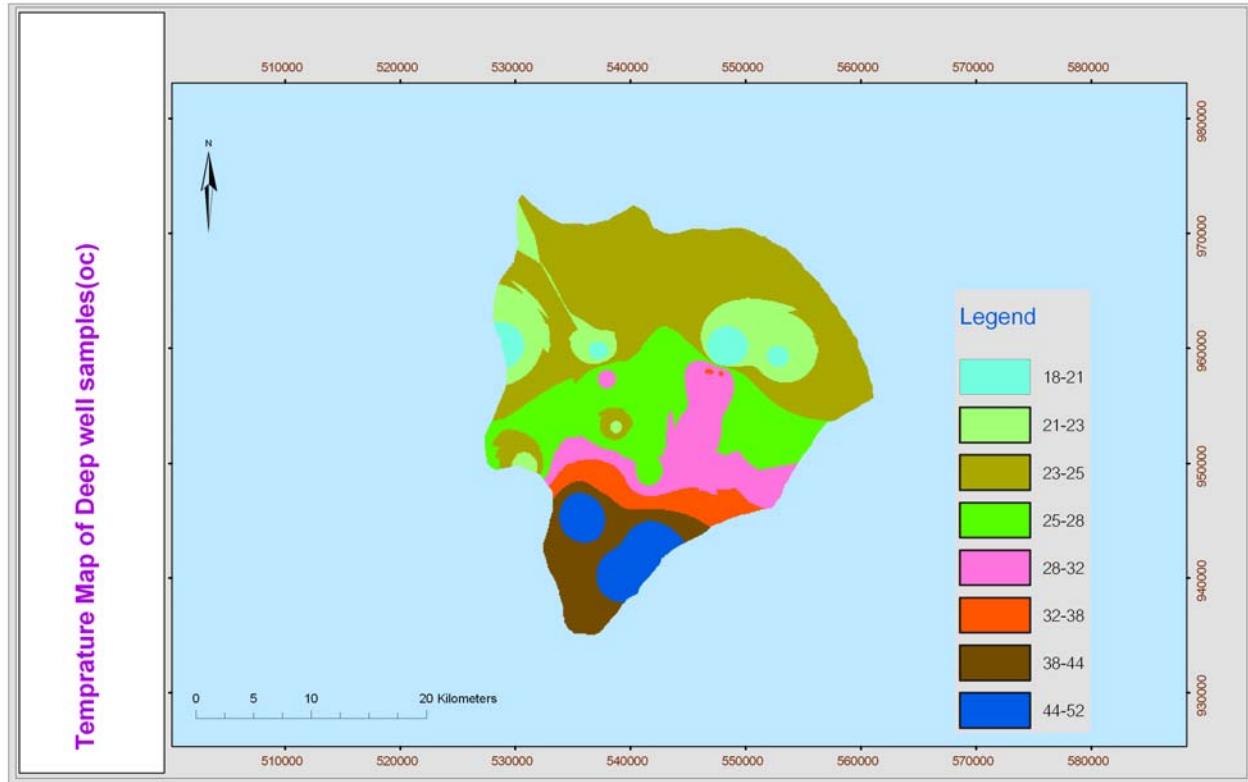


**Fig 6.1** Temperature map of the well samples of the study area

### 6.2.3 Total dissolved solids (TDS)

A total dissolved solid includes all solid materials in solution, whether ionized or not.

The Ethiopian rift is characterized by high salinity (TDS) due to high degree of water-rock interaction, evaporation and the discharge of thermal water (Tamiru Alemayehu, 2006).

From the water quality analysis result of the study area, the TDS varies in general ranging from minimum values for a relatively fresh groundwater of 300 to 400mg/L in the area close to highland escarpment and close to the recharge zone for the plain to some high values, which is saline water with a value ranging from 800 to 1030 mg/l in most boreholes around southern and south

west of Boseti mountain. Some lowest value of 200 mg/l is tapped in the handdug well of mukiyero (HD-6) area. The higher TDS value for deep wells in the southern tip area where there are highly fractured and jointed Bofa basalts and high temperature shows that the groundwater system in this water point is part of the groundwater flow system which favors active rock-water interaction resulting in high concentration of TDS. TDS values for groundwater are strongly controlled by the time of contact or rock- water interaction along the flow path. Some additional factor for high TDS value towards the southern part of the area could also be the dissolution of some salt minerals associated with surrounding lacustrine sediments resulting in evaporative enrichment. Where the rate of concentration of these minerals increase from the higher evaporation of the surface water and recharge deep into groundwater through the scoraceous , vesicular basalts and deep vertical joints.

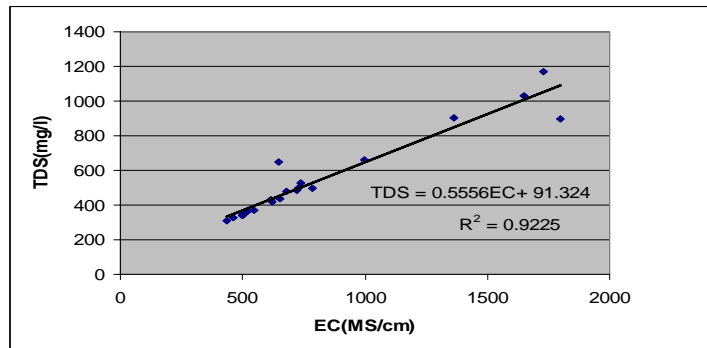


**Fig 6.2** TDS-EC correlation for the water sampled.

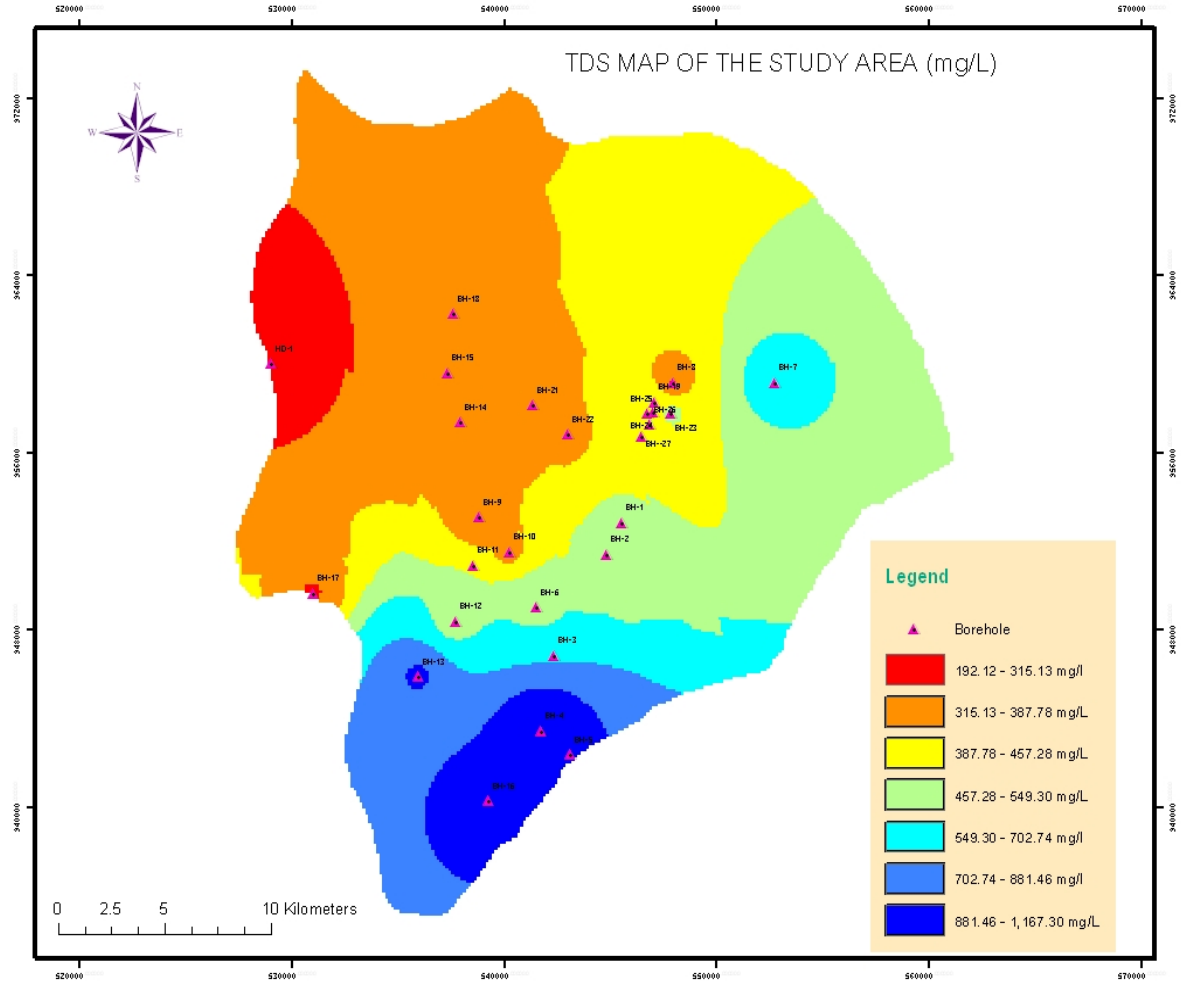


**FIG 6.3** TDS Map of the study Area

#### 6.2.4 Cations (Na + and Ca ++)

Out of the major cations of the groundwater in the study area, Sodium (Na<sup>+</sup>) and calcium (Ca<sup>++</sup>) are the most dominate cations where sodium in particular shows significant variations whose values range between 41 to 420 mg/L. The (Na<sup>+</sup>) concentration ranges from minimum values of 41 to 49 mg/L in the plain close to high land escarpment to maximum values of 420 mg/L in the south west of Boseti Mountain. Therefore Na<sup>+</sup> shows in general an increasing tendency from the highland escarpment to wards the southern tip of the study area.

This is because of long time of water-rock interactions. Sodium is a major constituent volcanic of lava flows and domes of Boseti Mountain. Most commonly occurring minerals in this unit are sodium plagioclase and alkali feldspars (sanadine anorthclase and albite (  $\text{NaAlSi}_3\text{ZO}_8$  ). The higher temperature in the groundwater facilitates the reaction between water and sodium-rich acidic volcanic rocks in the southern part of the study area. While deep aquifers close to highland escarpment have lower values due to slow groundwater interactions and to some extent sodium may be retained by adsorption on mineral surface of lacustrine deposits having high cation exchange capacities such as clay before directly recharge to groundwater.

On the contrary the calcium concentration which ranges between minimum values of 5.3mg/L in chelekiltu area, up to maximum values of 50mg/L in chemerijawis area, which is close to high land escarpment of the study area. Therefore from the samples analyzed, sodium and calcium in general shows a negative relation ship.

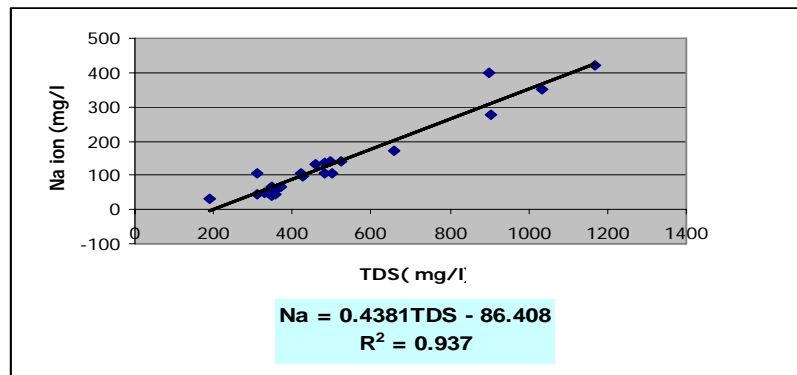


**Fig 6.4** correlation between Na and TDS

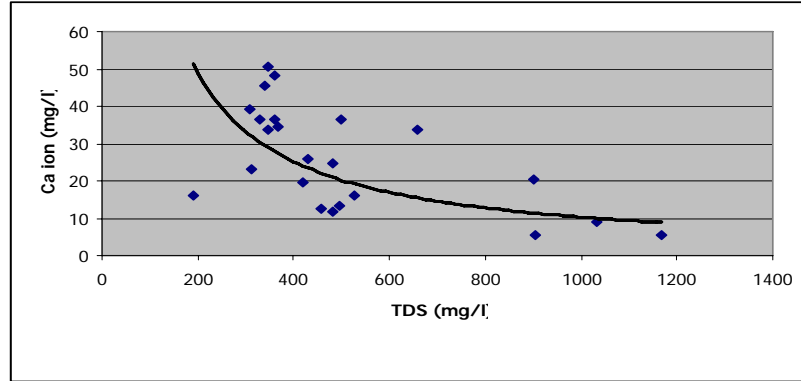


**Fig 6.5** correlation between Ca and TDS

### 6.2.5 Anions

Out of the major anions in the groundwater chemistry, bicarbonates and fluorides are the most dominating anions in the study area.

The higher concentration of bicarbonates to wards south of the area is due the reaction of dissolved carbon dioxide with Na and K silicate minerals emitted from deep geothermal sources to produce mica or clay minerals and bicarbonate ions (UN, 1973)

$\text{CO}_2 + \text{H}_2\text{O} + \text{Na, K-silicates} \rightarrow \text{HCO}_3 + \text{Na, K+H-silicate}$  in accordance with this reaction, Na and  $\text{HCO}_3$  are positively correlated in the study area. Pyroxene andesite produce less bicarbonate ions in the reaction of equation above but clay produces bicarbonates and  $\text{Na}^+$  ions in large quantities Koga (1969).

Concentration of bicarbonate considerable affects the extractions of Fluoride. If the PH of the groundwater remains constant, increasing or decreasing in bicarbonate Concentration (activity) will be accompanied by corresponding increasing or decreasing in the concentration (activity) of fluoride ions.

### **6.2.5.1 Fluoride**

The situation of relatively high fluoride concentration in the groundwater of the south and south west of the study area is related to the geochemical controls in relation to the site nature. Some maximum values have been observed in Golbomitimiti (BH-5) and Gorowagilo (BH- 16), areas on the foothills of Boseti Mountain, and Bofa basalts with a value of 11.25 and 9.2 mg/L respectively. Where as the northern part of the plain, close to highland escarpment, have a value ranging from 1.24 -1.92 mg/L. Minimum value of 1 mg/l has been observed in mukeyku (BH-9) area. In general the concentration of fluoride increase from north to wards the south and south west of the area.

Factor limiting the concentration of fluoride in groundwater system includes: the type of rock present, signs of previous hydrothermal alteration, the porosity of the rock, the temperature of interaction between rock and water, the concentration of  $\text{Ca}^{2+}$  and PH of the water (Mahon,W.A.J,1964).

Reasons for high concentration of fluoride in the area could be:

- From active volcanic mountain femoral gases, emanating from depth, could feed a lot of fluoride to the ground water. The relation of fluoride with temperature in the area shows that deep boreholes in the area are affected by geothermal activity. From water sample analysis, fluoride concentration is positively correlated with temperature.
- Rock consists of obsidian which covers Boseti mountain has high fluoride content. Mica amphiboles and pyroxene contain appreciable amount of fluoride by OH substitution. During precipitation surface runoff with high fluoride concentration from the obsidian and other recent volcanic rocks joins the ground water system in the southern part of the area.

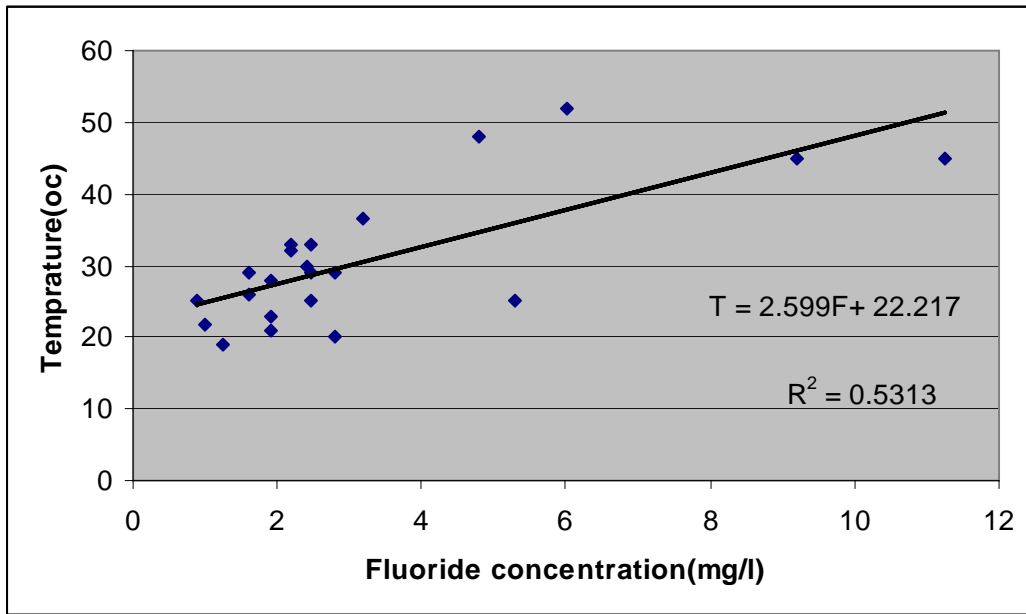


**Fig 6.6** Temperature –Fluoride correlation for the water sample

- Fluoride is quite mobile under most geochemical conditions, in water; stability is limited by the formation of calcium fluoride ( $\text{CaF}_2$ ). High fluoride concentration will thus mostly occur in low calcium water. As Calcium ion is precipitated or low in concentration, there is not enough  $\text{Ca}^{2+}$  to fix the  $\text{F}^-$ . Therefore it appears that fluoride is a mobile component in the acid volcanic terrain. In the study area fluoride ion is negatively correlated with calcium Ion (Fig 6.7) and positive correlation with PH of the water sample.

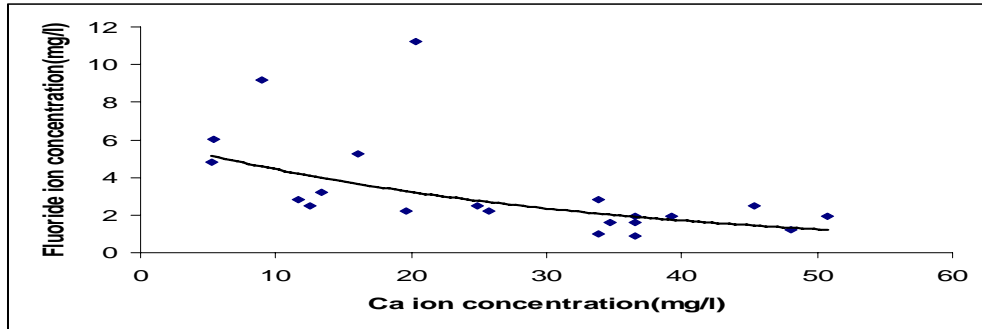


**Fig 6.7** Ca-Fluoride correlation for the water sampled

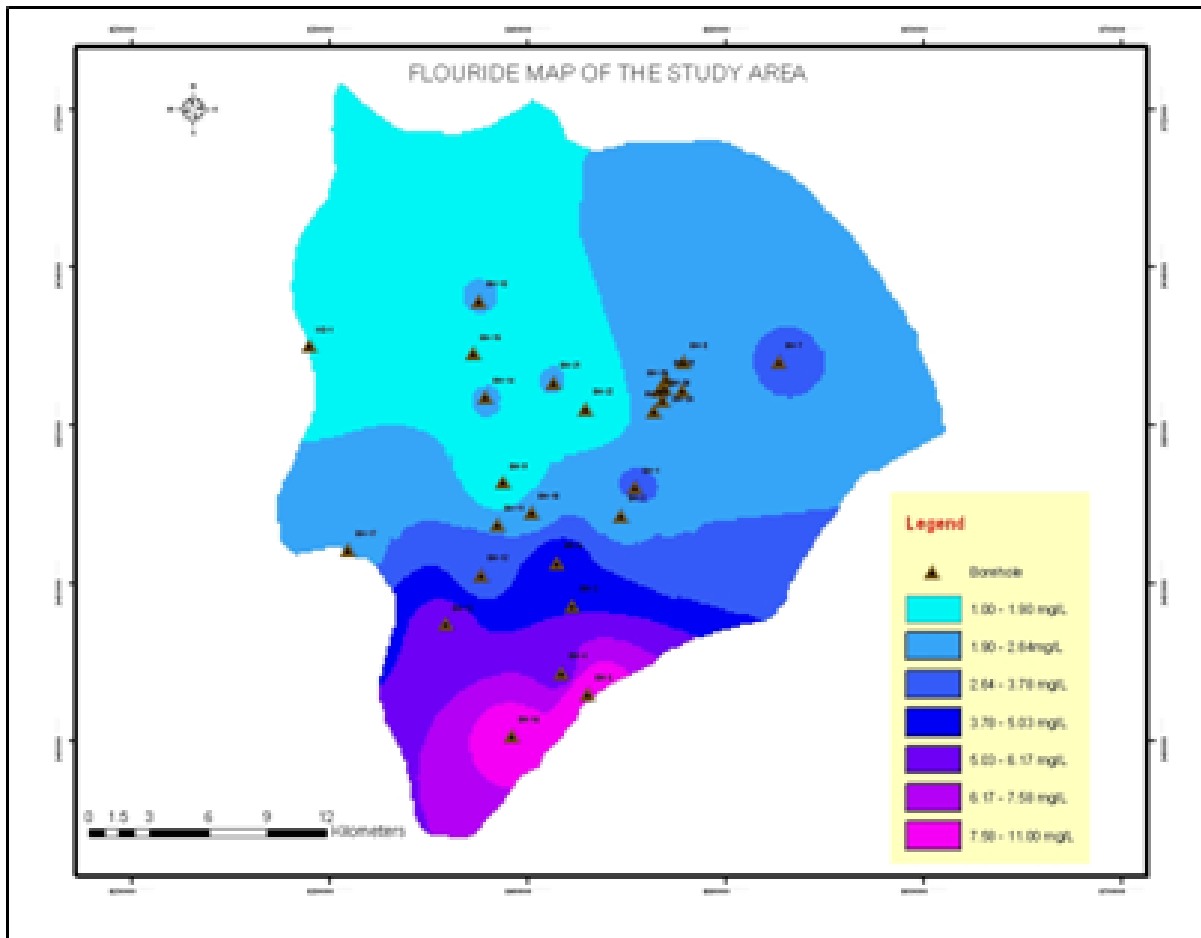


**Fig6.8** Fluoride map of the study area

Vertical distribution of TDS and Fluoride is variable in the study area based on the influence of thermal depth and composition of the rocks.

In general the central and northern part of the plain is relatively less affected by thermal activity in which the saline (TDS) and Fluoride concentration of the water samples is lower than the southern part of the area. The lower value of apparent resistivity at an average depth of 170m around Welenchiti town (Fig.5.5) is due to the nature and degree of fracturing in the water bearing ignimbrite rocks rather than salinity and thermal activities of the area. This can be manifested in boreholes around Welenchiti area, which have lower value of TDS (340-440mg/l), EC (500-620 $\mu$ s/cm), temperature (25-33 $^{\circ}$ c). The southern part of the study area is highly affected by thermal activities and composition of the rocks (Boseti volcanic rocks). In general concentrations of TDS and Fluoride increase as depth to groundwater increases. Well drilled in Golbomitimiti area having groundwater depth of 236m has the highest value of Fluoride ion (11.25mg/l) in the study area.

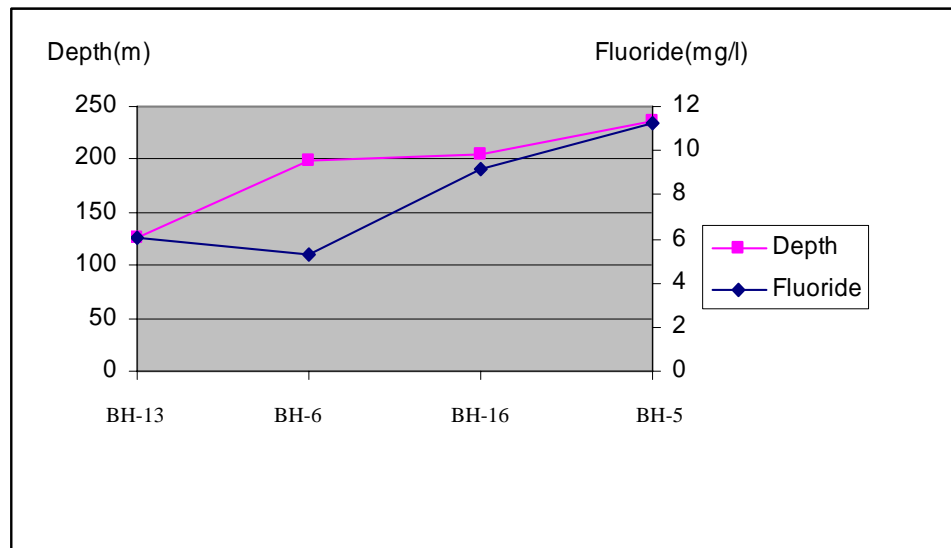


**Fig. 6.9** Vertical distribution of Fluoride in the southern part of the Area

Concentration of fluoride ion increases with depth except for a well drilled in Dibibisa area (BH-13). The higher value of fluoride at relatively shallow depth (126m) is due to shallow thermal depth in Dibibissa area (BH-13) where the

temperature of the water sample is around 52°C and enriched by deep thermal source.

The vertical distribution of TDS increases with depth as the influence of thermal source increases with depth. High temperature emanated from deep thermal source activates water-rock interaction resulting in high concentration of TDS.

#### **6.2.5.2 Chloride**

From the water quality analysis result on the study area, Chloride ion shows slight variation in concentration. Chloride concentration in the study area falls within a range of 4.9 mg/l – 92.2 mg/l. A relatively higher value is observed in chelekiltu, which is associated with water-rock interaction due to higher temperature of the groundwater system. However in general, chloride concentration is lower in the study area.

The lower chloride concentration in the study area is due to deep groundwater system, which is not highly affected by the solubility of some halites or evaporites in sedimentary formation, associated with lacustrine sediments and close to recharge zone resulting in dilution of the ions. The chloride-rich evaporites, formed from high evaporation probably do not infiltrate or recharge into groundwater in sufficient amount due to the low permeability of the lacustrine sediments.

#### **6.2.5.3 Sulfates (SO<sub>4</sub><sup>2-</sup>) and Nitrates (NO<sub>3</sub><sup>-</sup>)**

In most of the analyzed samples, these two anions have relatively low concentrations in the study area.

In general, the nitrate concentration for the most groundwater ranges from 0.4 - 20 mg/l. The relatively lower concentration of Nitrate is related to the absence of deep aquifers affected by anthropogenic source in related to agricultural fertilizers (inorganic) and animal manures (organic sources).

Similarly the sulfate values show relatively lower value ranging from 1.6mg/L in sekeklo area (BH -17) to higher value of 100.3mg/L in chelekiltu area (BH-4) may be due to some volcanic source (Boseti volcano).

### **6.2.6 Alkalinity**

The alkalinity of a solution may be defined as the capacity of solutes it contains to react with and neutralize acid. In almost all natural waters the alkalinity is produced by the dissolved carbonate species, bicarbonates, carbonate and non-carbonates such as hydroxides and silicates. The CO<sub>2</sub> gas from Atmospheric gas present in the soil as well as CO<sub>2</sub> from local magmatic source is the primary source for the production of Alkalinity in natural water. From the water quality analysis result of the study area it has been observed that the Alkalinity of the groundwater in general ranges from a minimum value of 226-266.7mg/l in the lacustrine sediment plain close to north escarpment to some highest values of 743.4mg/l in chelekiltu (BH-4) area on the foothill of Boseti Mountains. The highest values attained is most probably resulted from local CO<sub>2</sub> source for excess bicarbonate production from magmatic sources in relation to the active tectonic events to wards the southern tip of the area

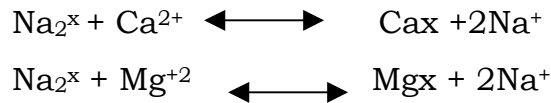
### **6.3 Geochemical Trend along flow paths**

It has been observed that there is a general increasing trend along the groundwater flow path for the sodium, Fluoride and bicarbonate ions attaining higher values in the south and south west of Mt Boset and south east. Similarly there is also an increasing trend for the total dissolved solids most possibly controlled by the rock water interaction along topographic flow paths. The higher TDS values in the south west of Mt Boseti is associated with the volcanic rocks of lava flows and domes of Boseti mountains and some cation exchange in association with lacustrine sediments, rich in clay that give rise to higher Na<sup>+</sup>

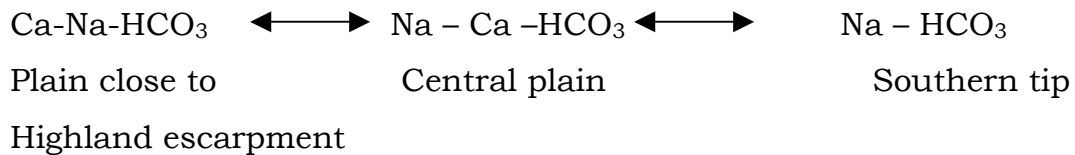
ions raising the TDS value. On the contrary, the  $\text{Ca}^{++}$  cation in general shows a decreasing geochemical trend toward the southern part of the study area.

The cation exchange is a reaction in which the calcium and magnesium in water are exchanged for sodium that was absorbed to aquifer solids such as clay minerals resulting in the higher sodium concentration.

The generalized equation is:



Therefore, from the above discussions of the spatial variation of some major cations and Anions along flow path and from discussions of major water types, the general geochemical trend or evolution of the ground water from plain close to Northern highland escarpment toward the southern tip and south east of the study area can be explained as follows:



#### **6.4 Evaluation of the hydrochemistry with respect to Drinking water quality standards in the study area.**

The chemical analysis results from the water samples in the study area have been evaluated and compared with WHO and Ethiopian guide line values for water quality standards to observe the lever of potability of the water with respect to some major ionic constituents like Fluoride, sodium, chloride, sulfate and etc that are the major threat in relation to health problem.

As can be seen from water quality data, the major anions and cations of sampled water fall with in the range of Ethiopian guideline values. But high fluoride concentration is the major problem that prevails in the study area.

The value of Fluoride ion for 90.9% of the borehole samples analyzed exceeds the WHO guide line. The incidence of medical problems in relation to dental and skeletal flurosis is well observed in the study area particularly in chelekiltu area.

Though it is not a major health threat, next to fluoride, sodium (Na) is also another major element that displays some higher values above WHO guide line in some samples analyzed. Around 5% of the borehole samples show sodium concentration above the guideline (>200 mg/L).

The only hand dug well in the area has both major cations and Anions below WHO and Ethiopian guide lines.

**Table 6.1** comparison with water Quality standards for drinking water

Element	WHO guide Line mg/L	Total % of borehole samples Above WHO guide line	Ethiopian guide line mg/L	Total % of Bore hole samples Above Ethiopian guide line
Fluoride	1.5	90.9	3	31.8
Sodium	200	15	358	5
TDS	1000	9	1776	0
Chloride	250	0	533	0
Sulfate	250	0	483	0
Nitrate	50	0	50	0

### 6.5 Water quality for irrigation purposes

Water quality, soil types and cropping practices all play a role in successful irrigation. Good quality of water permits maximum yields consistent with proper soil and water management.

Study of soil types is used to determine the infiltration rates and leaching of mineral salts. Leaching is essential to the reduction of salinity in the top soil; equally important is to have an understanding about the tolerance of specific crops to certain elements.

### **6.5.1 Salinity and Sodium Adsorption Ratio**

Excessive salinity occurs when there is an accumulation of salts in the topsoil. Salts in soils or water can reduce water availability to the crop to such an extent that yield is affected. Salts added to soil in irrigation activities will reduce crop yield if they accumulate in the rooting depth to damaging concentrations. The crop removes much of the applied water from the soil to meet its evapotranspiration demand but leaves most of the salt behind and become concentrated in the shrinking volume of soil water. A portion of the added salt must therefore be leached from the root zone before the concentration affects crop yield.

Sodium ion also has effects on soils. When sodium rich water is used for irrigation, some of the sodium is taken up by clay and the clay releases calcium and magnesium in exchange in the reaction known as base-exchange reaction. Clays of montmorillonites group can expand and contract in response to changes in the composition of the adsorbed cation between the clay plates resulting in decreasing in permeability of soils and degradation of soil agricultural productivity.

Since large part of the study area is covered with lacustrine sediments of which the top layer is dominated with clay soils, effect of sodium on soils during irrigational during irrigation should greatly be taken into consideration.

The United States salinity laboratory proposed the following relation to calculate the sodium hazard.

$$\text{SAR} = \text{Na} / (\sqrt{(\text{Ca} + \text{Mg}) / 2})$$

Where SAR is defined as Sodium Adsorption ratio expressed in milli equivalents per liter.

The United States Development of Agriculture has developed a widely accepted classification of irrigation waters based on the sodium adsorption ratio as an index for sodium hazard and specific electrical conductance (EC) as an index of salinity hazard.

**Table 6.2** Suitability of natural waters for irrigation

based on EC and SAR

Water class	EC in $\mu\text{s}/\text{cm}$	Alkali hazard (SAR)
Excellent	< 250	<10
Good	250-750	10-18
Medium	750-2250	18-26
Bad	2250-4000	>26
Very bad	>4000	

Based on EC as an index of salinity hazard (Table 6.2), the water samples of the study area can be classified as follows:

**Table 6.3** Suitability of Groundwater in the study area for irrigation  
based on EC

Water samples	Range of EC ( $\mu\text{s}/\text{cm}$ )	Waterclass
BH-1, BH-2, BH-8, BH-9, BH-10, BH-14, BH-15, BH-17, BH-18, BH-20, BH-21, BH-22, BH-23, BH-24, BH-25, BH-26, HD-1	283-740	Good
BH-4, BH-5, BH-12, BH-13, BH-16	783-1800	Medium

**Table 6.4** Suitability of Groundwater of the study area for irrigation  
purpose based on SAR

Water samples	Range of SAR	Water class
BH-1, BH-2, BH-7, BH-9, BH-10, BH-14, BH-15, BH-17, BH-18, BH-20, BH-21, BH-22, BH-23, BH-24, BH-25, BH-26, HD-6.	1.35-9.6	Very Good
BH-13	25.47	Medium
BH-16, BH-4	27.21-40.95	Bad

The SAR of all water samples in the study area except (BH-16, BH-4, and BH-13) is suitable for irrigation from the point of SAR values.

## 6.6 Water Types

Water type classification of the water samples collected from deep bore holes and hand dug well is made to observe the major water groups, their relation

ship and evolution along the flow path by using a graphical method. The piper diagram is the most widely used graphical form. The diagram displays the relative concentration of the major cations and anions on two separate trilinear Plots are projected.

According to this presentation, the water samples of deep wells from areas adjacent to the north highland escarpment shows in general Ca – Na – HCO<sub>3</sub> water type which consists of 19.1 % out of total water sample.

Similarly deep wells on the central part of the plain in general show a water type of Na – Ca bicarbonate consists of 23.8% of the total water samples.

Deep wells on the south west of Mt. Boseti show a water type of Na – HCO<sub>3</sub> consists of 57% of the total water sample.

Fluoride concentration in the Southwest of the study area particularly in Golbomitimiti and Gorowagilo areas Ranges from 9.2 to 11.25 mg/l. Fluoride concentration in areas close to northwest highland (Geldia, worsecha, Dibibsa and chemerijawis) ranges from 1-1.92 mg/l. While in the central part of the area around wlenchiti town the value ranges from 2.2 to 2.9 mg/l.

The possible source of fluoride concentration is a chemical weathering of acid volcanic rocks and magmatic emission. The situation of some high fluoride values for the boreholes having high temperature shows the deep thermal sources and high rock water interaction are the major factors.

From graphical presentation of the water types for the analyzed, different water types have been obtained from the piper plot, which shows some variations. In general boreholes from the north plain close to escarpment show Ca-Na-HCO<sub>3</sub> and boreholes sampled from the central part of the plain (around welenchiti town) show Na-Ca-HCO<sub>3</sub> water type. Deep wells sampled from south west of Mt Boset and eastern part show Na-HCO<sub>3</sub> water type. The only hand dug well in the North West highland shows water type of Na-HCO<sub>3</sub>.

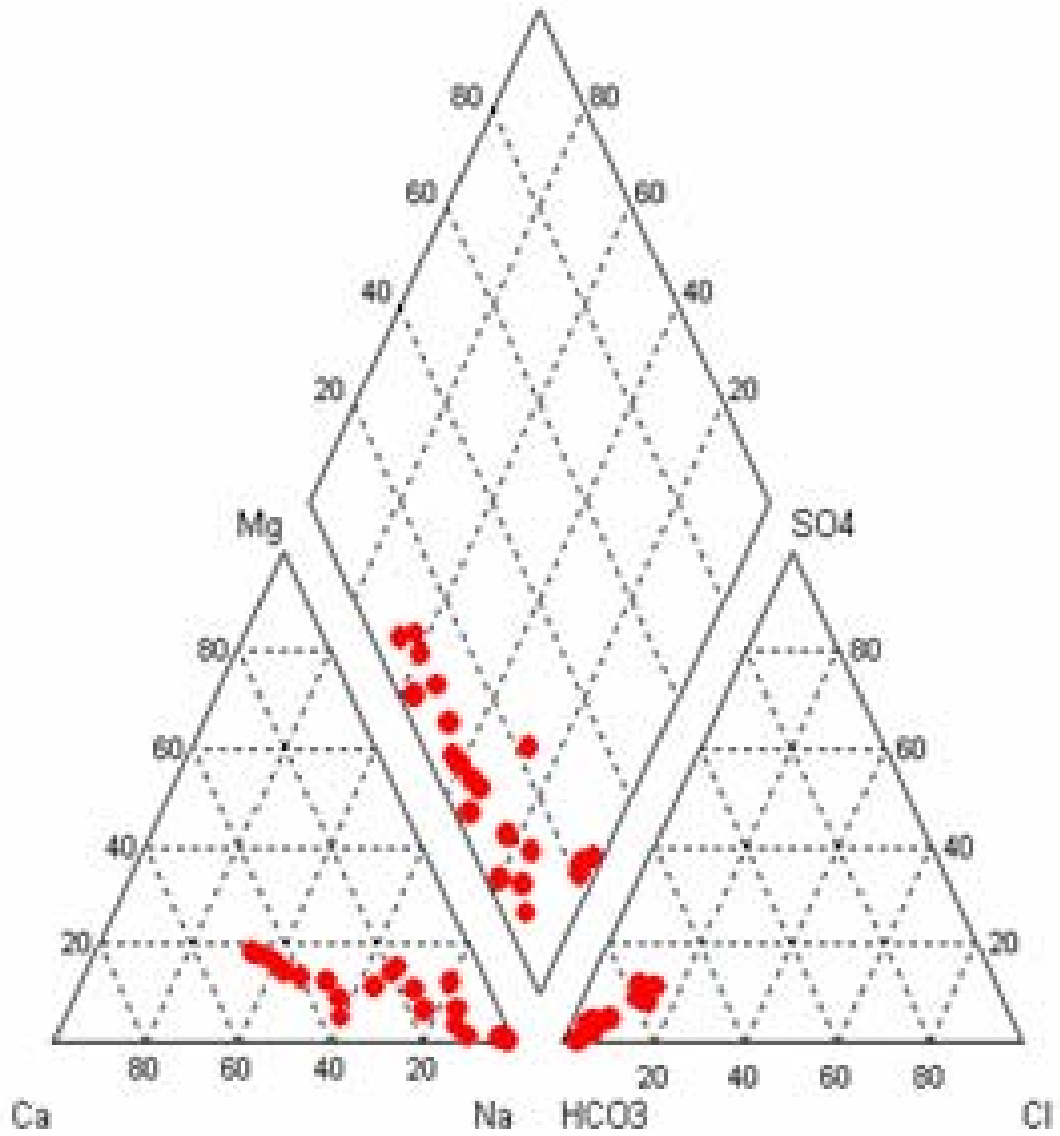


**Fig 6.10** Piper plot for all water samples analyzed from different sample Sources (Boreholes and Handdug well)

## CHAPTER SEVEN

### Synthesis

Annual depth of precipitation has been determined from gauge data of 20 years from three gauging Stations at Nazreth, welenchiti and Ejere.

The precipitation depth computed using Thiessen polygon and Isohytal methods is similar giving values of 874 and 874.5mm respectively. Temperature in the area in general varies from mean minimum monthly values of 14.4°C to mean maximum monthly values of 27.8°C with average of values of 21.1°C. Temperature value is maximum for the months of may and June. Similarly, the estimated mean annual values for wind speed and relative humidity are 2.8 m/s and 47.8% respectively.

The potential evapotranspiration for the area is computed from penman combination method using the necessary meteorological data and the ThornthWaite method using mean monthly temperature values.

The annual potential evapotranspiration from penman combination method is estimated to be 1481mm with relatively higher values for the months of May and June with potential evapotranspiration values of 140 and 135 mm/month. The higher value of potential evapotranspiration calculated from penman method is due to higher value of windspeed at Nazreth station in addition to higher temperature in the study area. The potential evapotranspiration values from Thornthwaite are under estimated with value of 655.4 mm/year.

The actual evapotranspiration of total annual value has been also empirically estimated from Turc's method using mean annual temperature and precipitation values. Using this formula, the annual actual evapotranspiration is estimated to be 697 mm/year. The weighted AET of different land uses using Thornthwaite and Mather soil water balance method gives 842 mm annually. In general actual evapotranspiration value is closer to the annual precipitation

values showing that evaporation is the main cause of water loss from precipitation.

In the study area there are many seasonal and intermittent rivers. Among which Tebo, Geldia and Marmarsa Rivers are the major rivers and gets surface runoff from the northern highland escarpment. The dendritic pattern of the drainage in the study area shows that the area is characterized by hard rocks, as intrusive and extrusive volcanic rocks, which are indeed impervious, less eroded, and tectonized. The flat plain near to welenchiti town is exposed to flooding due to the flat geomorphology of the plain, high intensity rainfall over the area surrounded by hilly terrain, high elevation difference (Fall) and landuse of the area. Therefore peak discharges of the streams during flooding period has been estimated for each streams using curve number method.

Since there is no measured river flow data, Surface runoff has been computed from empirical formula using chow for determining weighted runoff coefficient for different land uses. And runoff coefficient for the study area has been estimated to be 0.19. From this, the runoff depth for the study area is estimated to be 166mm or total amount of 129.5Mm<sup>3</sup>.

Recharge to groundwater has been estimated through water balance calculation giving value of 144mm/year. Only Tebo river has an outlet via southeast of the area. Therefore the surface runoff accumulated from all streams which haven't outlet from the study area is lost from evapotranspiration and infiltrate into soil.

From well log data, pumping test data, structure and local geology of the study area, four hydrostratigraphic units and deep aquifer system distributions have been identified.

The deep aquifer system extends through out the flat and undulating plain exists at an average depth of 170m below the ground surface. The scoriaceous and fractured basalts make up the major aquifer units in the southern and

southeast part of the area with permeability and transmissivity ranging from 5.7- 8m/day and 170-310m<sup>2</sup>/day respectively. From well log data, scoria and weathered basalts overlay these aquifer units. The aquifer units in the central and areas close to the northern highland are fractured ignimbrite aquifers at a depth ranging from 150-200m/day overlain by volcanic rocks and lacustrine sediments. The aquifer units close to the highland escarpment with transmissivity and well yield of 95-127m<sup>2</sup>/day and 3-5L/s respectively, are good potential aquifers than aquifer units around welenchiti town. The lower value may be due to the intercalation of volcanic rocks and remoteness from the tectonic discontinuities which act as conduits from the northern highland of the study area.

On the bases of hydraulic characteristics and water yielding capacity, in general four hydrostratigraphic units have been identified in the study area.

The only hand dug well in the area is found in the weathered part of rhyolite domes in mukeyeku area with groundwater depth and static water level depth of 8m and 5m respectively.

The deep aquifer system of the welenchiti plain gets indirect recharge possibly as groundwater inflow or through tectonic discontinuity like the Intra-rift and wonji faults from the northern highland and escarpment. And direct recharge from precipitation in the lacustrine sediments is less significant due to the prevailing higher evapotranspiration and low permeability of the lacustrine sediments. Topographic high areas or elevated mass of the study area or adjacent areas are recharge zones.

Due to the nature of deep groundwater system, groundwater discharge zones are not observed significantly in the study area.

Both topography and geology plays a major role for the groundwater flow direction in the area. There is in general groundwater flow direction from northern highland towards the plain or topographic low in the valley floor as observed from the potentiometric head map constructed. However the

groundwater flow is diverted away locally from areas, close to Guda and Baricca mountains due to the elevation of static water level which follows replica of the topography. This regional flow is also controlled by the regional tectonics. The groundwater flow direction in the northwest of the study area is NNE to SSW direction along the strike of wonji type faults.

From hydrochemical point of view, insitu or field measured parameters have been used in addition to laboratory analysis of the water samples.

Electrical conductivity for some deep wells sampled show values between 1800  $\mu\text{s}/\text{cm}$  to 435  $\mu\text{s}/\text{cm}$ . Some highest EC value of 1800  $\mu\text{s}/\text{cm}$  is observed in Golbomitimiti area in the south west of Mt. Boseti. Electrical Conductance is related to total dissolved solids and positively Correlated.

Water temperature for most deep wells sampled in the field shows values from 19 to 52 $^{\circ}\text{C}$ . The highest value is observed in south west of Mt. Boseti. Heat from deep thermal sources due to tectonic activities is the major cause for this high temperature. The TDS value varies from a minimum value of 300 to 400mg/l in areas close to the escarpment, which is close to the recharge zone for the plain to some high value of 800 to 1030mg/l in most boreholes in the southern part of the study area. The higher value of TDS in the southern part of the study area is related to water-rock interaction along flow path. The reaction is activated with higher temperature from deep geothermal sources.

Out of the major cations analyzed, sodium and calcium ions in general show some relationship spatially along groundwater flow path from northern escarpment toward the southern tip of the study area. As a result the ( $\text{Na}^+$ ) concentration ranges from minimum values of 41-68 mg/L in areas (adjacent to escarpment) to maximum values of 270-420 mg/L in the southern part of the area. On the contrary the calcium ion shows a decreasing trend from minimum values of 2.2-8.9 mg/L in southern part of the study area to maximum values of 38-51 mg/L to ward the highland escarpment. Sodium and Calcium have negative correlation in the study area. The higher value of sodium towards the southern part of the study area associated with acidic volcanic of rocks rich in

alkali feldspars and sodium plagioclase of which sodium is the major constituent.

The concentration of fluoride ion also varies from 9.2mg/l-11.25mg/l in the southwest of Mt. Boseti to 1.24-1.92mg/l in the northern periphery of the plain. Concentration of the fluoride is associated with acidic volcanic rocks. Obsidian rocks found in Boseti contains high fluoride. In addition; gases emanated from depth may feed fluorine gas to the groundwater. Fluoride concentration is positively correlated with temperature of the deep groundwater samples. Lower values of chloride are observed (4.9-92mg/l) in the study area. This shows infiltration of dissolved halites and evaporites deep into groundwater are restricted due low permeability of the lacustrine sediments and the lower residence time (close to recharge zone resulting in dilution). The lower value of sulfates and nitrates also related to deep nature of groundwater system, which is not affected by anthropogenic sources in related to agricultural activities.

From graphical presentation of the water types for the analyzed samples different water types have been obtained from the piper plot. From this it has been observed that boreholes close to northern escarpment in general show Ca-Na-HCO<sub>3</sub> and boreholes in the central part of the study area shows Na-Ca-HCO<sub>3</sub> While boreholes from southern part of the study area show Na-HCO<sub>3</sub> type.

The groundwater in general shows an evolution trend from Ca-Na-HCO<sub>3</sub> in areas close to the escarpment towards Na-HCO<sub>3</sub> types in the southern part of the study area.

## CHAPTER EIGHT

### Conclusion and Recommendation

#### 8.1 Conclusion

The current study revealed that the groundwater condition in the welenchiti area in general is characterized by the existence of deep aquifer units of fractured ignimbrites, fractured and scoriaceous basalts.

The deep aquifer units of fractured ignimbrites in the welenchiti plain show a moderate transmissivity and permeability values ranging from 36-124m<sup>2</sup>/day and 1-4.5m/day respectively with drawdown of 6-12m and well yielding of 2.4 – 8.4 l/s. The deep aquifers of scoriaceous basalts in the southern tip and eastern of the study area show higher transmissivity and permeability values ranging from 170-310m<sup>2</sup>/day and greater than 5m/day respectively and with well yield of 4.6-7 L/s .

Direct recharge into groundwater is percolation through fractures and hidden tectonic discontinuities. However direct percolation through soil is insignificant in the welenchiti plain covered with lacustrine sediments. This is due to high evaporation rate and low permeability of lacustrine sediments. Towards the southern part of the study area where the lithology is highly vesicular, scoriaceous and affected by deep and vertical joints, some amount of surface runoff from Mt. Boseti and local precipitation recharge to groundwater through tectonic discontinuity and groundwater inflow from adjacent areas.

In general groundwater recharge to the welenchiti plain is from the northern highland and escarpment through tectonic discontinuities particularly faults striking NNW to SSW and dipping towards the plain. Recent tectonic episodes like the wonji fault lines and associated fractures also play an important role for the groundwater circulation.

Groundwater flow direction is generally from NNE – SSW from the northern up land towards the southern tip and southwest of the study area but locally away from Boseti mountains.

The hydrochemical analysis of water samples in the area revealed that water samples from deep wells adjacent or close to north highland escarpment have relatively lower values of TDS, Temperature, sodium and Fluoride. While the water sampled from deep wells in southern part of the study area particularly south west of Boseti Mountain have high value of TDS, EC, sodium and fluoride. The relatively lower values of TDS in the areas adjacent to highland may be due to the close situation of these aquifers to the recharge zone and slow water- rock interaction. Where as higher values of TDS in the southern part is due to water rock interaction along the flow path. The relatively higher Fluoride in south west of Boseti is due to dissolution of high fluoride content of volcanic rock and emission from deep thermal source.

The general geochemical trend for the ground water follows the groundwater flow path evolving from calcium – sodium bicarbonate water type in the plain close to highland escarpment towards sodium bicarbonate water type in the southern tip of the study area.

## **8.2 Recommendation**

→ From the water resource development point of view, although the southern tip of the study area has high permeability and productivity to exploit deep aquifer system than the central and northern part of the plain, groundwater development activities should be avoided from the hydrochemical point of view where most deep wells are dominated with high fluoride concentration and high temperature. Where as areas close to northern west escarpment show moderate permeability and productivity with relatively better hydrochemistry recommendable for water source development.

→ Since the existing borehole data over the entire area is few and nothing in the north escarpment, some additional well drilling tests could give a good picture of permeability, productivity and thickness of aquifer units which are highly related to groundwater potential evaluation of the study area.

→ Most of the aquifers of the area not fully penetrated. Thus to establish detailed knowledge in depth of wells, aquifer thickness and consequently the actual yield and transmissivity of the aquifer of the study area, drilling should penetrate to the full depth of the aquifer thickness.

→ The hydro-geochemical trends and the most possible geochemical controls along flow paths from the escarpment to the plain needs a detail isotope analysis which could give a good result with respect to recharge mechanisms, tracing recharge source and recharge amount estimation for the groundwater potential in the Welenchiti area.

## References:

- Alua Damte, (1990).** Neotectonics of Nazreth – Dera area. M.SC. Thesis,AAU
- Berhanu Gizaw, (1996).** The origin of high bicarbonate and fluoride Concentration in waters of the MER valley.
- Brotzu P., Morbideli L., Piccirillo E.M., Traversa G. (1974)** petrological features of the Boseti Mountains, a complex volcanic system in the axial portion of the Main Ethiopian Rift. Bulletin volcanologique, 38.206-233.
- Brotzu P., Morbidelli L., Piccirillo E. M., Traversa G.(1980)** Volcanological And magmatological evidence of the Boseti volcanic complex (Main Ethiopian Rift). Att dei convegni lincci, 317-366.
- Chow Yen Te, (1988).** Applied hydrology, Mc Graw – Hill book Company.
- Esayas Gebre Kidan, (2005).** Water balance and effect of irrigated Agriculture on the water quality in Metehara area.
- Fetter, C.W., (1994).** Applied hydrogeology, 3<sup>rd</sup> edition.
- Freeze R. Allam and Cherry Jhon A. (1979)** Ground water Prentice Hall, NewJersy.
- Fournier, R.O., Truesdell, A.H.(1970).** Chemical indicators of subsurface tepmtrature applied to hot spring waters of yellow stone National park, USA. Geothermic, Special Issue 2, 529-535.
- Getahun Kebede, (1987).** Hydrogeology of Nazreth area.
- Gezahegn Yirgu, Dereje Ayalew, Peccerillo A, Barberio, M. R.; Donati, C.; Donato, P.; (1999)** Fluorite and chlorine distribution in the volcanic rocks from the Gedemsa volcano, Ethiopian Rift Valley, Acta Vulcanologica, 11(1): 169-176.
- Hem, J.D, (1985).** Study and interpretation of the chemical characteristics of natural water, USGS water supply paper 1473, 263p.
- Kazmin V.and seife Michael Berhe, (1978).** Geology and development of the Nazreth area northern Ethiopian rift.
- Keith E.Anderson, (1993).** Ground water hand book.

- Koga, A, (1969).** Formation of bicarbonate ion in hot spring water, In Report No, 20 on the springs in Iota prefecture (in Japanese), 59-62.
- Lerner, D.N., Issar, A.S. and Simmers, I. (1990)** Groundwater recharge, IAH, Vol. 8, Hannover, Germany, 344pp.
- Mahon, W.A.J. (1964).** Fluorine in the natural thermal waters of New Zealand. New Zealand Journal Science 7, 3-28.
- Mohr P.A., (1962).** The Geology of Ethiopia. University College of Addis Ababa press.
- P.K. Bhattacharya, (2003).** Elements of hydrology
- Seifu Kebede, and Travi, y. (2000).** Comments to an article entitled 'ageochemical survey of spring water from the main Ethiopian rift valley, southern Ethiopia: implications for well-head protection' by McKenzie et al, Hydrogeology journal (2001) 9:265-272.
- Shaw, E.M., (1988).** Hydrology in practice. Second edition, Chapman and Hall.
- Skuthan Bohumir, Kidane Araya, Berhanu Bekele, (1982).** Geophysical Survey for hydro geological study in the Nazareth area
- Tamiru Alemayehu and A. Vernier (1997).** Conceptual model for Boku Hydrothermal area, (Nazareth) Main Ethiopian Rift valley. Ethiopian Journal of Science, 20(2):283-291.
- Tamiru Alemayehu and Tenalem Ayenew, (2001).** Principles of hydrogeology.
- Tamiru Alemayehu, (2006).** Ground water occurrence in Ethiopia.
- Taye Zewde, (1987).** Geophysical Investigation for ground water exploration Nazareth-Welenchiti Area.
- Tesfaye Cherenet, (1983).** Hydrogeology of Ethiopia, Ethiopian Institute of Geological Survey, Addis Ababa.
- Teshome Dechasa, 1999.** Water balance and effect irrigated agriculture on Groundwater quality in the Wonji area, M. S. C Thesis, Addis Ababa University.
- Thornthwaite, C.W., (1944).** In report of committee on transpiration and evaporation: Am. Geophys. Union Trans., V. 25, pt.s P. 683 -693.

**UN, (1973).** Investigation of geothermal resources for power development: geology, geochemistry and hydrology of hot springs of the East African Rift system with in Ethiopia. UN Development program Report DP/SF/UN/116, 27SP.

**UNESCO, (1984).** Methods of Computation of the water balance.

**Visetin Tustin E, and piccirillo EM, Zanettin B. (1977).** Volcanic Succession, Tectonics and magmatology in Central Ethiopia.

**Zanettin B., And Justin-Visentin E., (1974).** The Volcanic Succession In Central Ethiopia , The Volcanics Of The Rift And Ethiopian Rift Margins. Mem. First Geol. Univ. Padova P73 31:1-19.

**Annex 1:** Location and Pumping test data of the boreholes used in this work

Index	Site name	UTME	UTMN	Elev(m)	Depth(m)	SWL(m)	DWL(m)	Yield(l/s)	T(m <sup>2</sup> /day)	specific yield(l/s/m)	permeability(m/day)
BH-1	Dengore Tiyo	545511	952863	1464	150			3			
BH-2	Dengore.N	544772	951424	1467.3	180			3			
BH-3	Borofa Kurkufa	542296	946871	1489.6							
BH-4	Chele Kiltu	541731	943438	1486.6							
BH-5	Golbomitimiti	543079	942366	1502.6	236	151.3		5.6	170		5.2
BH-6	Furda	541516	949046	1464.7				3.4			
BH-7	Feto	552712	959185	1379.3	200			4.5			
BH-8	Buta Dengore	547922	959185	1466.3	182.56	144.73	150.75	3	35.79	0.66	1
BH-9	Mukeyegu	538774	953120	1513.7	157	91.01	107.54	3.9	16.5	0.24	0.555
BH-10	Marmarsa	540218	951558	1481.6							
BH-11	Guraja Ferda	538498	950940	1495	164	84					
BH-12	Wachulafa	537673	948419	1492.4							
BH-13	Dibibibisa	535918	945906	1483.3	126	99.6	105.74	8.4	124	1.36	5.4
BH-14	Choba Chore	537928	957417	1572.1	145	104		2.4	95		
BH-15	Worsecha	537294	959643	1908.6	199	137.66	126.39	4.6	127.45	0.48	
BH-16	Goro Wagilo	539213	940271	1522.8	205	176.38		6.5	310		8
BH-17	Sekelo	530954	949680	1712.1	229	177.6		4.43			
BH-18	Chemeri Jawis	537592	962318	1666.2	262			4			
BH-19	Digelu wanga	547062	958304	1467.1	182	120					
BH-20	Rokecha Bokre	541516	949046	1464.7	199	132		1.5			
BH-21	merko Sala	541310	958167	1516.9	80			3			
BH-22	Warka	542960	956854	1482	145	95.2	101.6	0.8	6.9	0.125	0.52
BH-23	Wollenchiti 2	547842	957786	1457.5	180			4			
BH-24	Wollenchiti 1	547003	957874	1464.7	180			4			
BH-25	Wollenchiti 3	546727	957797	1465	171			4			
BH-26	Wollenchiti 5	546852	957290	1460.7	174			5			
BH--27	wollenchiti 4	546454	956736	1457.2							
HD-1	Mukiyero	528968	960038	2233	8			5			

**Annex 2: Hydrochemistry data used in this work**

Index	BH-1	BH-2	BH-4	BH-5	BH-7	BH-8	BH-9	BH-10	BH-12	BH-13	BH-14	BH-15
Temperature (oc)	29	27.8	48	45	20		21.7	26	36.6	52	29	19
Turbidity	4	3	4	3	4	1	3	2	4	3	5	3
TDS (mg/l)	482	500	1168	900	660	312	346	369	495	904	328	359
EC (MS/cm)	722	729	1729	1800	995	647	502	545	783	1361	464	511
PH	7.93	7.58	8.37	7.3	7.66	7.32	7.55	7.43	7.74	8.34	7.54	7.47
NH4 (mg/l)	0.13	0.13	0.113	0	0.06	-	0.25	0.113	0.15	0.13	0.113	0.188
Na (mg/l)	137	107	420	-	170	-	65	68	143	278	49	44
K (mg/l)	14.9	19	21	-	14.3	-	18.5	18	22	31	14.3	15.5
Total Hardness (mg/l)	75.5	133.2	19.98	-	139	-	97.7	111	59.9	31.1	122.1	166.5
Ca (mg/l)	11.6	36.5	5.3	20.4	33.8	-	33.8	34.7	13.3	5.4	36.5	48.1
Mg (mg/l)	11.3	10.3	1.62	8.16	13.5	-	3.2	5.9	6.5	2.2	7.6	11.3
Fe (mg/l)	0.02	0.02	0.02	0.07	0.02	-	0.02	0.02	0	0.03	0.03	0
Mn (mg/l)	0.02	0.07	0	0.01	0.02	-	0	0	0	0	0	0
F (mg/l)	2.8	1.92	4.8	11.25	2.8	2.4	1	1.6	3.2	6.04	1.6	1.24
Cl (mg/l)	7.8	9.7	92.2	8	42.7		6.8	8.7	23.3	56.3	8.7	11.6
NO3 (mg/l)	16.3	20	10.7	10.56	10.5	0.4	10	10	8	10.5	8.5	10
Alkalinity (mg/l)	378	363.3	743.4		428.4		246	266.7	368	571.2	226.8	243.6
CO3 (mg/l)	0	0	72	0	0		0	0	0	24	0	0
HCO3 (mg/l)	461	443.2	819.1	1191	522.6		300	325.4	448	648.1	276.7	297.2
SO4 (mg/l)	2.4	15	100.3		64.7	22.8	6.9	4.2	21.1	60.7	11.6	10.6
PO4 (mg/l)	0.4	0.37	0.6	0.64	0.512	0.306	0.27	0.287	0.19	0.369	0.348	0.185

Index	BH-16	BH-17	BH-18	BH-20	BH-21	BH-22	BH-23	BH-24	BH-25	BH-26	HD-1
Temperature(oc)	45	21	23	25	25	25	33	33		29	19
Turbidity	2	4	3	0	5	5	0	4	3	2	12
TDS(mg/l)	1032	310	348	526	340	362	480	420	428	458	192
EC(MS/cm)	1650	435	499	740	500	520	677	622	616	652	283
PH	8.71	8.02	7.42	7.81	7.42	7.64	7.63	7.64	8.11	7.9	8.75
NH4(mg/l)	0.38	0.113	0.188	0.13	0.188	0.113	0.15	0.25	0.15	0.188	0.28
Na(mg/l)	350	44.5	41	142	47	64	106	106	99	132	30.5
K(mg/l)	26.5	12.8	13.5	16	15.5	12.9	14.6	17.5	15.5	11.4	13.9
Total Hardness(mg/l)	31.1	131	175.4	53.3	155.4	124.3	115.4	68.8	111	35.5	44.4
Ca(mg/l)	8.9	39.2	50.7	16.02	45.4	36.5	24.9	19.6	25.8	12.5	16
Mg(mg/l)	2.2	8.1	11.9	3.2	10.3	8.1	12.96	4.86	11.3	1.1	1.1
Fe(mg/l)	0	0.03	0	0.04	0	0	0.02	0.03	0	0.03	0.1
Mn(mg/l)	0	0	0.07	0	0	0	0	0	0	0	0.05
F(mg/l)	9.2	1.92	1.92	5.28	2.48	0.9	2.48	2.2	2.2	2.48	0.8
Cl(mg/l)	83.4	4.9	7.76	15.5	7.8	7.8	7.8	11.6	9.7	9.7	16.5
NO3(mg/l)	7	11.75	7.5	11.75	13.5	8	16.25	10	12.5	7	18.3
Alkalinity(mg/l)	699.3	224.7	249.9	361.2	235.2	262.5	359.1	304.5	312.9	340	69.3
CO3(mg/l)	50.4	0	0	0	0	0	0	0	2.4	0	19.2
HCO3(mg/l)	750.7	274	304.9	440.7	286.9	320.3	438.1	371.5	376.8	415	45.5
SO4(mg/l)	65	1.6	6.1	12.4	12.1	12.1	2.1	14.8	13.5	6.6	31.7

**Annex.3.** Mean Monthly maximum Temperature (°c) at Nazreth station

<b>year</b>	<b>Jan</b>	<b>Feb</b>	<b>Mar</b>	<b>Apr</b>	<b>May</b>	<b>Jun</b>	<b>Jul</b>	<b>Aug</b>	<b>Sep</b>	<b>Oct</b>	<b>Nov</b>	<b>Dec</b>
1985	30	x	32	30	31	32	27	25.7	28	29	30	29
1986	30	31	30	34	34	30	28	28.4	31	28	29	30
1987	25	32	31	30	30	30	29	27	30	28	31	31
1988	31	33	32	33	33	32	25	27	28	31	25	27
1989	29	29	29	27	32	30	24	24.7	27	27	28	28
1990	27	28	26	27	30	30	26	27.5	26	28	27	26
1991	28	x	29	29	x	30	25	24.8	27	27	27	27
1992	26	26	30	30	31	30	25	24.4	25	27	26	26
1993	25	25	30	28	28	29	25	25.1	27	28	x	x
1994	x	x	x	x	31	29	26	25.4	26	26	26	25
1995	27	29	29	28	31	32	26	25.5	27	x	27	28
1996	29	30	30	29	29	27	26	25.5	27	27	28	26
1997	28	28	30	29	31	30	26	26.3	28	28	26	26
1998	27	29	29	32	32	x	x	25	26	28	27	26
1999	27	29	28	31	32	31	25	25.2	27	27	26	25
2000	73	28	30	30	31	30	26	25.6	27	27	26	25
2001	25	27	29	30	30	28	26	25.3	27	26	27	27
2002	26	29	30	31	33	31	29	26.6	28	26	29	27
2003	27	30	30	29	32	30	26	25.9	27	29	28	25
2004	28	28	29	29	x	30	26	26	27	27	27	26

**Annex 4:** Mean Monthly minimum Temperature (°c) at Nazreth station

year	Jan	Feb	Mar	Apr	May	June	July	Aug	Sept	Oct	Nov	Dec
1985	11		15	16	16	17	15	15	15	10	9.1	11
1986	11	15	13	14	15	16	16	14	16	11	11	16
1987	12	15	15	14	14	18	15	16	15	12	9.7	8.2
1988	12	15	13	13	15	17	11	14	15	10	7.6	8.2
1989	8.5	16	16	14	17	15	12	15	15	11	10	14
1990	13	15	14	14	17	18	16	16	15	12	12	12
1991	14	x	15	15	x	18	16	16	15	13	12	11
1992	14	15	16	16	16	17	15	16	14	12	12	14
1993	14	14	14	15	16	16	15	15	15	x	x	x
1994	x	x	x	x	16	17	16	16	14	11	13	11
1995	11	14	14	15	13	15	16	15	14	13	13	14
1996	14	14	15	15	15	17	16	16	15	12	13	12
1997	13	15	x	x	x	x	x	x	15	16	15	13
1998	14	16	16	16	17	18	16	16	15	14	13	11
1999	12	13	15	15	16	17	15	15	15	14	9.8	7.9
2000	9.2	13	15	16	17	18	16	16	15	14	13	12
2001	12	13	15	15	17	17	16	16	14	14	13	13
2002	14	14	16	16	18	18	17	17	15	14	13	15
2003	13	15	13	16	15	17	16	16	16	13	14	12
2004	15	13	13	16	17	18	16	16	15	14	14	14

**Annex: 5 Mean** monthly Rainfall (mm) at welenchiti station

year	Jan	Feb	Mar	Apr	May	June	July	Aug	Sept	Oct	Nov	Dec
1986	0	169	92.7	104	86	80.9	156	95.1	154.1	8	0	0
1987	0	37.7	220.4	132	272.6	1	91	166	24.7	9.7	0	0
1988	15	17.2	5.6	30.5	6.5	29.8	185	206	186.9	16.9	0	0
1989	0	189	149.5	286	0	83.4	186	244	119.2	1.4	0	14
1990	3.2	332.8	91.7	95	14.4	0	243	201	141.9	9.3	0	0
1991	2.7	90	137	16.9	7.1	23.8	223	184	44.4	4.8	1.2	5.6
1992	18.3	62.4		102	0	42.5	131	357	90.7	17.5	3.4	8.1
1993	47.1	50.7	0	114	31	42.2	211	140	140.8	19.6	0	0
1994	0	2.1	27.4	23.7	26	66.3	305	186	77.5	2.8	36.9	13.4
1995	0	57.4	163.4	95.7	12.9	46.1	156	310	135.5	12.1	0	3.5
1996	52.1	0	180	91.7	168.8	86.1	201	151	73.6	42.5	0	0
1997	29.8	0	38.2	23.2	44.7	145.7	255	131	88.6	117.8	51.4	0
1998	41.6	40.6	86.1	33.5	47	48.1	154	337	197.2	179	0	0
1999	11.1	0	104.1	0	0	39.1	247	233	52	167.4	3.6	0
2000	0	0	15.5	18.4	47.9	58.4	249	250	110.9	96.3	30.5	6.1
2001	0	0	128	20	65.9	76.5	241	305	91	33	10	0
2002	0	0	48.9	61.4	10	18.7	166	232	36	0	0	97.7
2003	32.5	32.1	119.6	153	0	61.2	393	322	7.5	0	0	28.3
2004	47.3	81.4	146.9	169	0	91.8	251	289	84	60	0	10.2
2005	30	24	93	65.9	110.4	91.5	69.4	123	50.6	0.4	2.3	0

**Annex 6: Mean monthly Rainfall (mm) at Ejere station**

year	Jan	Feb	Mar	Apr	May	June	July	Aug	Sept	Oct	Nov	Dec
1985	0.5	0	17.4	61.5	91.2	8.5	395	211	93.5	15.4	0	0
1986	0	67.8	59.5	103	22.9	160.7	98.3	134	76.3	8.4	0	0.4
1987	0	47.7	82.9	75.3	234.3	17.8	65	215	31.5	10.8	0	0
1988	3.3	20.8	12.5	16.7	41.2	29.1	166	245	120	22.1	0	0
1989	0	45.8	50.8	140	0	75.1	175		78.5	3.9	0	0
1990	2	145	41.3	67.7	8	18.3		197	152	1.7	0	0
1991	0	36	87.6	17	21.5	27.7	216	192	132	0	0	0
1992	2.4	18.6	43	63	19	32.5	232	175	99.6	7.1	2.3	3.7
1993	10.2	24.6	0	79.4	40.4	88.1	245	184	138	11.9	0	4.5
1994	0	0	5.4		43.8	91.6	210	110	134	0.9	27.1	4.1
1995	0	44.5	64.7	78.7	16.6	52.5	135	277	88.2	1.5	0	1.4
1996	105	0	94.6	30.2	151.7	170.7	192	151	121	0	17.5	0
1997	23.4	0	29	39.9	51.3	77	205	197	26.3	133	62.4	0
1998	2.2	128	4.1	32.8	47.6	63.6	252	270	107	153	0	0
1999	11.4	36.8	56	0	25.6	57.5	319	305	60.8	95.6	0	0
2000	0	0	10	20.9	16	97	259	163	143	21.4	32.6	10.2
2001	0	12.8	99.3	14.7	75.3	131.3	307	224	42.3	0	0	14.5
2002	2.2	9.5	49.3	4.3	39.4	29.2	203	254	100	0	0	49.2
2003	29.4	50.8	5.7	101	0	112.5	319	360	125	0	0	66.4
2004	27.2	2.9	76.4	64.9	0	74	166	393	100	28	0	0

**Annex 7:** Mean Monthly Rainfall (mm) at Nazreth staion

year	Jan	Feb	Mar	Apr	May	June	July	Aug	Sept	Oct	Nov	Dec
1985	3	17.1	23.1	183.4	67.3	8	399.4	327.4	174	0	0	0
1986	0	96.5	41	6.2	54.4	152.4	263.3		20.4		0	0
1987	0	11.2	80.2	81.1	259.6	0	161.6	243.4	30.8	0	0	0
1988	34	31.3	6.8	50.9	9.4	50.3	185.4	171.4	186.9	52.9	0	0
1989	0	29.9	21.7	95.4	0	54.7	182.5	281.2	80.3	5.7	0	3.5
1990	0.7	183.9	83	114.7	13.3	12	337.8	168.7	153.7	7	0	0
1991	0		111	13.5		43.5	332	232.8	89	13.1	0	1.7
1992	41.2	27.8	0	66.3	8.6	86.3	240.3	195.7	121.4	22.1	1.3	1.2
1993	4.6	51.9	0	102.6		64.1	345.2	142.4	79.3	20	0	0
1994	0	0	2.6	49.1	26.5	70.1	229.6	171.5	173.8	13.8	35.6	51
1995	0	26.5	46.9	127.2	33	46.5	203.1	251.4	88.2	14.7	0	2.8
1996	27.2	0	112	65.1	115.2	120.2	220.2	250	93.9	0	7.9	0
1997	14.4	0	75.3	28.5	6.9	94	193.1	240.9	75.5	117	31.5	0
1998	11.8	25.6	105	19.8	49.3	55.3	196.5	220.6	144.7	133	0	0
1999	9.2	0	34.6	1.2	18.6	74	283.2	194.4	66.3	165	3.1	0
2000	0	0	20.2	16.1	51.5	60.8	355.1	269	133.6	85.7	57.8	12.9
2001	0	6.2	108	28.7	177	51.2	216.8	145.3	107.8	1.7	0	6.6
2002	20.9	11.1		51.3	22.5	50.2	129.9	205.7	65.3	1.1	0	34.5
2003	46.5	69.1	151	88.9	3.6	75.2	235.6	279.7	122.8	0	5.3	48.8
2004	28.8	3.3	77.4	53.1	1.9	65.3	1144	227.3	77.1	58.6	12.8	1.6

**Annex 8:** Mean Relative Humidity (%) at 18:00 at Nazreth station

Year	Jan	Feb	march	Apr	May	June	July	Aug	Sept	Nov	Oct	Dec
1990	39	66	62	57	39	39	60	67	66	47	41	34
1991	36	X	45	38	38	35	62	62	62	38	36	37
1992	47	54	44	41	40	51	56	63	57	45	34	41
1993	49	53	32	52	50	48	63	58	62	60	x	x
1994	x	x	x	x	33	47	62	62	65	35	48	43
1995	32	44	49	49	39	36	59	65	56	37	41	49
1996	54	44	54	43	44	54	59	62	61	37	48	41
1997	47	34	46	49	40	44	54	56	47	59	61	48
1998	55	47	49	39	45	37	56	62	64	57	42	36
1999	36	26	48	29	33	40	58	59	60	66	36	36
2000	32	22	26	39	32	44	56	59	65	57	45	41
2001	36	33	44	35	39	46	55	63	54	36	35	32
2002	40	24	37	x	x	x	x	x	x	x	x	x
2003	x	x	x	x	x	x	x	x	x	x	x	x
2004	X	X	X	47	25	41	54	55	54	44	36	43
2005	43	27	41	40	47	40	56	54	57	38	36	37

**Annex 9:** Mean monthly Relative Humidity (%) at 12:00 at Nazreth station

Year	Jan	Feb	march	Apr	May	June	July	Aug	Sept	Nov	Oct	Dec
1990	51	55	61	56	42	49	72	74	66	47	43	44
1991	38	X	47	40	29	44	79	62	56	41	41	37
1992	45	52	45	45	35	41	55	55	51	48	37	55
1993	54	64	38	57	53	61	74	64	58	71	X	X
1994	x	x	x	x	38	53	58	63	53	35	47	45
1995	38	44	50	52	38	39	60	72	55	37	37	48
1996	58	48	54	46	51	60	66	68	63	39	50	44
1997	51	40	47	51	38	50	64	61	50	55	57	48
1998	56	53	56	42	50	47	61	68	59	58	41	32
1999	44	32	48	30	32	42	64	66	55	55	35	38
2000	36	30	28	32	32	37	53	60	64	62	39	41
2001	39	35	46	37	45	55	52	69	55	38	32	40
2002	51	33	44	x	x	x	x	x	x	x	x	x
2003	X	X	X	51	36	50	64	64	55	45	42	49
2004	51	35	50	43	52	51	66	62	58	41	41	42

**Annex 10:** Mean monthly sunshine hours at Nazreth station

<b>Year</b>	<b>Jan</b>	<b>Feb</b>	<b>march</b>	<b>Apr</b>	<b>May</b>	<b>June</b>	<b>July</b>	<b>Aug</b>	<b>Sept</b>	<b>Nov</b>	<b>Oct</b>	<b>Dec</b>
1990	7.4	X	X	7.1	9	9.1	6.8	6.9	7	9.2	9.6	9.7
1991	x	x	8.4	9.4	8.3	x	6.7	X	X	X	X	8.7
1992	7.2	7.2	9.2	8.5	9.6	8.5	6.4	5.1	7.3	9.2	9.3	8.7
1993	8.3	7.3	8.9	7.7	8.5	8.9	7.4	8.4	7.2	9.1	10.2	9.4
1994	10	9.8	8.5	8.3	9.8	7.3	6.1	7.2	7.7	10.3	9.2	
1995	10.3	9.3	8.6	8.3	9.9	9.9	6.1	6.9	8	9.8	10.6	9.8
1996	8.9	10	8.8	9.8	X	X	X	X	X	X	X	X
1997	x	x	x	x	x	x	x	x	x	x	x	x
1998	x	x	8.2	9.4	9	9.1	6.7	6.8	7.6	7.1	10.1	10.6
1999	9.4	5.2	4	5.2		9.3	6.5	7.9	8.6	7.9	9.9	10.3
2000	10.4	10	9.7	8.7	8.9	8.3	x	x	5.7	7.1	x	x
2001	10.4	9.9	8.1	x	x	x	x	x	x	x	x	x
2002	x	x	x	x	x	x	x	x	x	x	x	x
2003	X	X	7.7	8.4	10.5	8	7.2	7.6	8.2	8.8	10.5	8.8
2004	X	X	7.7	8.4	10.5	8	7.2	7.6	8.2	8.8	10.5	8.8
2005	8.9	11	9.3	8.5	7.5	7.7	6.1	8.8	7.5	9.8	9.4	10.7